

a NASA facsimile reproduction
PROPERTY OF: SCOTT J. DAVIS

REPRODUCED FROM MICROFORM

by the
Reproduced From
Best Available Copy
Scientific and Technical Information Facility

DISTRIBUTION STATEMENT A
Approved for Public Release
Distribution Unlimited



20011221 111

B057148

N64
17765
UNCLASS
CODE 1

2

1

N64-17765

SEARCH AND DEVELOPMENT OF S-1C
HEAT SHIELD BERYLLIUM PANELS

ER-764

ATRONCA MANUFACTURING CORPORATION
MIDDLETON, OHIO

Contract No. NASA-5221
Request No. TP-385154

Period of Performance January 29, 1964
to January 29, 1964, Inclusive

ABSTRACT

This report describes the work accomplished on Research and Development of S-1C Heat Shield Panels utilizing braze stainless steel honeycomb sandwich construction, for the period January 29, 1963, to January 29, 1964, inclusive.

The principal effort in this program was the stress, thermal and design analysis of two S-1C heat shield panel designs which differed by virtue of the panel mounting system. As a consequence of this analytical study and the NASA S-1C Heat Shield Panel Test conducted at Wyle Laboratories, either panel design appears to satisfy the S-1C requirements provided the M-31 insulation is retained on the panel by deformation of the honeycomb insulation reinforcement.

Additional items investigated include:

1. Application of Beryllium Sheet to S-1C Heat Shield Panels.
2. Deflection Characteristics of M-31 Insulation with Deformed Stainless Steel Honeycomb Reinforcement.
3. Analysis of Braze Defects, Braze Quality Standards and Repair Methods.
4. Analysis of Holes in Heat Shield Panels and Experimental Measurements of Stresses at Hole Boundaries.
5. Design Recommendations for Heat Shield Panels.

Submitted by:

ATRONCA MANUFACTURING CORPORATION
MIDDLETON, OHIO

Prepared by:

DONALD Y. POTTER
GEORGE W. SOMERS

MSFC Technical Supervisor
James O. Lysaght

DISTRIBUTION STATEMENT
Approved for Public Release
Distribution Unlimited

January 28, 1964

3

4

OTS PRICE

11/25/64
MICROFILM \$ 5
XEROX \$ 10

TABLE OF CONTENTS

<u>SECTION</u>	<u>PAGE</u>
ABSTRACT	1
TABLE OF CONTENTS	11
LIST OF TABLES	111
LIST OF ILLUSTRATIONS	v
I. TRANSIENT THERMAL ANALYSIS FOR S-1C HEAT SHIELD PANELS	1-32
II. STRESS ANALYSIS FOR S-1C HEAT SHIELD PANELS 30M12571 AND 60B20210	33-46
III. DESIGN PARAMETERS FOR BRAZED HONEYCOMB HEAT SHIELD PANELS WITH SIMPLY SUPPORTED EDGES	47-52
IV. APPLICATION OF BERYLLIUM SHEET TO S-1C HEAT SHIELD PANELS	53-70
V. DEFLECTION CHARACTERISTICS OF M-11 INSULATION WITH DEFORMED STAINLESS STEEL HONEYCOMB REINFORCEMENT	71-74
VI. ANALYSIS OF BRAZE DEFECTS, BRAZE QUALITY STANDARDS AND REPAIR METHODS FOR 30M12571 HEAT SHIELD PANEL	75-97
VII. ANALYSIS OF HOLES IN HEAT SHIELD PANELS AND EXPERIMENTAL MEASUREMENTS OF STRESSES AT HOLE BOUNDARIES	98-120
VIII. DESIGN RECOMMENDATIONS FOR S-1C HEAT SHIELD PANELS NOMENCLATURE	121-123 36-37

LIST OF TABLES

<u>NUMBER</u>	<u>PAGE</u>
1	1
2	2
3	3
4	4
5	5
6	6
7	7
8	8
9	9
10	10
11	11
12	12
13	13
14	14
15	15
16	16

PAGE

1	7
2	32
3	40
4	41
5	42
6	43
7	44
8	45
9	46
10	46
11	46
12	55
13	58
14	60
15	61
16	70

5

6

LIST OF TABLES (Cont'd)

NUMBER	PAGE	
17	FLEXURE TEST OF HEAT SHIELD TEST SAMPLE	72
18	SIZE AND SHAPE OF CORE TO FACING - ROSS VOID EFFECTS WITH MINIMUM SPACING REQUIREMENTS	40
19	SIZE AND SHAPE OF CORE TO FACING, INTERMITTENT CELL WALL VOIDS	41
20	METAL TO METAL AND CORE TO METAL BRAZE REQUIREMENTS	47
21	VALUES OF THE STRESS CONCENTRATION FACTOR K FOR VARIOUS SHAPES: HOLES WITHOUT FROBBER INSER	102
22	TEST PANEL DEFLECTION DATA	111
23	SUMMARY OF EXPERIMENTAL AND THEORETICAL VALUES OF STRESS CONCENTRATION FACTOR K FOR BIAXIAL LOADING	119

LIST OF ILLUSTRATIONS

NUMBER	PAGE	
1	TYPICAL S-1C HEAT SHIELD HEATING RATES & SURFACE TEMPERATURE AS A FUNCTION OF FLIGHT TIME (NASA SUPPLIED DATA 2-11-63)	2
2	TEMPERATURE PROFILE FOR HEAT SHIELD PANEL 30M12571: 100% NODE FLOW (.010 INCH WIDTH)	6
3	TEMPERATURE PROFILE - "W2" TYPE PANEL ATTACHMENT PANEL 30M12571	8
4	TEMPERATURE PROFILE FOR HEAT SHIELD PANEL SK60B20001 WITH 100% NODE FLOW (.010 INCH WIDTH)	9
5	TEMPERATURE PROFILE - CUP-TYPE PANEL EDGE ATTACHMENT	10
6	THERMAL CONDUCTIVITY OF HEAT SHIELD PANEL VS. CELL WIDTH AND NODE FLOW WIDTH	13
7	EFFECT OF NODE FLOW SIZE ON PANEL UNIT WEIGHT AND THERMAL CONDUCTIVITY	14
8	EFFECT OF NODE FLOW WIDTH & CELL SIZE ON TEMPERATURE DIFFERENTIALS ACROSS THE 30M12571 PANEL DESIGN FOR THREE DIFFERENT LOAD BEARING CORE SIZES	15
9	TEMPERATURE DIFFERENTIALS ACROSS THE HONEYCOMB AS FUNCTION OF CELL DEPTH AND NODE FLOW WIDTH. CORE SIZE 4-15	17
10	TEMPERATURE PROFILES IN HEAT SHIELD PANEL NO. 30M12571 ZERO NODE FLOW--CELL SIZE 4-15, VARIABLE M-31 REINFORCING	18
11	TEMPERATURE PROFILES, PANEL NO. 30M12571, ZERO NODE FLOW - CELL SIZE 3-15, OPEN CORE SIZE 8-15	19
12	TEMPERATURE PROFILES, PANEL NO. 30M12571, .005 INCH NODE FLOW WIDTH - CELL SIZE 3-15, OPEN CORE SIZE 8-15	20
13	TEMPERATURE PROFILES, PANEL NO. 30M12571, .010 INCH NODE FLOW WIDTH - CELL SIZE 3-15, OPEN CORE SIZE 8-15	21
14	TEMPERATURE PROFILES, PANEL NO. 30M12571, .015 INCH NODE FLOW WIDTH -- CELL SIZE 3-15, OPEN CORE SIZE 8-15	22
15	TEMPERATURE PROFILES - PANEL NO. 30M12571, ZERO NODE FLOW - CELL SIZE 4-15, OPEN CORE SIZE 8-15	23

7

8

LIST OF ILLUSTRATIONS (Cont'd)

<u>NUMBER</u>	<u>PAGE</u>	
16	TEMPERATURE PROFILES - PANEL NO. SK6018-0001 ZERO NODE FLOW - CELL SIZE 4-15, OPEN CORE SIZE 8-15	24
17	TEMPERATURE PROFILES - PANEL NO. SK6019-0001, .005 INCH NODE FLOW WIDTH - CELL SIZE 4-15, OPEN CORE SIZE 8-15	25
18	TEMPERATURE PROFILES - PANEL NO. SK6019-0001, .015 INCH NODE FLOW WIDTH - CELL SIZE 4-15 OPEN CORE SIZE 8-15	26
19	TEMPERATURE PROFILES IN HEAT SHIELD - PANEL NO. .015 INCH NODE FLOW WIDTH - CELL SIZE 8-15, VARIABLE M-31 REINFORCEMENT	27
20	TEMPERATURE PROFILES - PANEL NO. 10411571, ZERO NODE FLOW - CELL SIZE 6-20, OPEN CORE SIZE 8-15	28
21	TEMPERATURE PROFILES - PANEL NO. 10412571, .005 INCH NODE FLOW WIDTH - CELL SIZE 6-20, OPEN CORE SIZE 8-15	29
22	TEMPERATURE PROFILES - PANEL NO. 10412571, .010 INCH NODE FLOW WIDTH - CELL SIZE 6-20, OPEN CORE SIZE 8-15	30
23	TEMPERATURE PROFILES - PANEL NO. 10412571, .015 INCH NODE FLOW WIDTH - CELL SIZE 6-20, OPEN CORE SIZE 6-20	31
24	MOUNTING SYSTEM FOR 60B2020 PANEL SHOWING CALCULATION DIMENSIONS ONLY	38
25	VARIATION OF MODULUS OF ELASTICITY WITH TEMPERATURE (ELASTIC PROPERTIES OF PH15-7HO (TH 1050) BASED ON 1958 ARMC DATA IN ARDC TR 59-66)	39
26	DEFLECTION AT CENTER OF PANEL VS. CORE THICKNESS	48
27	THERMAL DEFLECTION AT CENTER OF PANEL VS. HEIGHT OF PANEL FOR CONSTANT TEMPERATURE DIFFERENCES	49
28	THERMAL + AIR LOAD DEFLECTION AT CENTER OF PANEL VS. HEIGHT OF PANEL FOR CONSTANT TEMPERATURE DIFFERENCES AND 1 psf	50
29	THERMAL + AIR LOAD DEFLECTION AT CENTER OF PANEL VS. HEIGHT OF PANEL FOR CONSTANT TEMPERATURE DIFFERENCES AND 1 psf	51
30	THERMAL + AIR LOAD DEFLECTION AT CENTER OF PANEL VS. TEMPERATURE DIFFERENCE FOR CONSTANT CORE THICKNESS (\bar{t})	52
31	FLEXURE TEST OF SANDWICH SECTION WITH M-31 INSULATION	73
32	FLEXURE TEST OF SANDWICH SECTION WITH M-31 INSULATION AT FAILURE	74
33	QUALITY MODIFYING CONDITIONS REVEALED BY RADIOPHIC EXAMINATION	76
34	QUALITY MODIFYING CONDITIONS REVEALED BY RADIOPHIC EXAMINATION	77
35	QUALITY MODIFYING CONDITIONS REVEALED BY RADIOPHIC EXAMINATION	78
36	QUALITY MODIFYING CONDITIONS REVEALED BY RADIOPHIC EXAMINATION	79
37	QUALITY MODIFYING CONDITIONS REVEALED BY RADIOPHIC EXAMINATION	80
38	QUALITY MODIFYING CONDITIONS REVEALED BY RADIOPHIC EXAMINATION	81
39	BASIC VOID AND BUCKLING CONFIGURATIONS	83
40	EFFECT OF GROSS Voids - LOCAL UNIAXIAL COMPRESSION ALLOWABLE PH15-7HO (RH1050)	85
41	EFFECT OF CELL WALL Voids - LOCAL UNIAXIAL COMPRESSION ALLOWABLE PH15-7HO (RH1050)	87
42	EFFECT OF UNDERSIZE FILLET ON FACE SHEET STABILITY	88
43	TYPICAL METAL TO METAL BRAZE VOID REPAIR WITH MECHANICAL FASTENERS (RIVETS)	95
44	HOLE DIAGRAMS, TYPICAL	100
45	STRESS CONCENTRATION FACTOR, K AT $\theta = \pi/4$ FOR SQUARE AND DIAMOND HOLES	101
46	VACUUM BOX TEST FIXTURE	108
47	SIDE VIEW, TEST ASSEMBLY, PANEL NO. 1	109
48	END VIEW, TEST ASSEMBLY	110
49	DIAL INDICATOR POSITIONS FOR TEST PANELS	112

10

9

LIST OF ILLUSTRATIONS (Cont'd)

NUMBER	PAGE
50	113
51	114
52	115
53	116
54	117
55	120
56	123
57	124

SECTION I
TRANSIENT THERMAL ANALYSIS
FOR S-1C HEAT SHIELD PANELS

PAGE

STRESS COAT, PANEL NO. 1, INITIAL HOLE PATTERN
CENTER HOLE STRESS COAT CLOSE-UP PANEL NO. 1,
INITIAL HOLE PATTERN

EDGE HOLE STRESS COAT CLOSE-UP PANEL NO. 1,
INITIAL HOLE PATTERN

CENTER HOLE STRESS COAT CLOSE-UP PANEL 1
MODIFIED HOLE PATTERN

PANEL NO. 2, STRESS COAT PATTERN, QUARTER
SECTION VIEW

STRAIN GAGE LOCATIONS ON TEST PANELS USED FOR
EXPERIMENTAL DETERMINATION OF STRESS CONCENTRATION

FACTOR, K

RECOMMENDED ZEE SECTION CORNER JOINT ASSEMBLY

ECONOMICAL ZEE SECTION CORNER JOINT ASSEMBLY

Introduction

Presented in this section are the transient heat transfer analyses of the Saturn base heat shield panel for design drawing Nos. 30R12571 and 5K 60B-20001 and shown in Figure 1, Page 2. All analyses are three dimensional in nature and are based on heating rates and surface temperature profiles from NASA Huntsville data. Included are the maximum temperature profiles of the edge attachment scheme for the two panel designs. The temperature profiles presented are for the condition of 100% brazing allow node flow in the honeycomb support structure. All other assumptions and ground rules which govern the analysis are presented in "Methods of Analysis".

In addition to the thermal analyses of the two panel concepts, a set of parametric curves is presented illustrating the temperature differences across the honeycomb support structure as a function of brazing node flow size, cell dimensions and M-31 reinforcement honeycomb dimensions. While these parametric studies are confined to the dimensions bounded for the most part by the dimensions of the panel considered, they do present the possible trade-offs that could be considered for possible panel design optimization from thermal considerations.

Methods of Analysis

Aeronca has developed a digital computer program which has general applicability to thermal analysis of high temperature structures. For purposes of analysis, the structure is represented by a set of spatially distributed points or nodes. The temperature of each node is determined by solving the generalized heat balance equation in finite difference form:

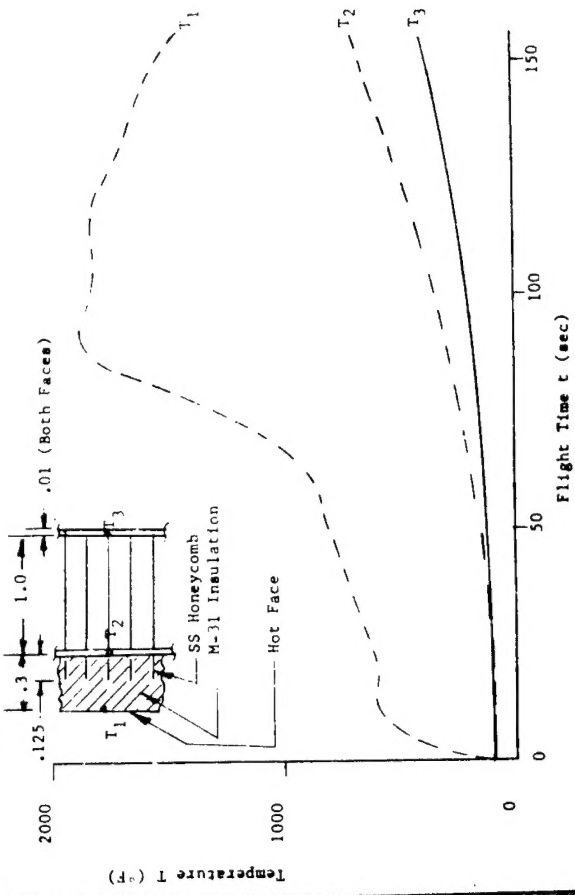
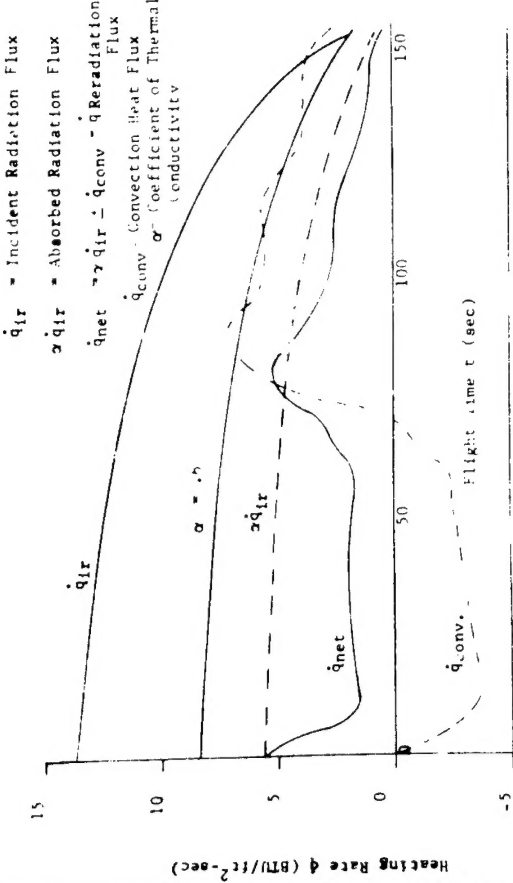
$$T_j' - T_j = \frac{\Delta r}{\rho V C_p} \left[Q_j + \sum_{i=1}^n U_{ij} (T_i' - T_j) \right] \quad (1)$$

T_i' and T_j' represent the temperatures at the end, and beginning of the time step, respectively. The parameters Q_j and Q_i represent volumetric heating and incident surface flux, respectively. U_{ij} is the thermal conductance between the adjacent nodes i and j . The program does an iteration for T' and re-evaluates temperature dependent functions (radiation coefficient, etc.) on the temperature at the midpoint of the time step. This is the so-called Implicit Method.

*MSFC Memorandum, "Estimated Temperatures for S-1C Heat Shield Attachment", dated 2/11/63, M-PSVE PH 26-63.
See Figure 2.

12

11



The program can use the Explicit Method, in which T_j and T_i are the same as in the Implicit Method. The heat balance equation will become explicit in T_j

$$T_j - T_j = \frac{\Delta t}{\rho V C_p} \left[\dot{Q}_j^{***} + \dot{Q}_j^{**} - \sum_{i=1}^n U_{ij} (T_j - T_i) \right] \quad (2)$$

There is now a limit on the length of time step Δt which the program calculates and is given by $\Delta t \leq \frac{\rho V C_p}{\sum_{i=1}^n U_{ij}}$ and taken so that the expression $\sum_{i=1}^n U_{ij}$ is a minimum for the entire nodal system. Here, n is the total number of thermal connections.

The expression used to evaluate zero-volume nodes (surface) and steady-state calculations is

$$\sum_{i=1}^n U_{ij} (T_j - T_i) - \dot{Q}_j^{***} - \dot{Q}_j^{**} = 0 \quad (3)$$

The parameters \dot{Q}_j^{***} and \dot{Q}_j^{**} are the same as defined previously.

The thermal conductance term, U_{ij} , is used in three basic forms: (1) solid to solid conduction, with contact coefficient; (2) solid to solid radiation, with radiation coefficient; and (3) solid to fluid, with conduction and film coefficient.

There are several important features in this computer program. The amount of data necessary to run a problem is quite large and would include such things as: (1) time, boundary variables; (2) time, rate tables; (3) Nusselt number correlation tables; (4) material property tables; (5) node description data for each node; and (b) connection data for each node. Although a large amount of input data is necessary, the engineer requires little or no knowledge of computer programming or techniques to use the program. Use of stacked storage is employed rather than the bulkier reserved storage, so that problems with greater than 1000 nodes can be run.

The program is divided into five chains: Chain 1 accepts data in a form which is easy for the user to prepare and stores it for further processing—in other words, Chain 1 is just to input the problem; Chain 2 processes data from Chain 1 into a form which the program can use; Chain 3 takes this processed data and performs the computation of Equations (1) or (2); Chain 4 is an editing chain which will (1) give a time-temperature history if requested, and (2) if the run is pulled for time, punch the current temperature distribution or decimal cards so that the run can be restarted; Chain 5 sets up change cases. A more detailed description of the program is presented in Ref. 1*.

Figure 1 Typical S-1C Heat Shield Heating Rates & Surface Temperature As a Function of Flight Time (NASA supplied data 2-11-63)

*Ref. 1 - Niehaus, W. R., Criss, R., Cannizzaro, R., "A Transient Heat Transfer Computer Analysis for Space Vehicle Application", Aeroneca Manufacturing Corporation, ER-638, February 1963.

A second method of heat transfer which was employed was to assemble "n" heat balance equations, one for each temperature point in the panel and for given time intervals and time dependent boundary conditions use the Gauss-Seidel iteration method to determine the unknown temperatures.

This process is repeated for each time interval until the desired transient analysis is complete.

The general form of the heat balance equation for one point in the panel for a single time interval is given below.

$$\frac{\partial V_C}{\partial T} (T - T') = \sum_{n=1}^6 \left[\frac{A_n}{K} + \frac{\Delta X_{11}}{K_{11}} + \frac{1}{h_n} + \frac{1}{h_C} \right] (T_i - T) +$$

Fluid flow input

$(W_e/W)h_C (T_n - T)$

Surface Flux

$A_s \dot{Q}_s$

Solid Radiation

$$\sum_{n=1}^3 \sum_{i=1}^3 \sigma A_h F_i \epsilon_1 \epsilon_2 [T_h^4 - T_i^4]$$

Basically, the transient analysis was one of using the finite difference technique of dividing the panel geometry into a three-dimensional network of nodes. Each node had a finite volume enclosed by a maximum of six sides. Material properties and states were considered to be uniform within a given node and correspond to the temperature at the center of the node.

Design Point Analysis

2-Type Edge Panel (Dwg. 30M12571):

The temperature histories at various levels throughout the panel are given in Figure 2 and are based on the effective thermal properties of the various layers as given in Table 1. The temperature histories at various points on the Z-type edge attachment are given in Figure 3.

Cup-Type Panel (Dwg. SK 60B20001):

The temperature histories at various levels throughout the panel are given in Figure 4 and are based on the effective thermal properties of the various layers given in Table 1.

The temperature histories at various points on the cup-type edge attachment are given in Figure 5.

Assumptions Made in the Preceding Analysis:

The following assumptions and/or ground rules were made and incorporated in the transient heat transfer analysis:

1. When composite layers existed in the heat shields (i.e., where parallel heat transfer paths exist), an effective thermal conductivity and density were used. The effective thermal conductivity is equal to the sum of the parallel conductances divided by the total panel heat flow area.
2. The temperature differential across the honeycomb support structure facing was considered small and the unit conductance (k/s) was substituted as a contact coefficient to account for thermal conductance through them. The volumetric heating was neglected.

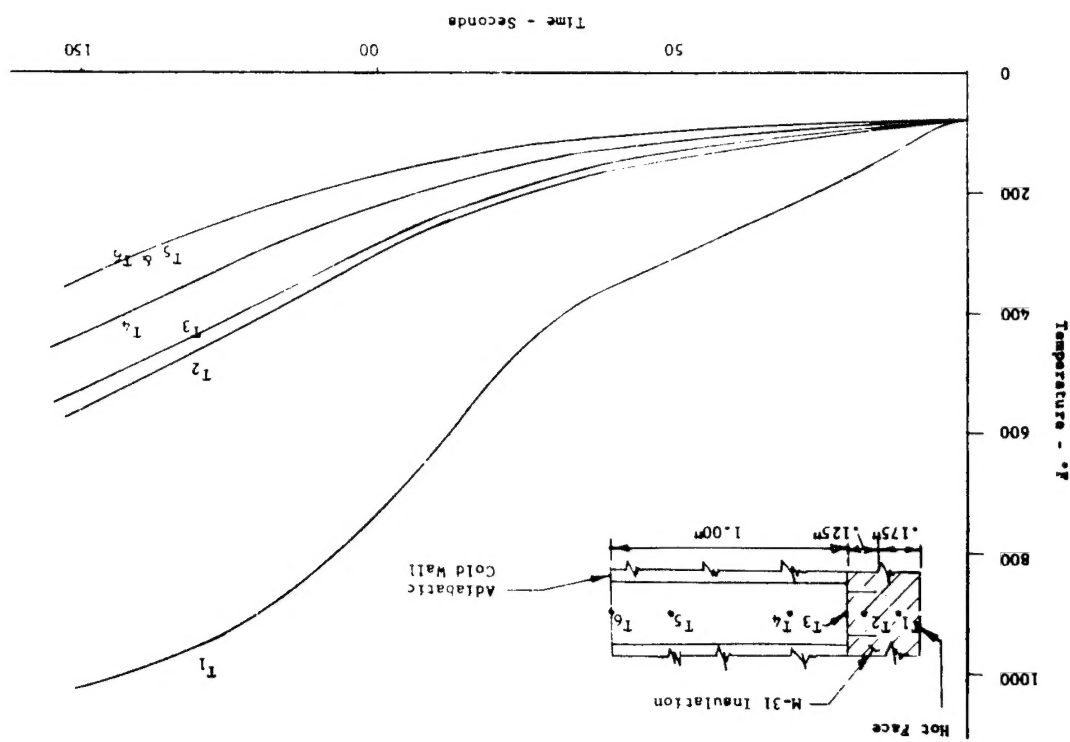
3. Node flow was included in the thermal conductance of the honeycomb support panel. Two (2) braze nodes per honeycomb cell were considered having an effective cross sectional area equal to that of an equilateral triangle of side 0.010 inch. This dimension was based on measurements of the node flow width made from 30M12571 panel X-rays.
4. The cold face surface was adiabatic.

5. The radiation exchange and natural convection were both considered negligible in the honeycomb cells.
6. The contact coefficients between the panel edges and the attachment bolts were based on a nominal air gap of 0.001".

TABLE 1
THERMAL ANALYSIS,
EFFECTIVE MATERIAL PROPERTIES
BASED ON HOMOGENEOUS LAYERS

Material Layer	T ₀ F	K _{effective} BTU/Hr/Fe/°F	Specific Heat - B BTU/#°F		Density - D Lbs/Cu.Ft.
			11	7.19	
1. Honeycomb Structure (4.15) Cell Size PH15-7Mo	0 800	.228 .265	.11 .11	7.19 7.19	
2. M-31 Plus Honeycomb Support	0 800	.130 .152	.31 .31	50.1 50.1	
3. M-31	3000	.083 .083	.31 .31	47.0 47.0	

Figure 2 Temperature Profile for Heat Shield Panel 30M12571
100% Node Flow (.010 inch width)



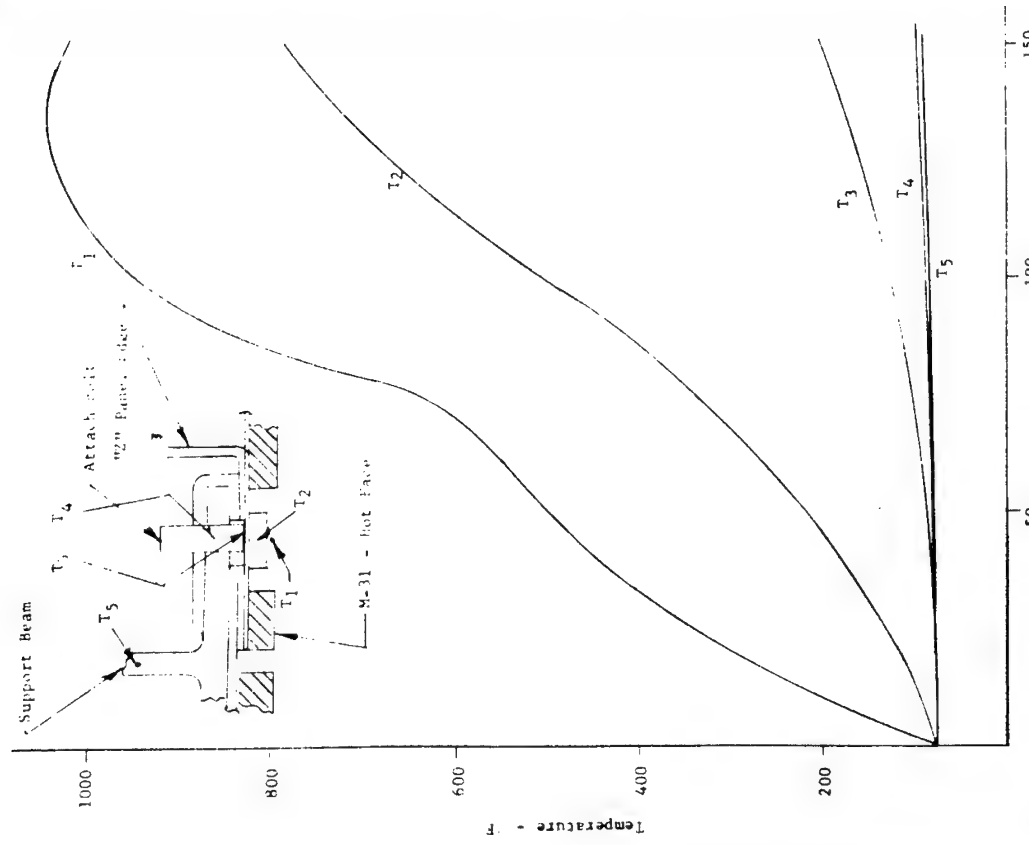


Figure 3 Temperature Profile - "Z" Type Panel Attachment
Panel 30M12571

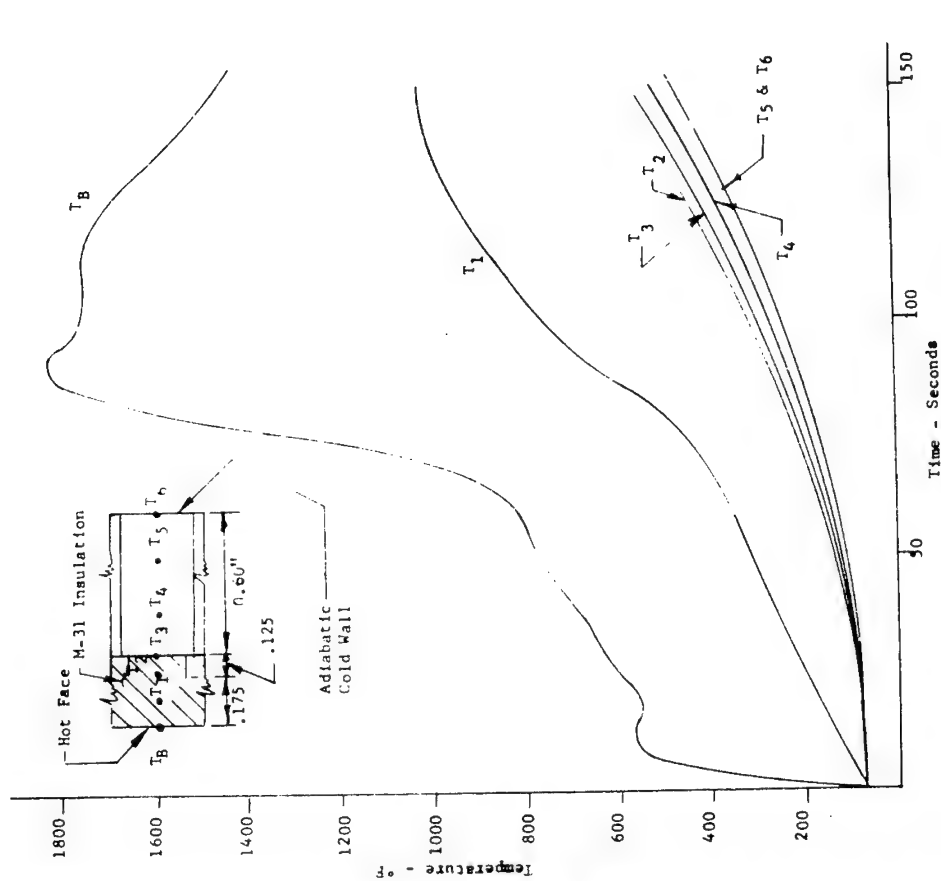


Figure 4 Temperature Profile for Heat Shield Panel SK 60B20001
with 100% Node Flow (.010 inch width)

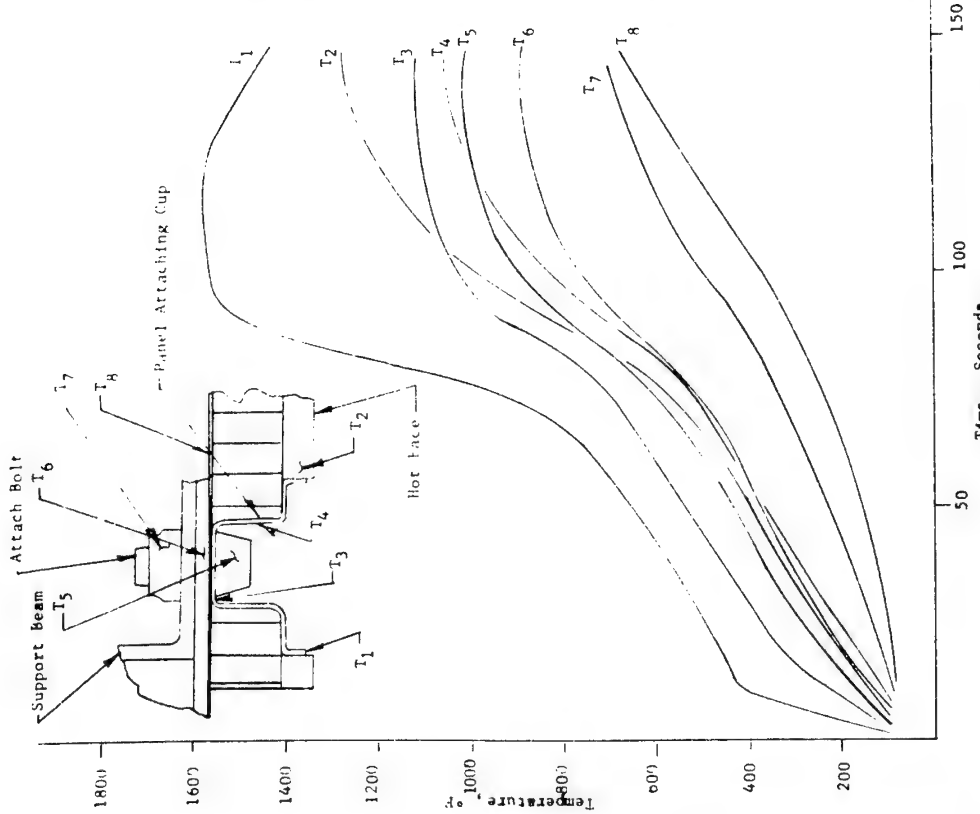


Figure 5 Temperature Profile - Cup-Type Panel Edge Attachment

Design Point Temperatures

The maximum temperature differentials to be used for design purposes across the brazed honeycomb sandwich panels are as follows:

Panel Configuration	Silver Brazing Alloy Node Flow Condition	ΔT, °F	Time Duration, Second*
SK60B20001 0.6" Thick Core	Complete--0.010"	80	155
30M12571 1.0" Thick Core	Zero	320	155
30M12571 1.0" Thick Core	Complete--0.005"	280	155
30M12571 1.0" Thick Core	Complete--0.010"	180	155
	Width		

The beneficial effect of brazing alloy node flow in the lead tearing honeycomb core, reducing the temperature difference and the resultant thermal stress, is shown for the 30M12571 heat shield panel design by the above data.

Parametric Analysis

As a result of the thermal analysis performed on the two heat shield panel concepts, a parametric analysis was made which considered the effects of node flow width, cell dimensions, and M-31 reinforcing honeycomb effects on the transient temperature differentials across the honeycomb support structure.

A careful review of the thermal analyses of honeycomb panels in the past has indicated that the presence of good node flow with the use of high thermal conductivity brazing alloy is the probable cause of the high rate of heat conduction through honeycomb panels.

The term "node flow" refers to the phenomenon of the formation of fillets of braze alloy which connect the panel faces, in the corners of the honeycomb core cells. Such metal "bridges" offer conduction paths between the panel faces which are orders of magnitude better than that in the air gap within the cells and which, at reasonably low temperature levels, transfer considerably more thermal energy between panel faces than is transferred by thermal radiation. If the thermal conductivity of the node-flow metal approaches that of silver, which is on the order of 20 times that of a high-nickel-content brazing alloy, the node-flow conduction path will be by far the dominating factor in the transmission of heat through the panel.

Reference 2* presents an analysis of sample test data wherein it is shown, on the basis of a reasonable set of assumptions, that of the total heat passing through the test panel, 5.2% was by radiation between the panel faces, 17.0% was by conduction through the core foil, and the remaining 77.8% was by conduction through the high-silver-content brazing alloy. While the exact magnitude of the numbers may be subject to some questions on the basis of the assumptions used in calculating them, the relative magnitudes are felt to be quite correct.

The parametric analyses presented here are intended to furnish in limited way the trade-offs to be made in designing a heat shield panel from thermal considerations. The range of honeycomb cell dimension considered brackets the dimensions of the two design panels. As such the material discussed in this section and the feasible trade-offs that can be derived from the curves apply only in the neighborhood of the dimensions and environments of the previously mentioned design panels.

Node Flow Effect

Figures 6 to 8 show the effects of node flow width on the effective thermal conductivity of the honeycomb, the weight of the honeycomb panel, and the temperature differential across the honeycomb panel.

Figure 6 shows that in doubling the cell width the effective conductivity of the panel is reduced by a factor of from $2 - 2\frac{1}{3}$ for node flow widths of about 0.010". Also, it is evident that for a node flow width above 0.010" the effective conductivity increases rapidly. However, with this increase in thermal conductivity, which is desirable from a thermal stress standpoint, there is an increase in panel weight. Figure 7 shows the trade-off between effective honeycomb density and increase in effective conductivity as a function of cell width and node flow width. For a node flow width of 0.010", the per cent increase in density of a honeycomb having a 3-15 cell (.188" cell width, .0015" foil width) when such a brace node flow is added in 21% of the original density with no node flow. The per cent increase in thermal conductivity, however, is 118%. In values of density the increase would go from 9.3 to 10.03 lb/ft³ while the conductivity would increase from .136 BTU/ft²·F to .387 BTU/ft²·F·°F.

Figure 8 gives the effect of node flow width and cell width on the temperature differential across a 1.0" thick honeycomb panel (Panel No. 30812571). The temperature differential decreases with an increase in both cell width and node flow width. This is to be expected since an increase in either of these increases the effective thermal conductivity across the panel.

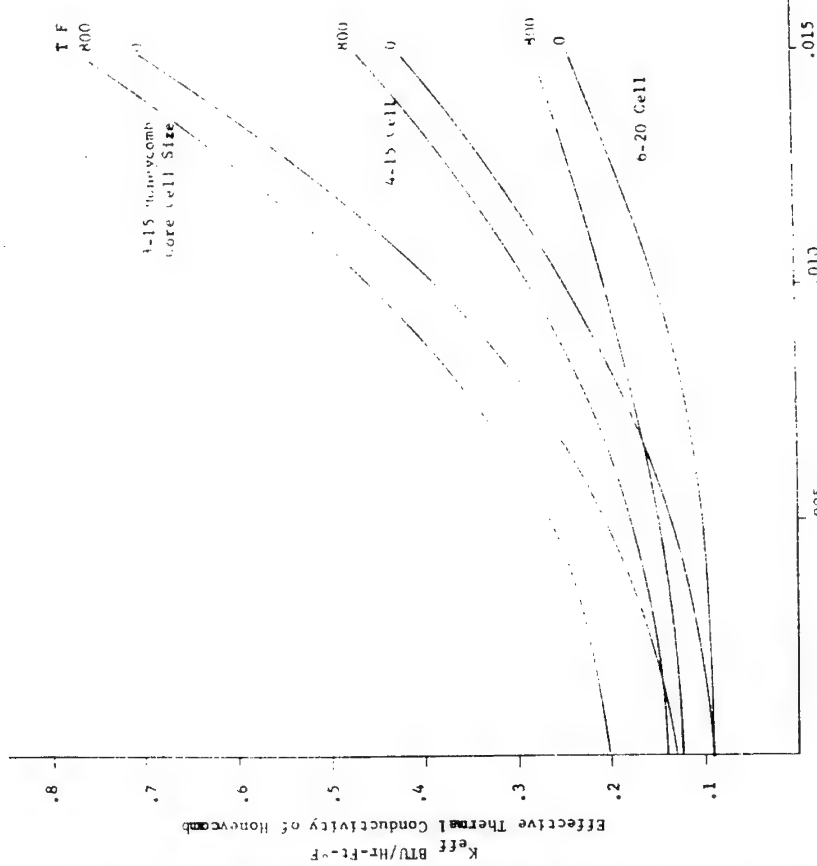


Figure 6 Thermal Conductivity of Heat Shield Panel vs.
Cell Width and Node Flow Width
(Based on Equilateral Triangle Cross-Section)

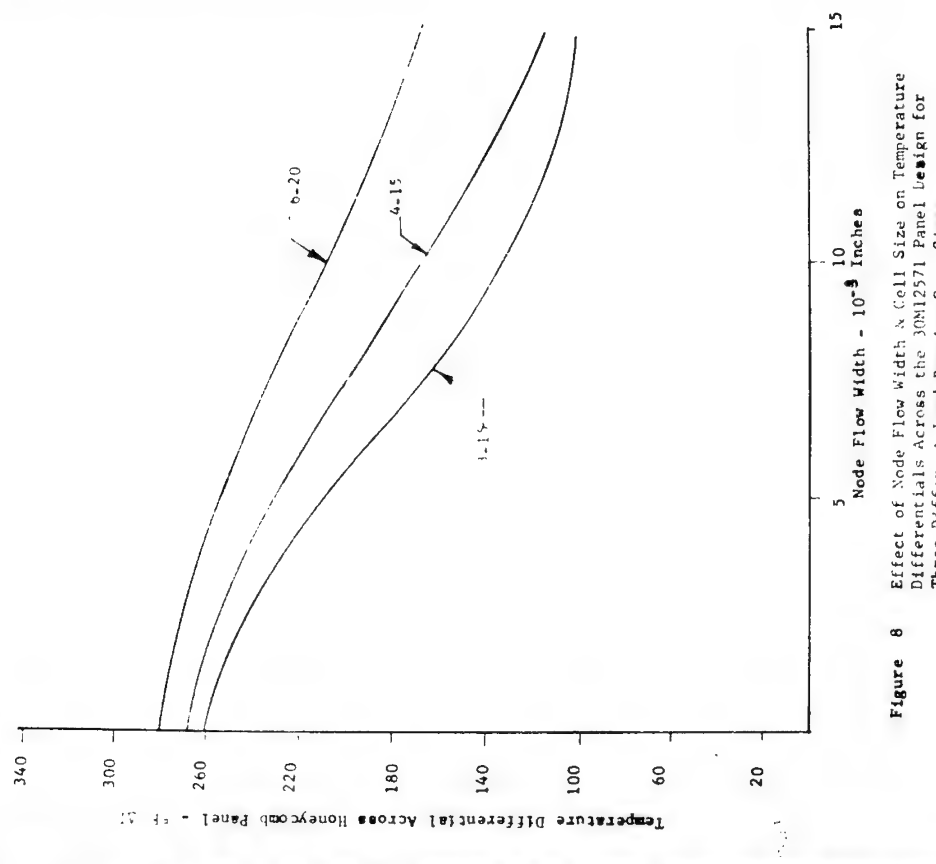
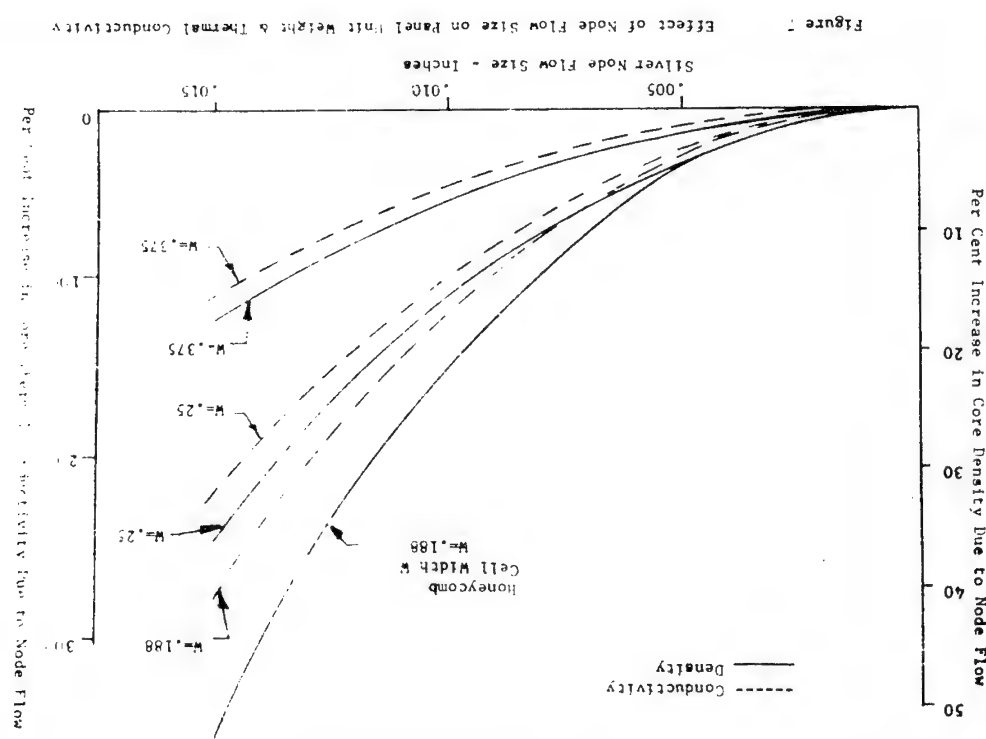


Figure 8 Effect of Node Flow Width & Cell Size on Temperature Differentials Across the Honeycomb Panel Design for Three Different Load Bearing Core Sizes

Cell Depths

In Figure 9, the adiabatic temperature differentials are given across the honeycomb core as a function of cell depth and node flow width for a constant cell size of 4-15" wide and 0.015" cell thickness. It is quite evident that for any one cell depth, the temperature drop across the honeycomb decreases with an increase in node flow width. Also, for a constant node flow width the ΔT approaches zero as the cell depth is decreased, as would be expected.

It should be pointed out here that holding all parameters constant and decreasing the cell depth for the adiabatic case increases the (hot side) temperature of the honeycomb panel. This is in contrast to the fact that the boundary conditions are the same so that there is no cell mass to absorb the same amount of heat.

M-31 Reinforcing Honeycomb Effects

Figure 10 gives the temperature profiles for the heat shield panel No. 30M-12571 as a function of variable M-31 reinforcement cell width. The cell size was varied from 8-15 to 4-15, respectively. As is evident from the curves, there was no noticeable effect on the temperature distribution in the honeycomb structure. Although not shown on the curves, a slight variance was noted in the temperatures T_1 and T_2 , but was of such a magnitude ($\pm 10^\circ$) as to make it negligible.

Supplementary Information Relating to Parametric Studies

The temperature profiles given in Figures 11 to 23 were the basis for the preceding parametric analyses. Table 2 shows in tabular form the characteristics of the three honeycomb panels that served as the models for the parametric analyses.

Discussion

The methods of thermal analysis and the design point analysis presented here have been discussed previously (Ref. 1) and have been given to consolidate the thermal analysis and its results into a single unit for reference.

In reference to the information given in the section on the parametric analyses, it should be pointed out that the curves can be used most accurately in predicting the trend or trade-offs that occur for any one set of cell dimensions. This is especially so when predicting the effect of node flow width on temperature differentials across the honeycomb panel. It is quite evident from the curves that the node flow size is of prime consideration.

It should also be noted here that the ΔT ($166^\circ F$) for the 4-15 cell having 0.010" node flow width in Figure 8 differs from the ΔT given in the section on Design Point Temperatures for the design point ($180^\circ F$). The difference is due to a refinement in the effective thermal conductivity of the honeycomb panel which was made for the parametric analyses. However, since the design point value was conservative, it was not changed.

Figure 9 Cell Depths

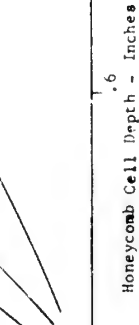
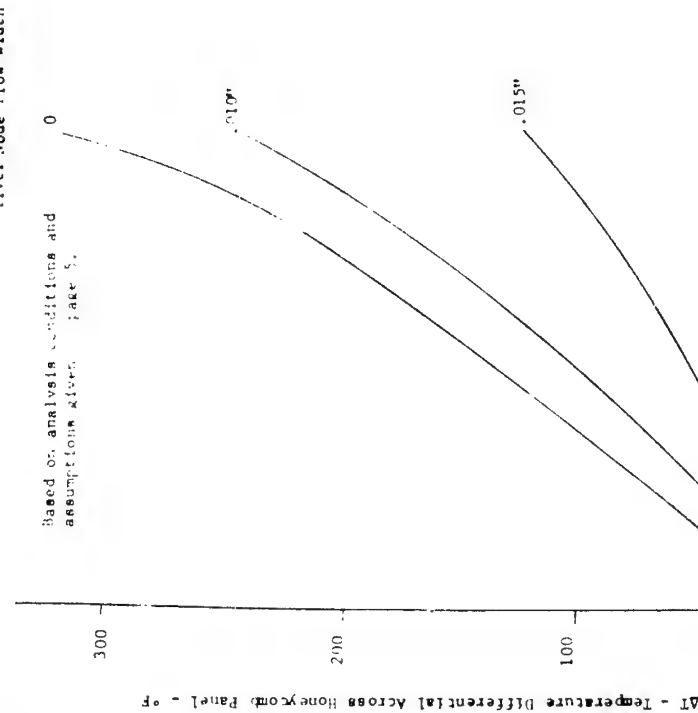


Figure 9 Temperature Differentials Across the Honeycomb Core as a Function of Cell Depth and Node Flow Width, Core Size 4-15

30

Figure 11 Temperature Profiles, Panel No. 30M12571
Zero Node Flow - Cell size 3-15
Open Core Size, 8-15

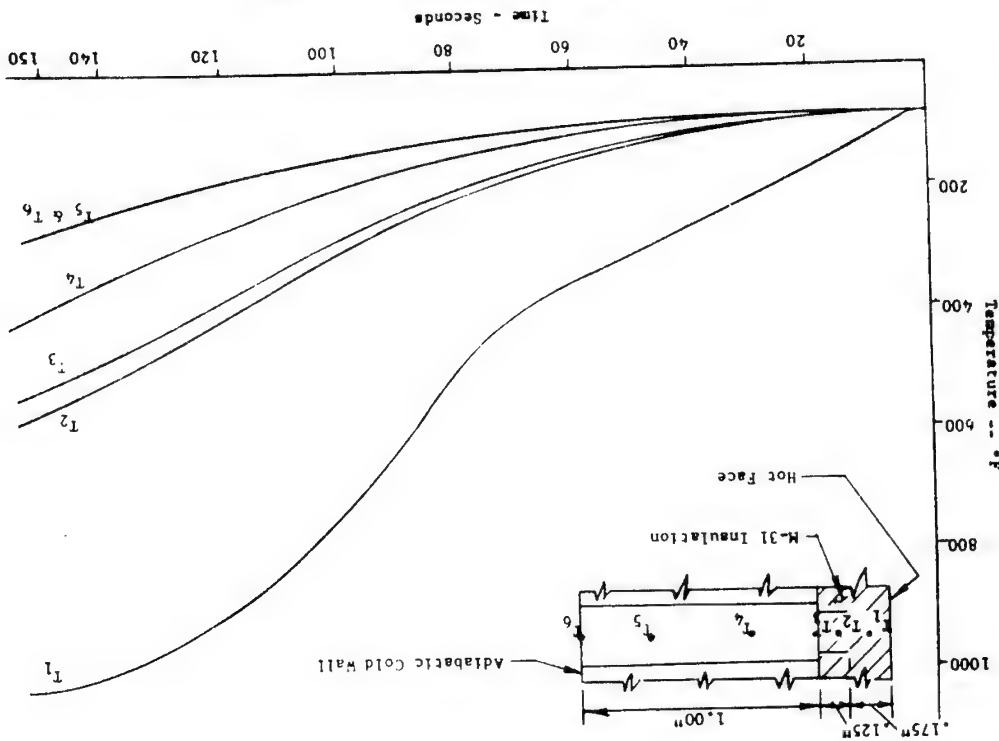
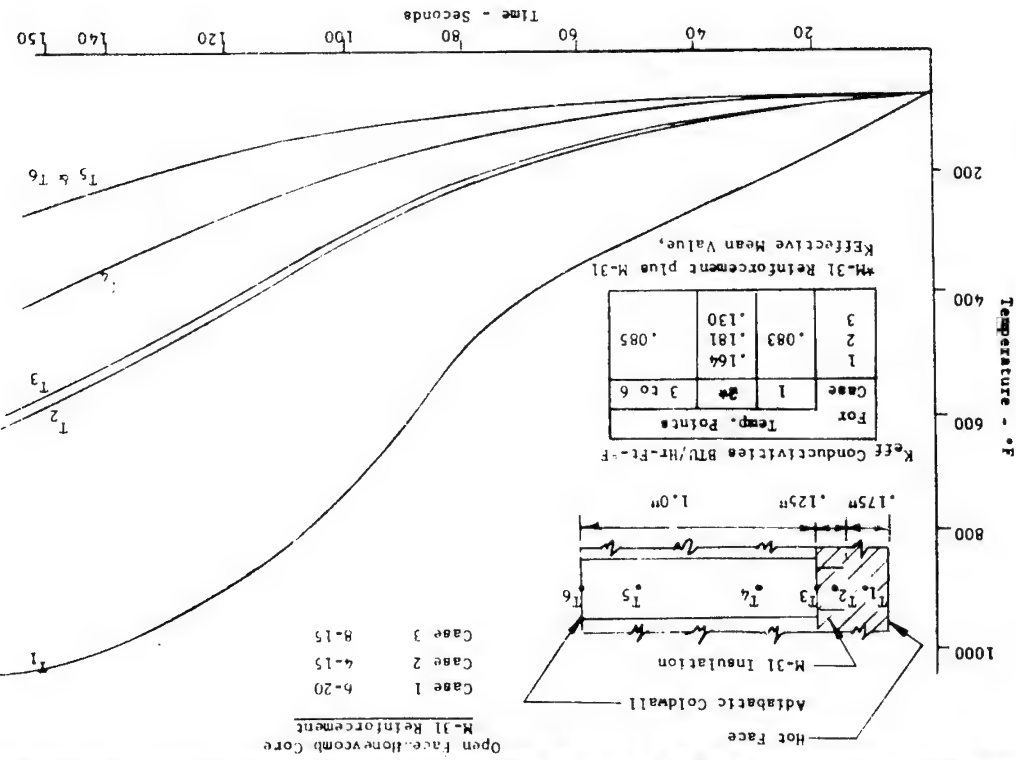


Figure 10 Temperature Profiles in Heat Shield Panel No. 30M12571
Zero Node Flow - Cell Size 4-15, Variable M-31 Reinforcement



29

32

Figure 13 Temperature Profiles, Panel No. 30M12571
.010 Inch Node Flow Width - Cell Size 3-15
Open Core Size, H-15

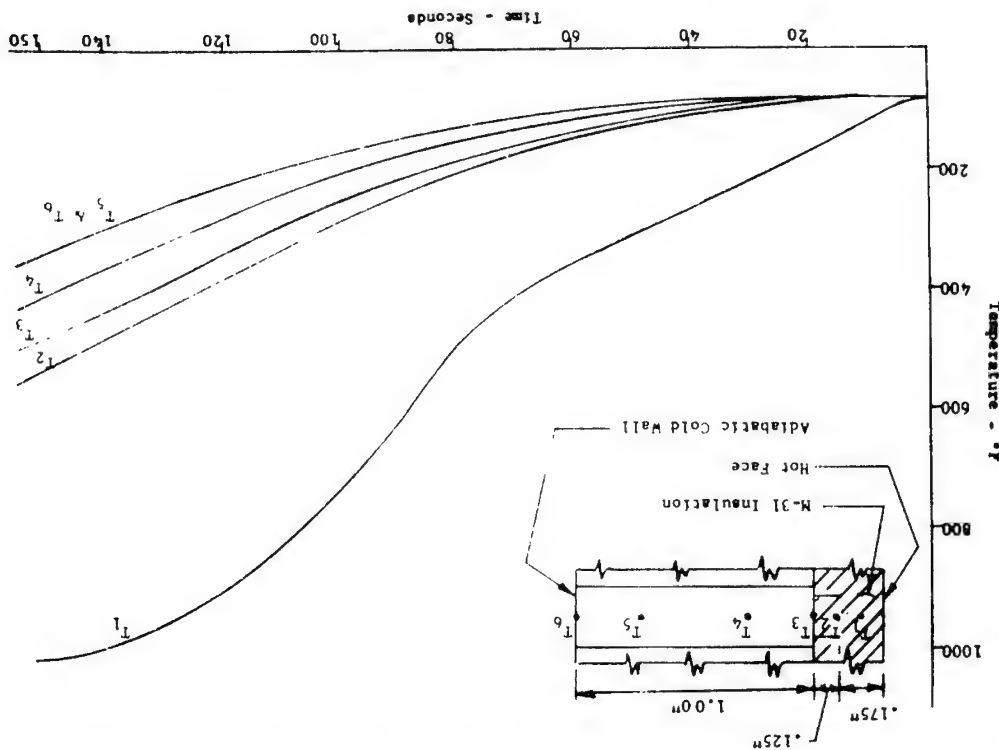
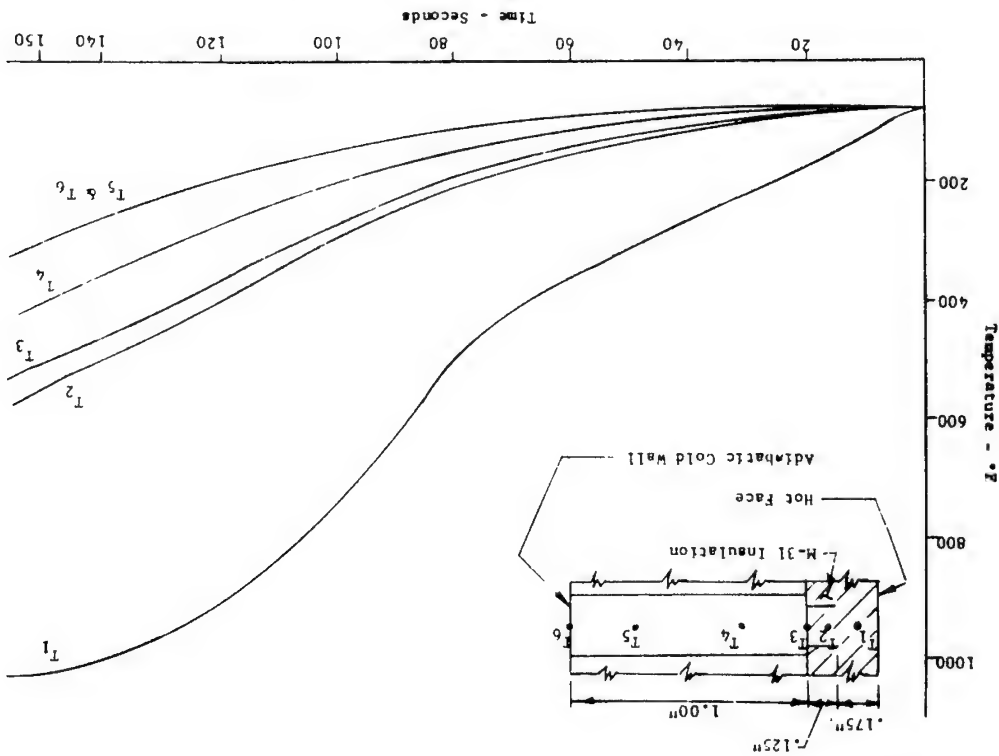
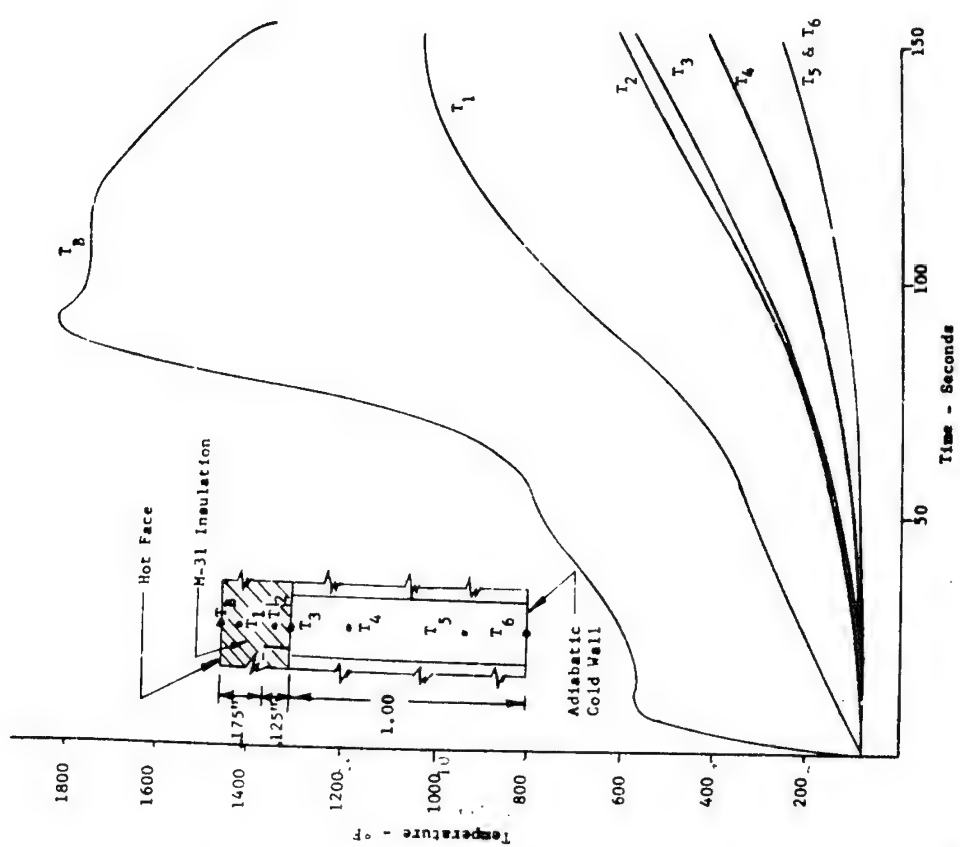
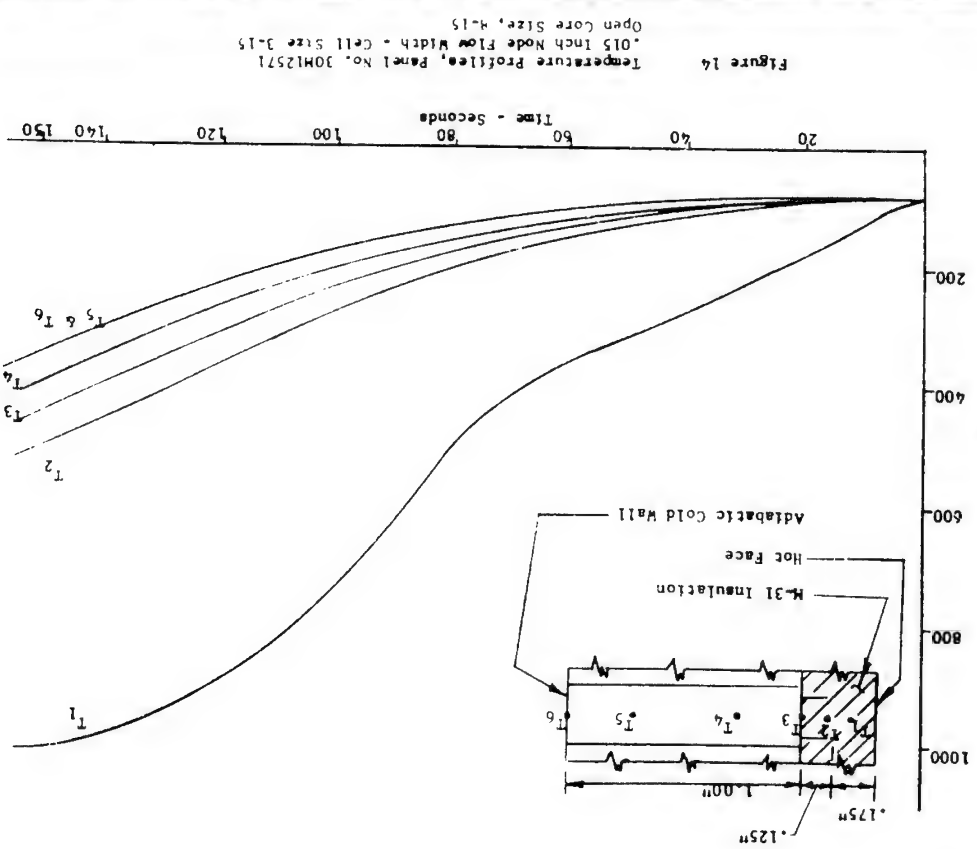


Figure 12 Temperature Profiles, Panel No. 30M12571
.005 Inch Node Flow Width - Cell Size 3-15
Open Core Size, B-15



31



35

Figure 16 Temperature Profiles - Panel No. SK 60B20001
Zero Node Flow - Cell Size 4-15
Open Core Size, 8-15

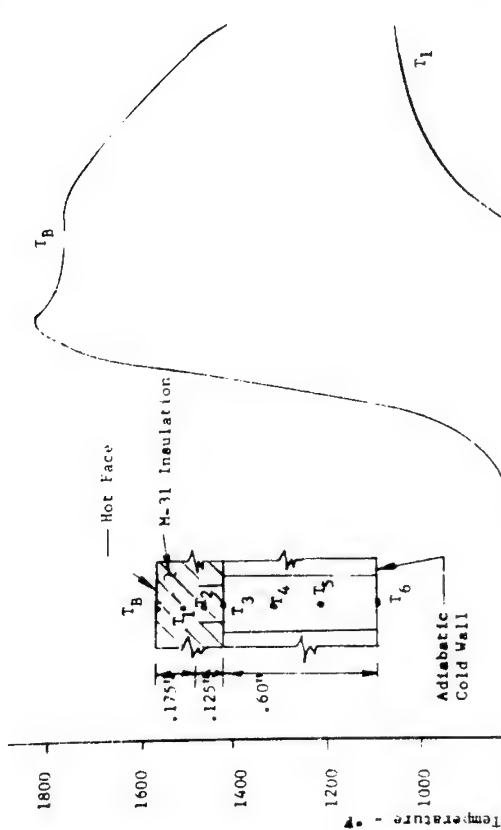
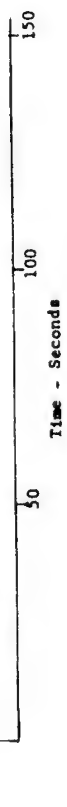
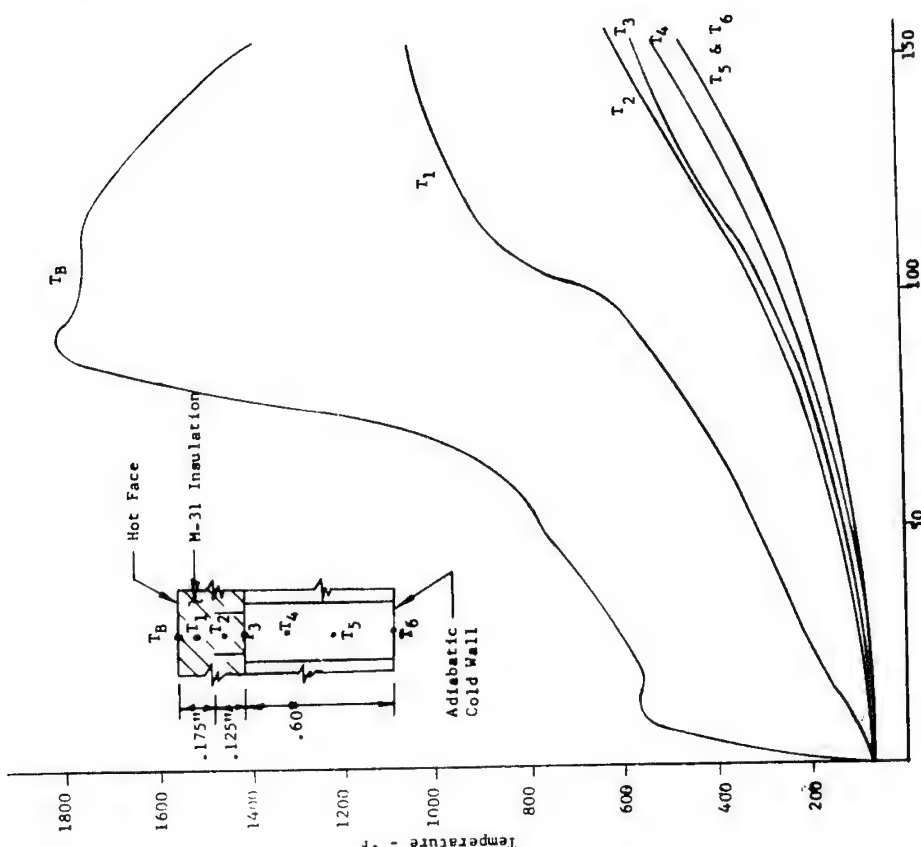


Figure 17 Temperature Profiles - Panel No. SK 60B20001
.005 Inch Node Flow Width - Cell Size 4-15
Open Core Size, 8-15

Time - Seconds

150
100
50

36



150
100
50

Time - Seconds

150
100
50

Figure 18
Temperature Profiles -- Panel Sk 60B20001
.015 Inch Node Flow Width - Cell Size 4-15
Open Core Size, R-15

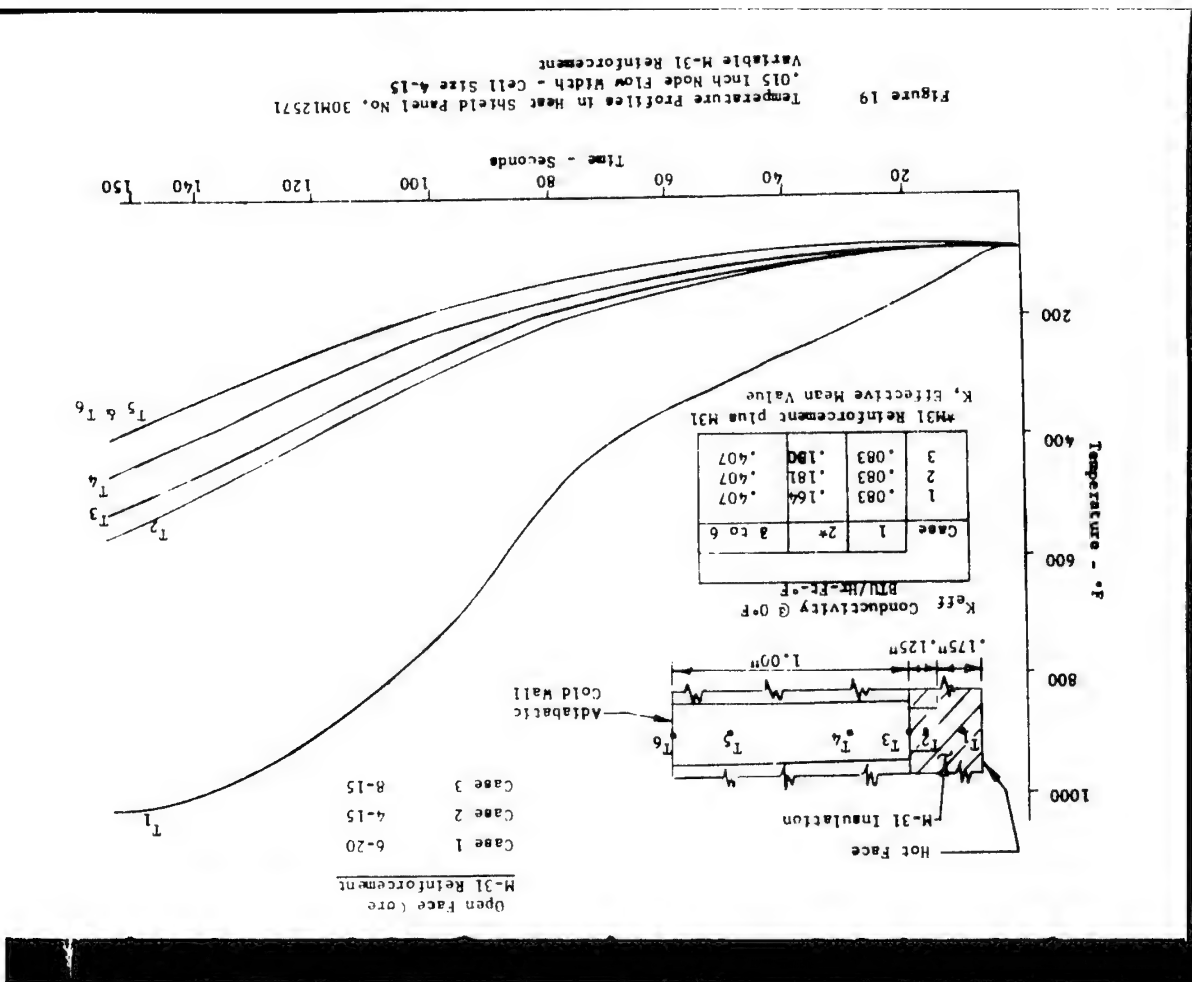
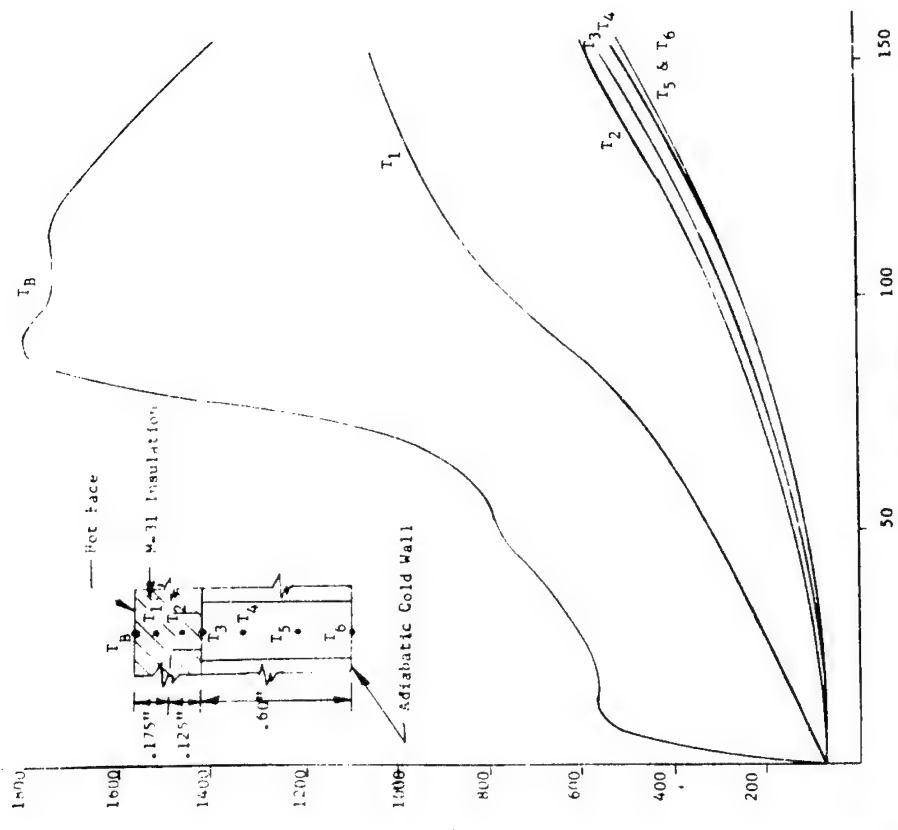
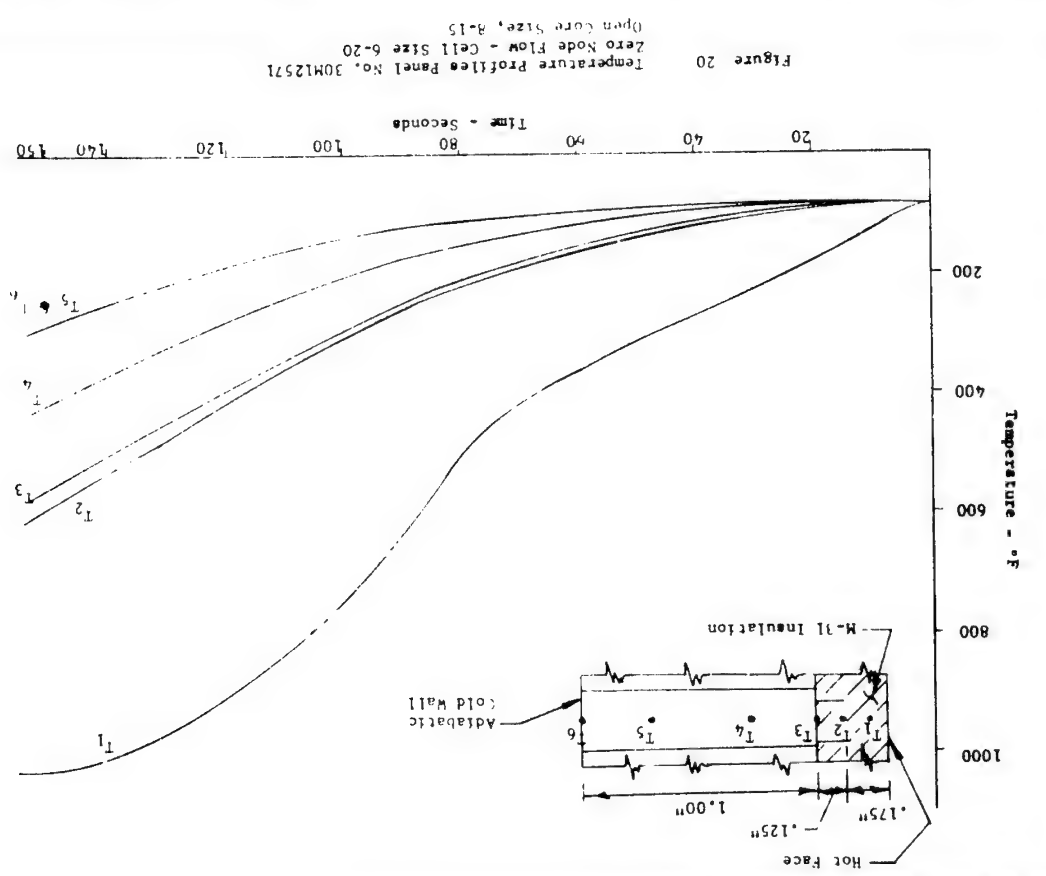
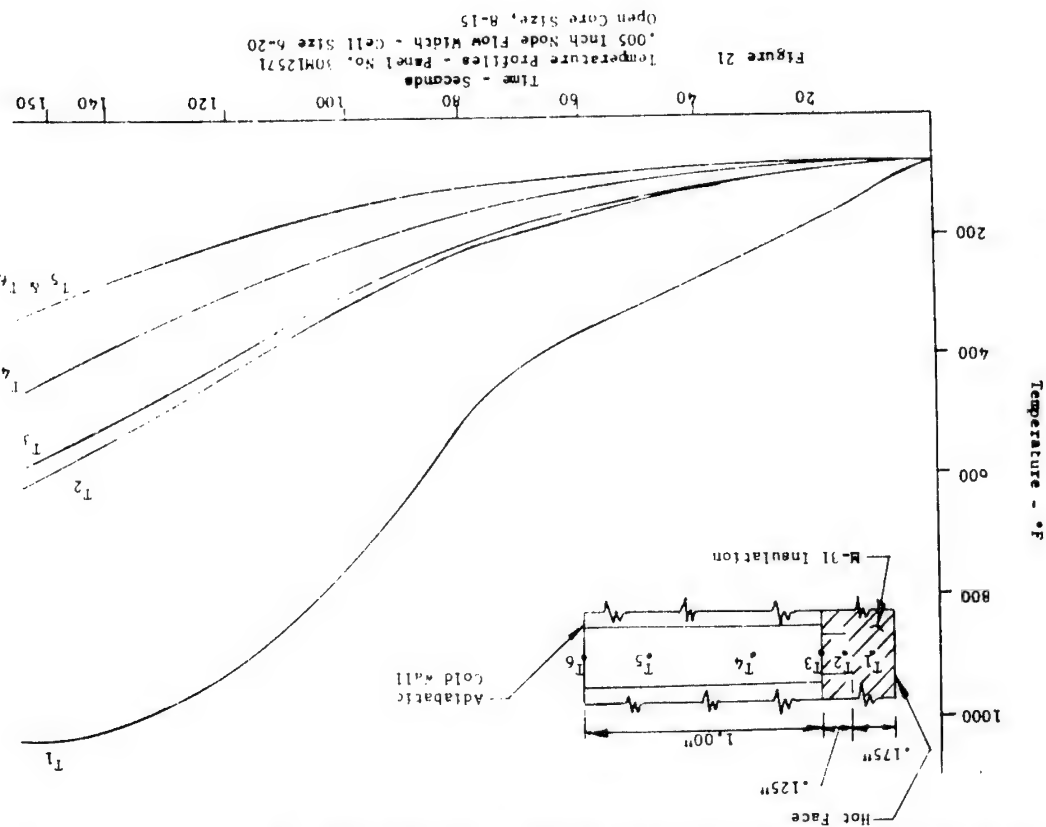


Figure 19
Temperature Profile in Heat Shield Panel No. 30H12571
.015 Inch Node Flow Width - Cell Size 4-15
Variable M-31 Retention



42

41

Figure 23 Temperature Profiles - Panel No. 30M12571
.015 Inch Node Flow Width - Cell Size 6-20
Open Core Size, 6-20

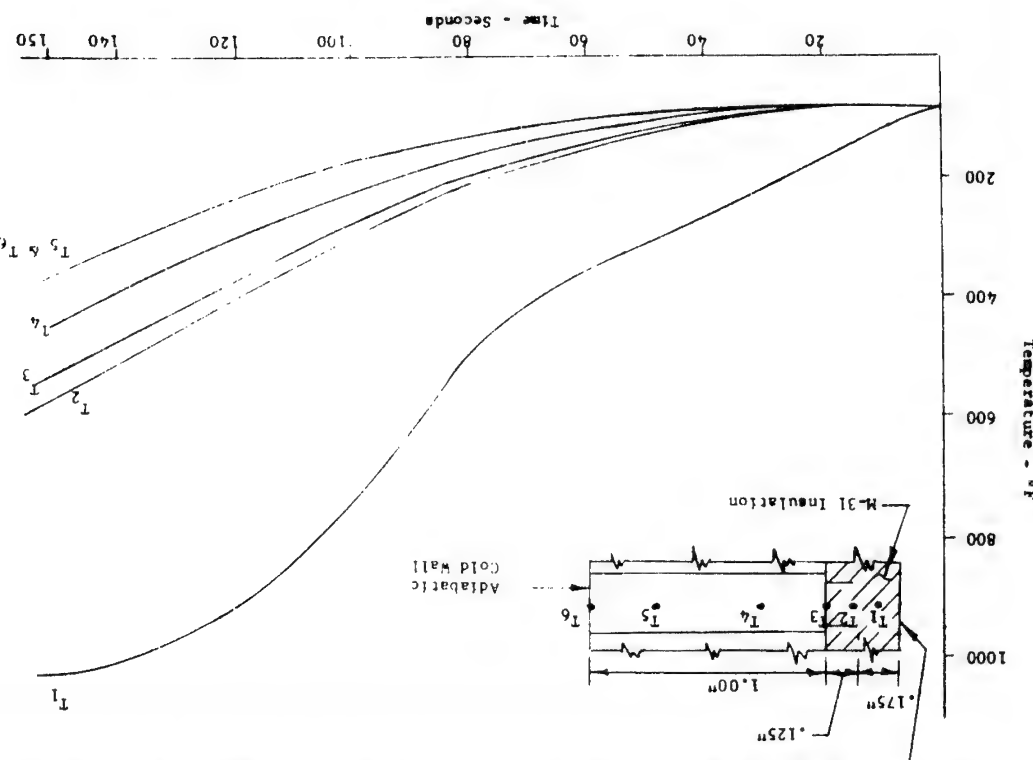
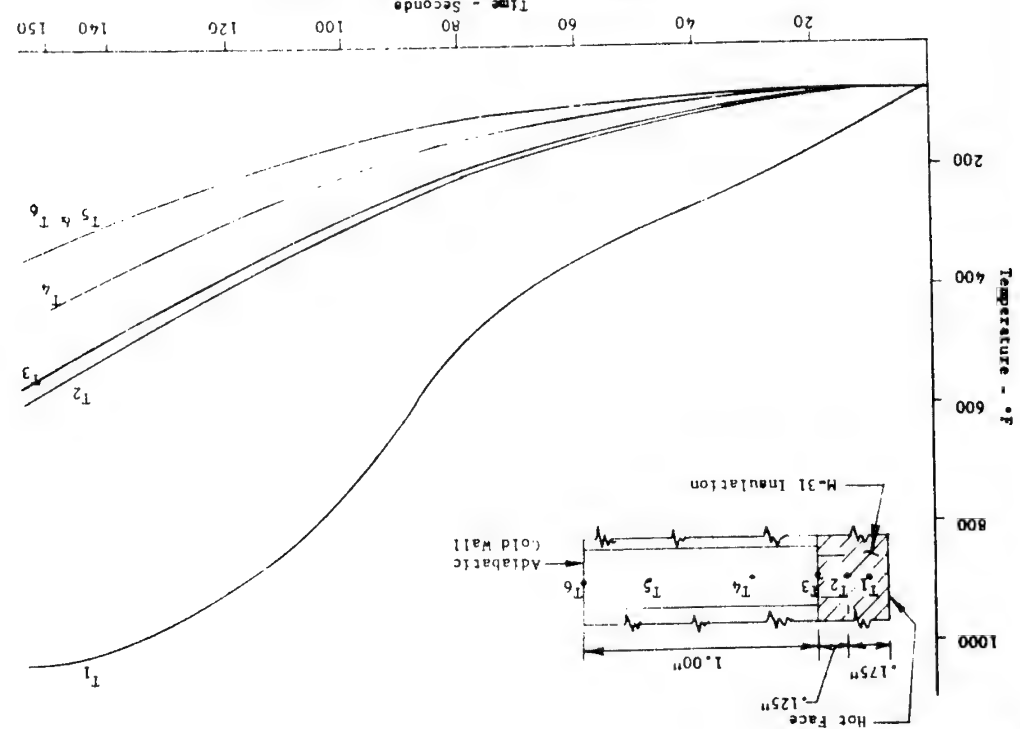


Figure 22 Temperature Profiles - Panel No. 30M12571
.010 Inch Node Flow Width - Cell Size 6-20
Open Core Size, 6-15



SECTION II

STRESS ANALYSIS FOR 5-1C HEAT SHIELD PANELS
30M12571 AND 60820210

For small deflections within the elastic range, the sandwich heat shield panels behave as homogeneous plates when the proper modulus of rigidity is used. An approximate formula for D which has been used for all calculated data is:

$$D = \frac{E_1 E_2 h_f (h_c + h_f)}{(E_1 + E_2) (1 - \nu^2)}$$

This expression assumes both facings to be of the same material and thickness, and thin compared to the height of the core.

Three panels were considered: the one panel 30M12571, $h_c = 1.0"$; the two cup panels 60820210, with $h_c = 0.6"$ and 1.0". Each panel was calculated for every reasonable combination of conditions. The results are shown in Tables 4 through 7.

Table 3 lists all the pertinent stress functions as they apply to the heat shield panels. Formulas taken from Timoshenko have had the various series in his expressions evaluated for the maximum value for a square for either the edge or center as required.

Table 4 shows the calculations for the simple support condition on the cup panel, 60820210. The most severe loading occurs at the center for the maximum ΔT and is 79,524 psi and 63,416 psi for the two thicknesses, respectively. Since the allowable for the maximum ΔT is 140,000 psi*, there is an adequate margin of safety.

Table 5 shows the fully clamped condition for the same panel. Here, the maximum stress occurs at the edge and is 97,885 psi and 81,099 psi for the two panels, respectively, at the maximum ΔT . Again, an adequate margin of safety is indicated.

It is easily recognized that in actual practice neither of the above two edge mounting conditions represent the physical picture. The panel loading imposes a stress condition on the flange and insulation both of which are elastic materials. Table 6 considers the flexibility of the panel, flange and the JM-146 insulation as a system. The per cent of edge fixity was calculated and tabulated for the various conditions for the two panels, and presented in Table 6.

* $f_{ty} = 170,000$ psi at room temperature, Ref. MIL-HDBK-5

44

43

(TYPE 6-20 Honeycomb Core)														
Node Flow Width	Node Flow Depth	Node Flow Area	Cell Area	Cell Depth	Cell Width	Cell Dimensions	Core Area	Core Effective Conductivity	Core Effective Thermal Conductivity	Core Density	Core Flow Depth	Core Node Flow Area		
.375	.002	2048	.011	.0002	.0007	.0016	5.6	.124	.43	.990	.112	.157	.237	0
.188	.0015	4096	.016	.0007	.0028	.0064	8.3	.435	1.73	3.960	.199	.387	.79	0
.25	.0015	2304	.012	.0004	.0016	.0036	6.2	.148	.99	2.23	.138	.245	.424	.00
(TYPE 4-15 Honeycomb Core)														
.188	.0015	4096	.016	.0007	.0028	.0064	8.3	.435	1.73	3.960	.199	.387	.79	0
.25	.0015	2304	.012	.0004	.0016	.0036	6.2	.148	.99	2.23	.138	.245	.424	.00
(TYPE 3-15 Honeycomb Core)														
.188	.0015	4096	.016	.0007	.0028	.0064	8.3	.435	1.73	3.960	.199	.387	.79	0
.25	.0015	2304	.012	.0004	.0016	.0036	6.2	.148	.99	2.23	.138	.245	.424	.00
(TYPE 6-15 Honeycomb Core)														
.188	.0015	4096	.016	.0007	.0028	.0064	8.3	.435	1.73	3.960	.199	.387	.79	0
.25	.0015	2304	.012	.0004	.0016	.0036	6.2	.148	.99	2.23	.138	.245	.424	.00

Table 7 utilizes the edge fixities determined in Table 6 and tabulates the stress functions for both the edge and center conditions. The results show an appreciable reduction in maximum stresses in the center and a substantial reduction in edge stresses. It is believed that this table represents a realistic resume of stresses to be expected in the 60B20210 panel. The 1.0" thick panel meets the maximum deflection criteria of 0.5" for all conditions under 280 °F. The maximum deflection of 1.41" inch at a ΔT of 450° indicates that the M-31 would be cracking and probably breaking off from vibration. Since there is now relatively good indications of appreciable cooling on the back face of the heat shield, the maximum ΔT 's are more probable for the terminal flight condition.

If the M-31 deflection values obtained for the radius of curvature at cracking deflection on these panels is about 0.8", then, it appears that the cracking would not start until the latter stages of the flight and probably would be of no actual significance.

Table 8 shows the panel calculations for the mounted 30M1251 unit 1.0" thick. The zee mounting approximates a simple support condition and all path calculations for this table are based on the assumption of ample support for the panel edges. The maximum deflection is seen to be less than that for the comparable cup panel (1.10") by about a tenth of an inch. $\Delta T = 750^{\circ}\text{F}$ for 450 °F. Thus, the danger of cracking and flaking off of the M-31 is lessened. Further, the maximum stresses are only nominally greater than the cup panel (elastic support) at maximum ΔT and less at zero ΔT . The zee mounting is better able to withstand shock than the cup panel mounting as it is essentially a cantilever spring. The damping effect of the zee mounting on vibration is sufficient whereas vibration loads add directly to the possibility of exceeding the core crushing load at the cup area on the 60B20210 panel.

Table 9 shows the calculations for the edge member for the zee type mounting of the 30M1251 panel. The h_2 shown is the thickness of the edge member and extended facing to which it is brazed during manufacture. Although the 30M1251 design called for a combined $h_2 = 0.060$ (0.050 + 0.010), it is seen that the maximum stresses do not exceed the allowable (140,000 lb/in^2 at $\Delta T = 450^{\circ}$) except for $h_2 = 0.30$ and 0.20 ". Thus, an appreciable weight saving could be effected by using an $h_2 = 0.040$ ". This thinner edge member would also increase the vibration damping effect over the present design.

All calculations in the tables are based on the following data and procedures.

The 165 db noise level was converted to an equivalent pressure of 0.72 psi. This noise loading was used (for both ignition and flight) as an equivalent moment of 102.8 inch pounds per inch. It was assumed to be uniformly distributed over the panel surface for the fully clamped condition; a maximum at the center and zero at the edge for the simply supported condition.

* Ref: NASA memorandum M-P&VE-PH 217-63, Aug. 16, 1963, Figure 5.
** Ref: S-1C Base Heat Shield Design Criteria

*Ref: NASA correspondence M-P&VE-SB 3/15/63.

45

46

NOMENCLATURE SYMBOLS AND UNITS

SUMMENCLATURE SYMBOLS AND UNITS (Cont'd)

A	Area, square inches	RT	Room Temperature
a	Panel width, inches	T	Temperature - $^{\circ}$ F
b	Panel length, inches	ΔT	Temperature difference, $^{\circ}$ F; subscript, temperature difference, $^{\circ}$ F
C	Center	V	Edge reaction force, pounds per inch
c	subscript, core	W	Deflection, inches
D	Modulus of rigidity, inch pounds	x	Axis
E	Young's Modulus, psi	y	Axis
E_m	Average of two values of Young's modulus	z	Subscript, zee edge member
E.F.	Edge Fixity	α	Temperature coefficient of expansion, in/in/ $^{\circ}$ F
F	Flange, subscript	ϵ	Strain, microinches per inch
f	Stress, psi; subscript, facing	θ	Rotation of panel edge, Radians
f_{tu}	Tensile ultimate strength, psi	$\Delta\theta$	Differential rotation of zee edge member, $\Delta\theta = \theta_1 - \theta_2$
f_y	Tensile yield strength, psi	ν	Poisson's Ratio
h	Thickness, inches; core height, inches	σ	Stress, psi
I	Moment of inertia; insulation; subscript, insulation		
K	Spring constant, in-pounds/in/in		
L	Length, inches		
M	Moment, in-pounds/in.		
$M_{\Delta\theta}$	Differential moment due to $\Delta\theta$		
P	Subscript, panel		
q	Unit pressure loading, psi; subscript, unit pressure loading, psi		
Q	Shear, lbs/in		
R	Corner reaction force, pounds; radius, inches		

47

48

49

50

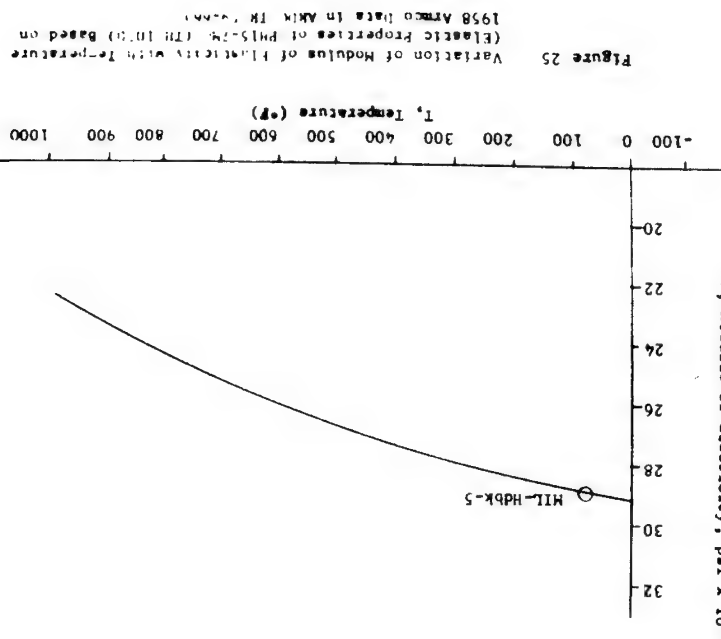
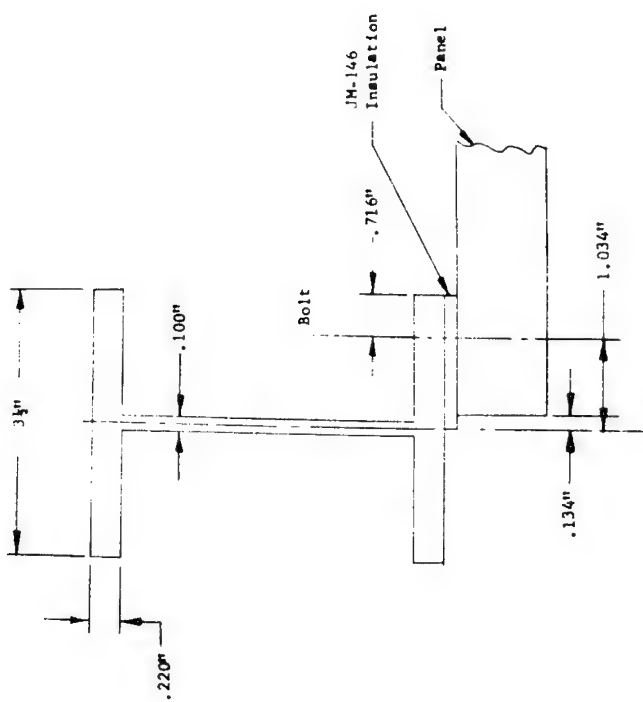


Figure 24 Mounting System for 60B20210 Panel
Showing Calculation Dimensions Only



MAXIMUM VALUES FOR 60B2020 PANEL
SIMPLY SUPPORTED EDGE CONDITION

All other formulas from S. Timoshenko, Plates & Shells, 2nd Ed., 189 q₁ = 297 q₂ = 3086 2₁ = 716₁ 2₂ = 900₁ $\int_0^L q_1 = 3086$ $q_2 = 2097$

३०

支
3

TABLE 5

6. 2008

KF = 14, 637 Ignition, 16, 667 Flight
Program, support beam flange and J-H145 insulation rotate. The spring connectors are:

K₁ = 1330.7 Ignition, 1509.7 Flight

14,637 Ignition, 16,667 Flight

Panel, support beam flange and JH-146 1

SECTION III

DESIGN PARAMETERS FOR BRAZED HONEYCOMB HEAT SHIELD PANELS
WITH SIMPLY SUPPORTED EDGES

MAXIMUM BENDING STRESSES IN E-VEE MEMBER FOR 30ft12571 PANEL, ZEE EDGE MEMBER 1.0" CORE THICKNESS						
TABLE 9						
Ignition Condition						
q_p	$h_z = .060$	$h_z = .050$	$h_z = .045$	$h_z = .040$	$h_z = .030$	$h_z = .020$
l_z	18-6	10.42-6	7.59-6	5.34-6	2.25-6	0.666-6
q_p	.0254	.0503	.0870	.1192	.1694	.4022
$\Delta\theta$		-.0249	-.0616	-.0938	-.1440	1.3580
H_q	52.58	52.58	52.58	52.58	52.58	52.58
$H_{\Delta\theta}$	13.58	19.45	21.57	23.30	25.70	26.90
H_{total}	39.01	33.13	31.01	24.28	26.88	25.68
S_2	65,000	79,486	91,927	109,663	179,200	385,200
Flight Condition						
q_p	.0203	.0363	.0510	.0708	.1680	.5670
h_z	21.23	21.23	21.23	21.23	21.23	21.23
H_q	.0103	-.0100	-.0260	-.0407	-.0605	-.1577
$\Delta\theta-0^\circ\Delta T$.0268	+.0065	-.0095	-.0242	-.0440	-.1412
180°						-.5402
280°						-.5310
320°						-.5273
340°						-.5154
450°						
$H_{\Delta\theta-0^\circ\Delta T}$						
180°	-5.45	-8.21	-9.36	-9.79	-10.75	-11.25
280°	+3.54	+3.00	+5.59	+7.12	+9.63	+10.91
320°	8.56	-0.09	-3.45	-5.63	-9.00	-10.93
340°	10.58	+1.07	-2.60	-5.03	-8.75	*10.65
450°	17.07	4.83	+0.14	-3.11	-7.94	-10.41
$H_{\Delta\theta-0^\circ\Delta T}$						
180°	15.78	13.02	11.87	11.44	10.48	9.98
280°	24.77	18.23	15.66	14.11	11.60	10.32
320°	29.79	21.14	17.78	15.60	12.23	10.50
450°	31.81	22.30	16.63	16.20	12.48	10.58
S_2	38.30	26.06	21.37	18.12	13.29	10.82
$\Delta\theta-0^\circ\Delta T$						
180°	26,289	31,235	35,183	+2,343	69,860	149,700
280°	41,267	43,754	46,416	52,842	77,326	154,800
320°	49,630	50,715	52,700	58,222	81,525	159,500
450°	52,995	53,498	55,219	60,669	83,192	158,700
S_2	63,808	62,518	63,341	67,859	88,591	162,300

NOTE: The value of the moment arm z used for the zee calculations was 0.957", the distance from center line of mounting hole to the vertical leg of the zee.

57

58

60

59

Thermal Deflection $\sim W$ in Inches

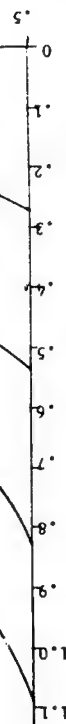


FIGURE 27 Thermal Deflection at Center of Panel W_s , Height of Panel

for constant Temperature Differences
Height of Panel ($E + 2E$) in Inches

0.5

0.6

0.7

0.8

0.9

1.0

1.1

1.2

1.3

1.4

1.5

1.6

1.7

1.8

1.9

2.0

$\Delta T = 100^\circ F$

$\Delta T = 200^\circ F$

$\Delta T = 300^\circ F$

$\Delta T = 400^\circ F$

$\alpha = .30$

$q = 6.1 \times 10^{-6}$

Panel Size 48.4" x 48.4"

Deflection $\sim W$ in Inches
Air Load Only

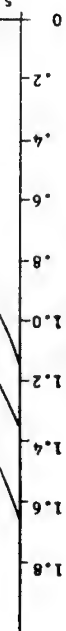


FIGURE 26 Deflection at Center of Panel W_s , Core Thickness

Deflection at Center of Panel W_s , Core Thickness

0

.5

.6

.7

.8

.9

1.0

1.1

1.2

1.3

1.4

1.5

1.6

1.7

1.8

0

.2

.4

.6

.8

1.0

1.2

1.4

1.6

1.8

Constant Face Thickness $\sim c'$

Core Thickness $\sim c$ in Inches

Core Thickness $\sim c$ in Inches

Deflection $\sim W$ in Inches

Air Load $q = 2.7 \text{ psf}$

$c' = .008 \text{ in}$

$c' = .010 \text{ in}$

$c' = .012 \text{ in}$

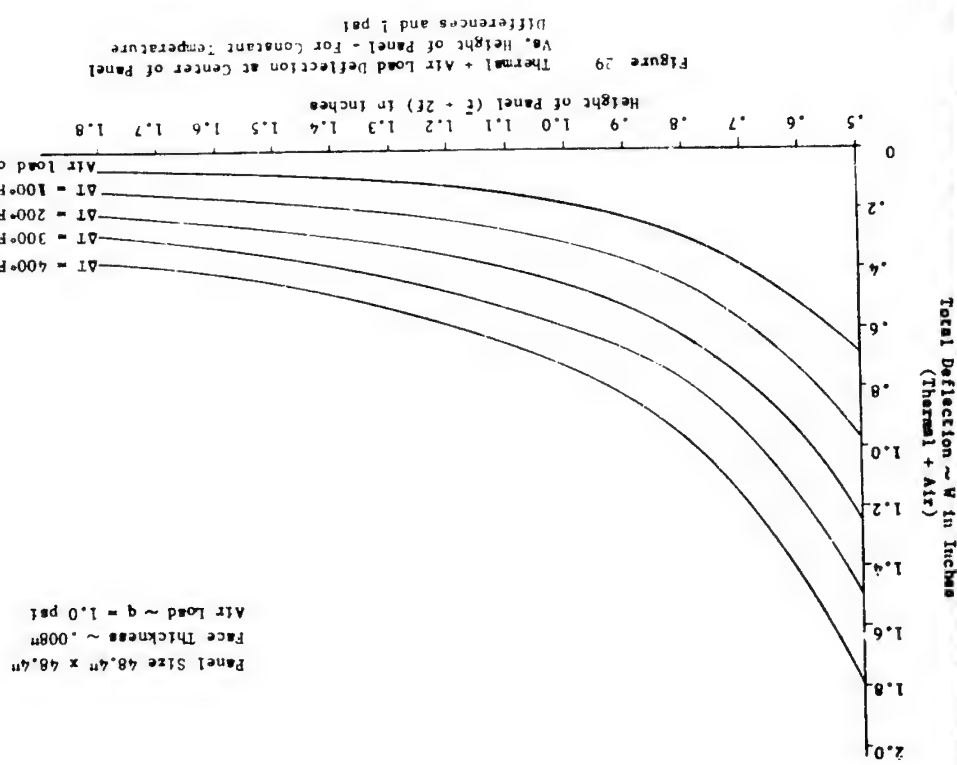
$c = .012 \text{ in}$

$c = .010 \text{ in}$

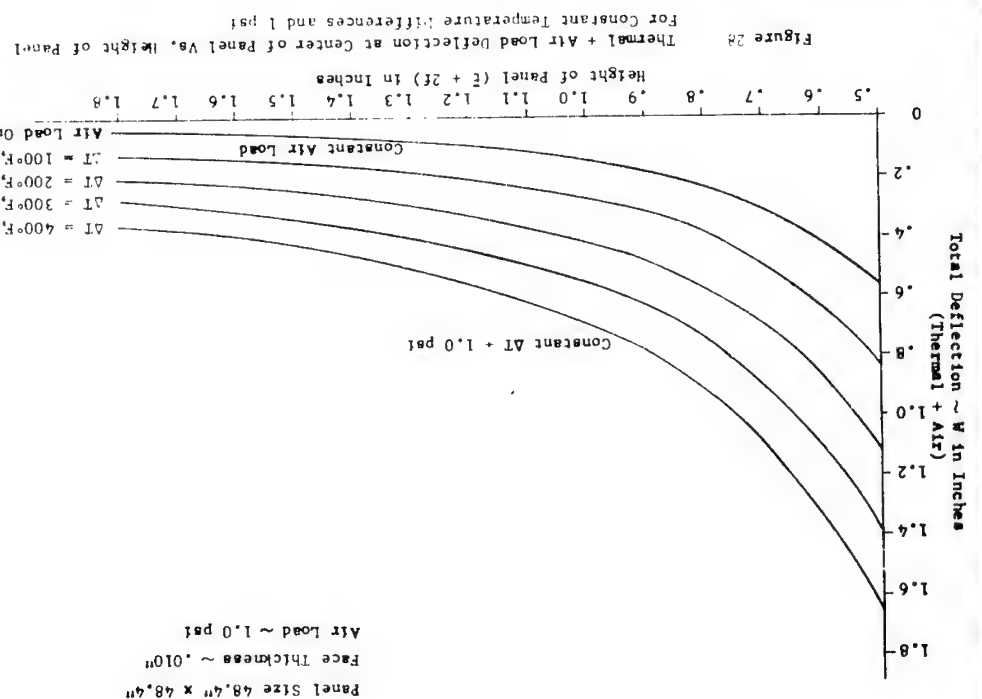
$c = .008 \text{ in}$

$c = .00$

62



61



SECTION IV

APPLICATION OF BERYLLIUM TO HEAT SHIELD PANELS

Preliminary Analysis of Zee Section Edge Member Heat Shield Panel with Beryllium Facings and Edge Members

The use of cross rolled beryllium sheet components for facings and edge members were evaluated for potential heat shield panel application using the JOM12571 panel design as a basis.

Panel stresses, deflections and margins for the ignition and flight conditions are given in Table 10. The critical item from a stress view point is the relatively high stress in the zee section edge member which would require a minimum thickness of .08".

The allowables for silver brazed beryllium sheet employed were:

$$f_{t_u} = 50,000 \text{ psi}$$

$$f_{t_y} = 35,000 \text{ psi}$$

$$\% \text{ Elongation} = 1.21\%$$

and reflect our experience in beryllium brazing and fabrication*. These values for .04" gauge material are substantially less than the allowables for unbrazed beryllium sheet, which presently are:

$$f_{t_u} = 70,000 \text{ psi}$$

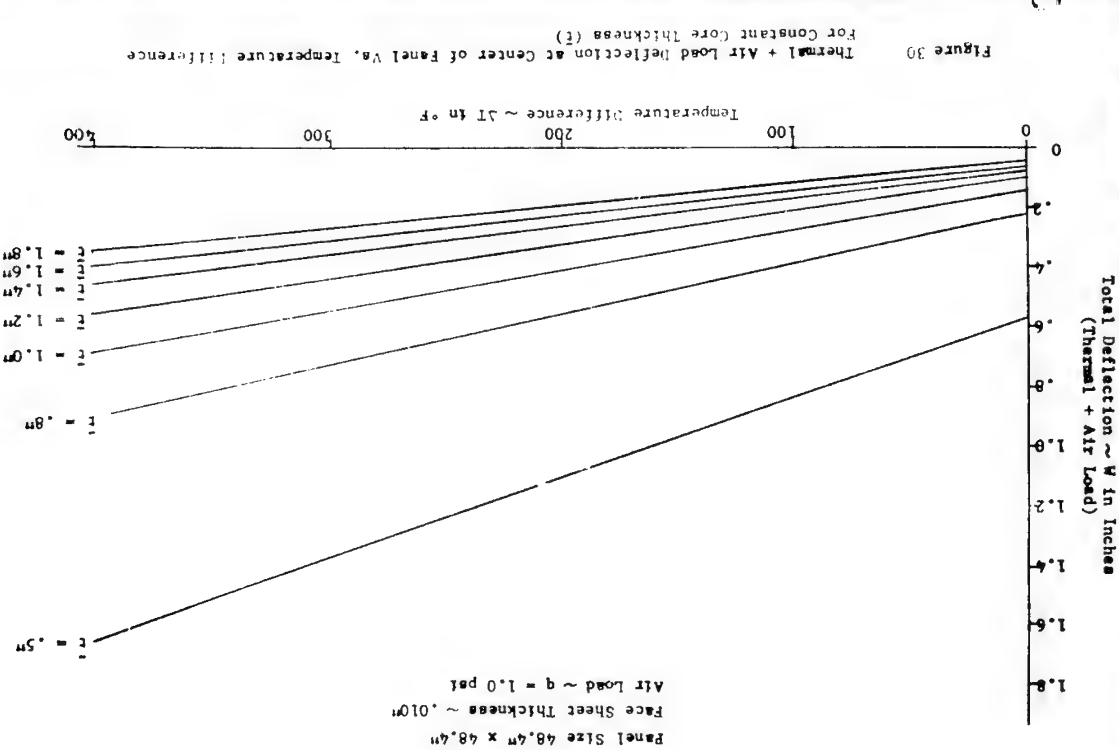
$$f_{t_y} = 50,000 \text{ psi}$$

$$\% \text{ Elongation} = 5\%$$

The reduction in strength and loss of ductility results principally from the reaction between the beryllium and the silver brazing alloy (99.5Ag-5Li) and cannot be eliminated or further minimized with presently available brazing methods or brazing alloys within the current state of art. Current studies being conducted at Aeroneca are aimed at the development of low melting braze alloys for beryllium. A reduction of braze temperatures below recrystallization and diffusion temperatures would overcome many of the problems which cause embrittlement and loss of strength. The braze alloy compositions which show the greatest promise in this regard would either be zinc base or aluminum base with zinc additions.

*Contract AF 33(657)-715;
Sheet Beryllium Composite Structures

53



63

64

Other characteristics of beryllium which make it undesirable for braze heat shield panels are:

1. The high modulus, 43,000,000 psi, while desirable for stiffness is undesirable for thermal loads which produce a high thermal moment. The high moment along with the relatively low strength of beryllium soon produces stresses comparable to the yield or ultimate of the material.
2. The highly directional tensile properties of beryllium sheet, with low ductility in the short transverse direction, results in sharply limited and unpredictable capacity to accept multi-axial loads without catastrophic failure. Consequently, an extensive test program would be required to support a production design.
3. The maximum width sheet at present is 36" which would require a load-carrying splice. The poor welding characteristics of beryllium and erratic joint properties preclude the use of fusion welding; consequently, the facing sheet splices would have to be accomplished during the panel braising and would consist of a butt joined sheet with a braised on doubler reinforcement. For the open faced core side of the panel, the reinforcing doubler would probably have to be located in a ribbed machined in the load bearing honeycomb core (at increased cost).
4. The susceptibility of beryllium sheet in the large sizes required and in edges less than .04" to breakage during shop handling imposes additional fabrication problems.
5. An experimental program to determine the material allowances for braised beryllium sheet for a range of thicknesses would be required as well as an optimum braising cycle for beryllium panels of this size (53" x 53").

As a consequence of the foregoing considerations, the use of beryllium sheet is not recommended for braze, honeycomb sandwich heat shield panels within the present state of art.

Preliminary Analysis of Heat Shield Panel with Beryllium Facings and Cup Type Edge Attachments per drawing 60B20210

The use of cross rolled beryllium sheet facings was evaluated for potential use in the cup type edge heat shield panel design shown in NASA drawing No. 60B20210 based on the following assumptions:

1. A facing edge of .030" beryllium sheet, load bearing core Type 4-15 PH 15-7 Mo 1.0" thick

2. Allowables for braze beryllium sheet using a braze alloy of choice
Silver with 0.5% lithium.

$$f_{t_u} = 50,000 \text{ psi}$$

$$f_{t_y} = 35,000 \text{ psi}$$

$$\% \text{ Elongation in } 2^{\text{in}} = 1.24\%$$

$$E = 43 \times 10^6 \text{ psi at R.T.}$$

$$E = 37 \times 10^6 \text{ psi at } 600^{\circ}\text{F}$$

$$v = 0.1$$

Panel stresses, deflections and margins were calculated for the flight conditions at four levels of edge fixity and are given in Tables 1 and 13. The compressive stresses in the honeycomb core area under the cup flange were also calculated for the same loading conditions and three levels of edge fixity (Tables 14 and 15).

Based on any degree of edge fixity and 180° AT representative of the 100% node flow condition this panel design shows positive margins for .030" beryllium sheet facings. As the thermal gradient increases, the margins decrease rapidly as shown in Table 13 for a 320°F AT representative of the zero node flow condition; however, small positive margins exist for most of the edge fixity conditions. Consequently, the use of beryllium facings of cross rolled beryllium sheet .030" thick appear feasible from a stress viewpoint for this panel design. However, the use of beryllium sheet facings in this application is subject to the same qualifications (Items 1 thru 5) previously noted and is not considered to be a suitable material for braze honeycomb sandwich heat shield panels.

Compression load on insulation (RH-146)

$$\frac{P}{A} = \frac{M}{G \cdot r \cdot v} = \frac{16}{.6 \times .9 \times 1} = 30 \text{ psi}$$

Simply Supported Edge Condition

$$W_A = \frac{.00006 \times 1.0 \times 50.9784}{624,018} = .00447$$

$$W_T = \frac{.01T(1+\frac{1}{3})44.25708}{n \cdot h} = \frac{6.0110-6 \times 18021.1 \times 4 \times 50.9784 \times .5708}{32,86654}$$

$$W_T = .2147$$

$$W_{TOTAL} = .2587$$

70

Code: PH15-TM0 Material

CY 35,000 psi

CU 50,000 psi

(Facility) Material: Beryllium, Room Temperature, After Brazing

Moment is normal to panel surface.

M.S. based on a load factor of 1.1 and yield strength.

* Beam flanges, flange insulation and panel rotate.

Edge Fixity	Deflection W (inches)	Deflection M (in-lb)	Bearing Stress f_b (psi)	Margin of Safety	M. S.
0%	0.475	828C	26,796C	+0.19	
*2.514%	0.464	807C	1091E	-0.10	+Very Large
34.91%	0.319	539C	26,117C	+0.22	
100%	0.027	1530E	17,282E	+0.84	

Load Condition - Flange 10 psi after load + 1.15 psi dynamic (C.15 psi) plus 320° AT

OF THE 60B20210 PANEL DESIGN WITH BERYLLIUM FACINGS
DEFLECTION AND STRESS CHARACTERISTICS

TABLE 13

69

Code: PH15-TM0 Material

CY 35,000 psi

CU 50,000 psi

(Facility) Material: Beryllium, Room Temperature, After Brazing

Moment is normal to panel surface.

M.S. based on a load factor of 1.1 and yield strength.

* Beam flanges, flange insulation and panel rotate.

Edge Fixity	Deflection W (inches)	Deflection M (in-lb)	Bearing Stress f_b (psi)	Margin of Safety	M. S.
0%	0.258C	439C	14,207	+1.24	+0.56
*1.927	0.253C	431C	13,948	+1.28	+0.59
94.91	0.172	286C	13,236	+1.40	+2.44
100%	.012	832E	26,926E	+0.18	

Load Condition - Flange 10 psi + 180° AT

OF THE 60B20210 PANEL DESIGN WITH BERYLLIUM FACINGS
DEFLECTION AND STRESS CHARACTERISTICS

TABLE 12

2

2

COHPRESSIVE STRESSES IN HOLLOW CIRCULAR PANELS FOR DESIGN

CALE 15

60

1. Edge Fixity	Core	Compressive Stress	in core area under edge fixity	100% beam flange. (PH15-70M Meterial)	7,371 psi	Panel and flange insultal action rigid	1,0.0 psi + 180° LT (100% node allow)
2. Fixing Condition	Core	Compressive Stress	in core area under fixing condition	100% beam flange. (PH15-70M Meterial)	7,371 psi	Panel and flange insultal action rigid	1,0.0 psi + 180° LT (100% node allow)
3. RT-760 Test	600° - 675 psi	340° - 722 psi	for Type 4-15	Core, Ref. NAA	2,570 psi	Panel and flange insultal action rigid	34.91% beam flange and Manual
4. RT-760 Meterial	600° - 675 psi	340° - 722 psi	for Type 4-15	Core, Ref. NAA	2,570 psi	Panel and flange insultal action rigid	1. 97% beam flange
5. Structural Design	600° - 675 psi	340° - 722 psi	for Type 4-15	Core, Ref. NAA	142 psi	Panel and flange insultal action rigid	rotate

$$M_A = .0479 q a^2 = .0479 \times 1.0 \times \frac{55.978^2}{1.06} = 124.68 \text{ in-lbs/in at center of panel}$$

$$M_T = \frac{2 M(1-q^2)D}{h} = \frac{180 \times 1.0 \times 10^{-6} \times .89 \times 624.018}{1.06} = 629.43 \text{ in-lbs/in at edge of panel}$$

Clamped Edge Condition

$$W_T = 0$$

$$W_A = \frac{.0137 \times q \times a^4}{12 \times D(1-q^2)} = \frac{.0137 \times 1.0 \times 50.978^4}{12 \times 624.018 \times .99} = .012"$$

$$M_A = .0513 q a^2 = .0513 \times 1.0 \times \frac{50.978^2}{1.06} = 133 \text{ in-lbs/in at edge of panel}$$

$$M_T = \frac{2 \Delta T D (1-q^2)}{h} = \frac{6.0 \times 10^{-5} \times 180 \times 624.018 \times 1.0}{1.06} = 699 \text{ in-lbs/in at edge of panel}$$

$$M_{\text{total}} = 832 \text{ in-lbs/in at edge}$$

Then the edge moment of panel with 34.91% fixity is:

$$M = 832 \times .3491 = 290 \text{ in-lbs/in.}$$

Load reacted by cup:

$$P = \frac{290 \times 7.463}{.9} = 24.05 \text{ lbs/cup}$$

Compression load on panel core:

$$\frac{2405}{.93593} = \underline{\underline{2570 \text{ psi}}}$$

Assume rotation of panel, flange and insulation

Use $K_c = .0066 \text{ lb/in-in}^2$ (25-50 psi)

$$C = .60^{\circ}$$

$$K_1 = \frac{C k A^2}{2} = \frac{.6 \times 3086 \times .9^2}{2} = 750 \text{ in-lbs/in/Rad.}$$

$$K_p = 30.753 \text{ in-lbs/in/Radian}$$

$$K_F = 19.11 \text{ in-lbs/in/Radian}$$

$$K_1 = .0066 \text{ in-lbs/in/Radian}$$

$$\text{Edge Fixity} = \frac{36.753}{750} \cdot \frac{1}{19.711} = \frac{1}{51.759} = 1.927.$$

$$M = K_1 \times .01927 = 15 \text{ in-lbs/in}$$

Load reacted by cup:

$$P = \frac{16}{9} \times \frac{7.463}{.9} = 133 \text{ lbs/cup}$$

compression load on panel core:

$$\frac{133}{.93593} = 142.151$$

Detail calculation

⁽¹⁾ 30% servilium factor and blight condition: $1 \sim 10^6 \times q = 1.0 \text{ psi}$
panel 50.928" $\underline{\underline{L}}$ of fasteners.

$$f_{t,y} = 35,000 \text{ psi}$$

$$f_{t,u} = 50,000 \text{ psi}$$

$$\alpha = 6.0 \times 10^{-6} \text{ (R=500)}$$

$$E = 4.3 \times 10^6 \text{ RT psi}$$

$$E = 37 \times 10^6 \text{ 6000°F psi}$$

$$\nu = .1$$

$$H = .94736 \text{ in-lbs/in}$$

$$D = \left[\frac{1.0372}{1.04736} \right] \left[\frac{37.8 \times 10^6 \times .030}{1 - \nu^2} \right]$$

$$D = 624,018 \text{ in/lb.}$$

Assume no rotation:

$$M_T = \frac{6.0 \times 10^{-6} \times 1.30 \times 624,018}{1.06} (1.1) = 699 \text{ in-lbs/in}$$

$$M_A = .0513 \times 1.0 \times \frac{50.978^2}{50.978} = 133 \text{ in-lbs/in}$$

$$M_{\text{total}} = 832 \text{ in-lbs/in}$$

Load reacted at cup:

$$P = \frac{832 \times 7.463}{.9} = 6,895 \text{ lbs/cup}$$

Compression load on panel core:

$$\frac{6899}{19,711} = 7,371 \text{ lb/in}^2$$

Assume the insulation to be incompressible and allow the flange and panel rotate.

Assume the spring rate of the panel is the average of the pressure and thermal condition.

Thermal

$$K_p = \frac{M_{\text{clamp}}}{\theta_{\text{Free}}} = \frac{\alpha \Delta T \cdot 0.1 \times 2}{h \cdot a \cdot \Delta T} = \frac{2D(1+\alpha)}{a}$$

$$K_p = \frac{2 \times 624,018 \times 1.1}{50.978} = 26,930 \text{ in-lbs/in/Radian}$$

Pressure

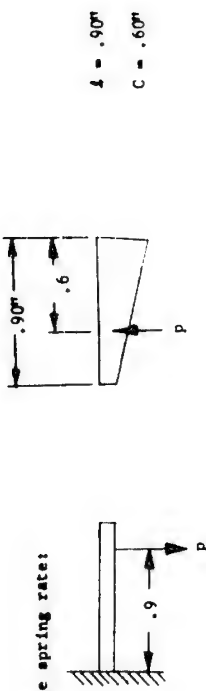
$$K_p = \frac{M_{\text{clamp}}}{\theta_{\text{S.S.}}} = \frac{0.013 \times \pi^4 \times D}{1.31330 \times 50.978} = \frac{.0513 \times \pi^4 \times 624,018}{1.31330 \times 50.978}$$

$$K_p = 46,576 \text{ in-lb/in/Radian}$$

Use average spring rate:

$$K_p = \frac{46,576 + 26,930}{2} = 36,753 \text{ in-lb/in/Radian}$$

Flange spring rate:



$$A = .90^2$$

$$C = .60^2$$

$$M_T = \frac{M}{\theta_F} = \frac{M \cdot 2EI}{M} = \frac{2 \times 10 \times 10^6 \times 687 \times 10^{-6}}{.9} = 19,711 \text{ in-lb/in. Rad.}$$

$$E.F. = \frac{\theta_p}{\theta_{\text{total}}} = \frac{\theta_p \left(\frac{K_p}{K_F} + 1 \right)}{\theta_p + 1} = \frac{\frac{1}{K_p} + 1}{\frac{1}{K_F} + 1}$$

$$E.F. = \frac{1}{\frac{16,753}{19,711} + 1} = \frac{1}{2.86459} = 34.91\%$$

Flight Condition:

$$q = 2.15$$

$$\Delta T = 320^\circ F$$

.030 Beryllium Facing

Panel size 50.978 in. of bolts

$$D = 624,018$$

Assume no rotation:

$$M_T = \frac{6.0 \times 10^{-6} \times 320 \times 624,018 \times 1.1}{1.06} = 1243 \text{ in-lbs/in}$$

$$M_A = .0513 \times 2.15 \times \frac{50.978^2}{.9} = 286 \text{ in-lbs/in.}$$

$$M_{\text{total}} = 1529 \text{ in-lbs/in}$$

$$\text{Load reacted at cup:} \\ P = \frac{1529 \times 7.463}{.9} = 12,679 \text{ lbs/cup}$$

63

64

75

76

Compression load on panel core:

$$\frac{12,679}{.93593} = 13,547 \text{ lb/in}^2$$

Assume the insulation to be incompressible and allow the flange and panel to rotate.

Assume the spring rate of the panel is the average of the pressure and thermal condition.

Thermal

$$K_p = \frac{M}{\theta} = \frac{2D(1+\mu)}{a}$$

$$K_p = \frac{2 \times 624,018 \times 1.1}{50,978} = 26,930 \text{ in-lb/in/Radian}$$

Flange

$$K_p = \frac{.0513 \times \pi^4 \times 624,018}{1.31330 \times 50,978} = 46,576 \text{ in-lb/in/Radian.}$$

$$\text{Average: } K_p = \frac{46,576 + 26,930}{2} = 36,753 \text{ in-lb/in/Radian}$$

Flange spring rate:

$$K_F = 19,711 \text{ in-lb/in/Radian}$$

$$E.F. = 34.91\% \text{ same as above (page 65)}$$

Then the edge moment of panel with 34.91% fixity is:

$$M = 1529 \times 34.91\% = 534 \text{ in-lb/in.}$$

Load reacted by cup:

$$P = \frac{536 \times 7,463}{.9} = 4,428 \text{ lbs/cup}$$

Compression load on panel core:

$$\frac{4428}{.93593} = 4,731 \text{ psi}$$

Assume rotation of panel, flange, and insulation.

$$\text{Use } K = 4098 \quad (50-75 \text{ psi}) \text{ Ref.}$$

$$C = .6\pi \quad \theta = .9\pi$$

$$K_I = \frac{CK\theta^2}{2} = \frac{.6 \times 4098 \times .9^2}{2} = 996 \text{ in-lb/in Radians}$$

$$K_p = 36,753 \text{ in-lb/in. Radians}$$

$$K_F = 19,711 \text{ in-lb/in. Radians}$$

$$K_I = 996 \text{ in-lb/in. Radians}$$

$$\text{E.F.} = \frac{36,753}{996} + \frac{36,753}{19,711} = \frac{1}{39,76519} = 2.5147$$

$$M = 1529 \times .02514 = 38.4 \text{ in-lb/in.}$$

Load reacted by cup:

$$P = \frac{38.4 \times 7,463}{.9} = 318 \text{ lbs/cup}$$

Compression load on panel core:

$$\frac{318}{.93593} = 340 \text{ psi}$$

Compression load on insulation (JM-146)

$$\frac{P}{A} = \frac{M}{C \cdot \theta \cdot W} = \frac{38.4}{.6 \times .9 \times 1} = 71 \text{ psi}$$

which is within the limits (50-75 psi) assumed above.

Simply Supported Edge Condition:

$$q = 2.15 \text{ psi} \quad \Delta T = 320^\circ \text{F}$$
$$W_A = \frac{.02406 \times 2.15 \times 50.978^4}{624,018} = .094\pi$$
$$W_T = \frac{\alpha \Delta T (1+\nu)}{\pi^3} \frac{4\pi^2}{h} = \frac{6.0 \times 10^{-6} \times 320 \times 1.1 \times 4 \times 50.978^2 \times .5708}{32,86654}$$
$$W_T = .381\pi$$
$$W_{\text{total}} = .475\pi$$

77

78

$$M_A = 0.0479 q a^2 = 0.0479 \times 2.15 \times \frac{50.978^2}{1000} = 268 \text{ in-lb/in center of panel}$$

$$M_T = \frac{\alpha \Delta T (1-\beta^2) D}{h} = \frac{6.0 \times 10^{-6} \times 99 \times 320 \times 624,018}{1.06} = 1119 \text{ in-lb/in at edge of panel.}$$

Clamped Edge Condition:

$$q = 2, 1, \text{ per}$$

$$\Delta T = 120^\circ F$$

$$w_T = 0$$

$$M_A = \frac{0.0137 \times 2.15 \times \frac{50.978^2}{1000}}{1.2 \times 624,018 \times .99} = .0277 \text{ in-lb/in}$$

$$M_A = .0513 \times 2.15 \times \frac{50.978^2}{1000} = 287 \text{ in-lb. edge}$$

$$M_T = \frac{6.0 \times 10^{-6} \times 320 \times 624,018 \times 1.1}{1.06} = 1243 \text{ in-lb. edge}$$

$$M_{\text{total}} = 1530 \text{ in-lb/in.}$$

Preliminary Design Considerations for Beryllium Faced Honeycomb Heat Shield Panels

Based on the previously indicated feasibility of using beryllium facings for the cup type edge design heat shield panel, and assuming that none of the previously described undesirable characteristics of beryllium sheet is applicable, the following design considerations are recommended.

Using the cup type edge design, per drawing 60820210, with the changes noted below:

1. 0.03" beryllium facings
2. Cup 0.063" Ti-13V-11Cr-3Al

The weight reduction would be 5.69 lbs., or 9.2%, compared with the all-stainless steel configuration having a calculated weight per drawing of 61.75 lbs.

Cost Considerations for Beryllium Faced Heat Shield Panels

The principal item of additional cost in a brazed honeycomb sandwich heat shield panel with beryllium facings for the 60820210 design compared with the all-stainless steel design is the material cost for the beryllium sheet since the fabricating and/or brazing operations are essentially unchanged. The experience factor of considerable importance in handling and fabricating beryllium is also significant but is not readily determinable from a cost viewpoint and will not be evaluated.

The material cost of the 0.03" thick cross rolled beryllium sheet for one (1) heat shield panel per 60820210 drawing is \$3677 (Table 16). This compares with a cost of \$240 for two (2) 0.01" x 52" x 56" PH 15-7 Mo facings having one fusion weld splice, roll planished and radiographically inspected.

79

80

SECTION V

DEFLECTION CHARACTERISTICS OF M-31 INSULATION
WITH STAINLESS STEEL HONEYCOMBS REINFORCEMENT

An important consideration in the use of ceramic materials for heat shield panel applications is the deflection allowable; i.e., the amount of bending the composite panel can withstand before failure of the ceramic occurs from the resultant tensile stresses. The deflection characteristics of M-31 were recently determined by Aerones as part of the S-1B heat shield panel program (Contract NAS8-4016) and are included as pertinent design information.

The test arrangement employed, shown in Figures 1 and 12, utilized a 3x15" specimen with two point loading. Specimen configuration was a 1.02" thick load bearing panel with 0.250" thick S-15 open faced core deformed to about 0.2" in height. M-31 thickness was 0.3". The test data is given in Table 17.

The radius of curvature for the deflection at which failure occurred may be calculated by

$$R = \frac{(C/2)^2}{2H} \quad \text{where } C = \text{chord length}$$

H = deflection

$$R = \frac{(7/2)^2}{.029} = 418 \text{ inches}$$

For the 30M12571 panel using the 4" deflection allowable, the corresponding radius of curvature is:

$$R = \frac{(48.3/2)^2}{1} = 583 \text{ inches}$$

Therefore, the safety factor with regard to the deflection produced cracking of the M-31 is approximately 583/418 or 1.38.

The requirement for deformed honeycomb core to insure adherence of the M-31 insulation was established by the NASA S-1C Heat Shield Panel Test Program. These tests showed conclusively that deformation of the open faced honeycomb core was necessary to prevent separation of the M-31 under a simulated S-1C acoustic and thermal environment.

Note: The doubler strips are required for the brazed facing sheet splice accomplishment during the panel brazing.

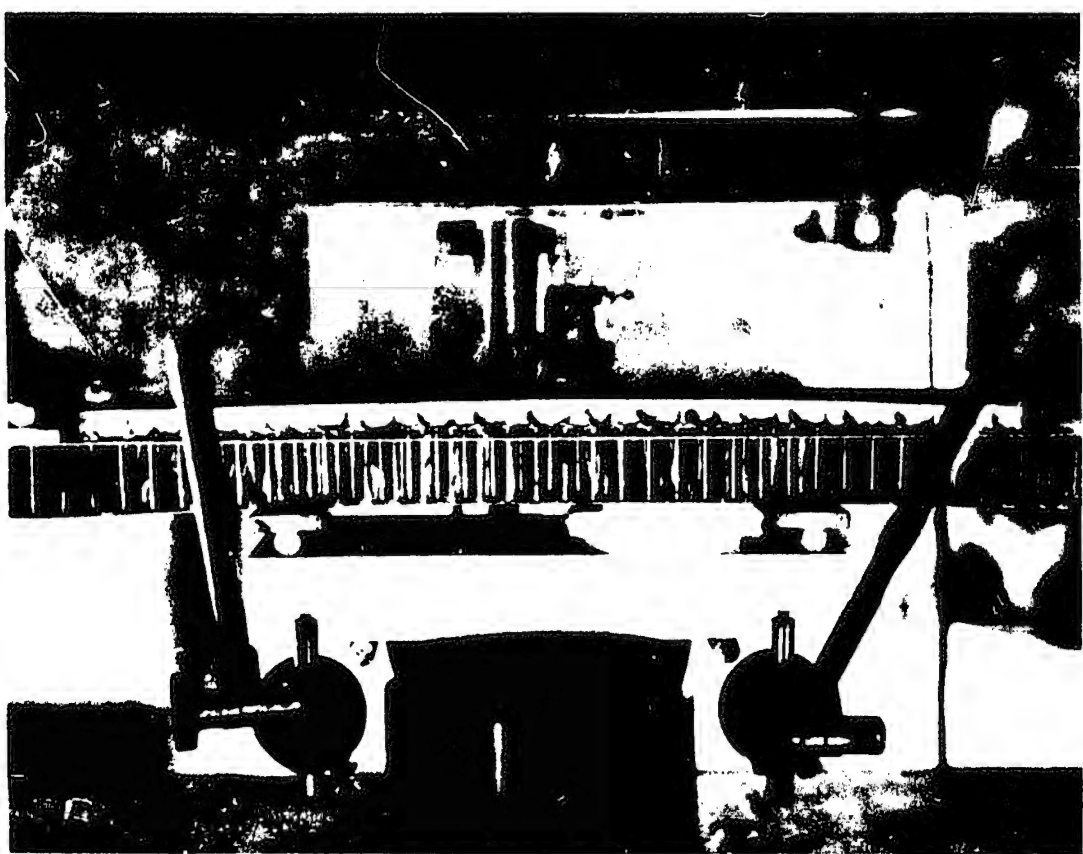
Material Cost for Beeryllium Faced Heat Shield Panel			
60B20210 Design			
Size	Quantity	Cost	beeryllium sheet
53" x 36"	2	159	
53" x 17"	2	1802	2. Doubler strips - .03" cross rolled beeryllium sheet
53" x 36"	2	\$3816	1. Facings - .03" cross rolled beeryllium sheet
			for one (1) panel
			55877

84

83

*Ref: Aerofence Test Report TR-50-63

Load	Load	Load	Load	Load	Load	Load	Load	Load	Load	Load	Load	Load	Load	Load	Load	Load	Load	Load	Load
REFLECTOMETER MIRROR REFLECTION																			
0.0105	0.012	100	0.0104																
0.0185	0.02	200	0.0195																
0.026	0.027	300	0.0274																
0.033	0.034	400	0.0357																
0.0405	0.0405	500	0.0440																
0.047	0.047	600	0.0524																
0.054	0.054	700	0.06																
0.061	0.061	800	0.0688																
0.0685	0.0685	900	0.0784																
0.076	0.075	1000	0.0875																
0.093	0.096	250	0.09																
0.1085	0.1065	1310	0.122																
FOR THE UPWARD																			
FAILURE OF M-31 ACCURSED AT THE																			
SLIGHT CRACK EXCENDING THE FULL																			
POINT. FILTER CONSTRUCTED OF A																			
Panel which through the entire																			
depth of the M-31. Separation																			
the M-31 from the panel failing																			
not occur.																			



SECTION V1
ANALYSIS OF BRAZE EFFECTS
QUALITY STANDARDS AND REPAIR METHODS

Heat Shield Panel Braze Quality

The types and sizes of typical braze discrepancies that are acceptable for heat shield panels of the 30M12571 design produced by Aeroneca for NASA or contract NASA-6976 are shown in Figures 3 through 37. The discrepancies include:

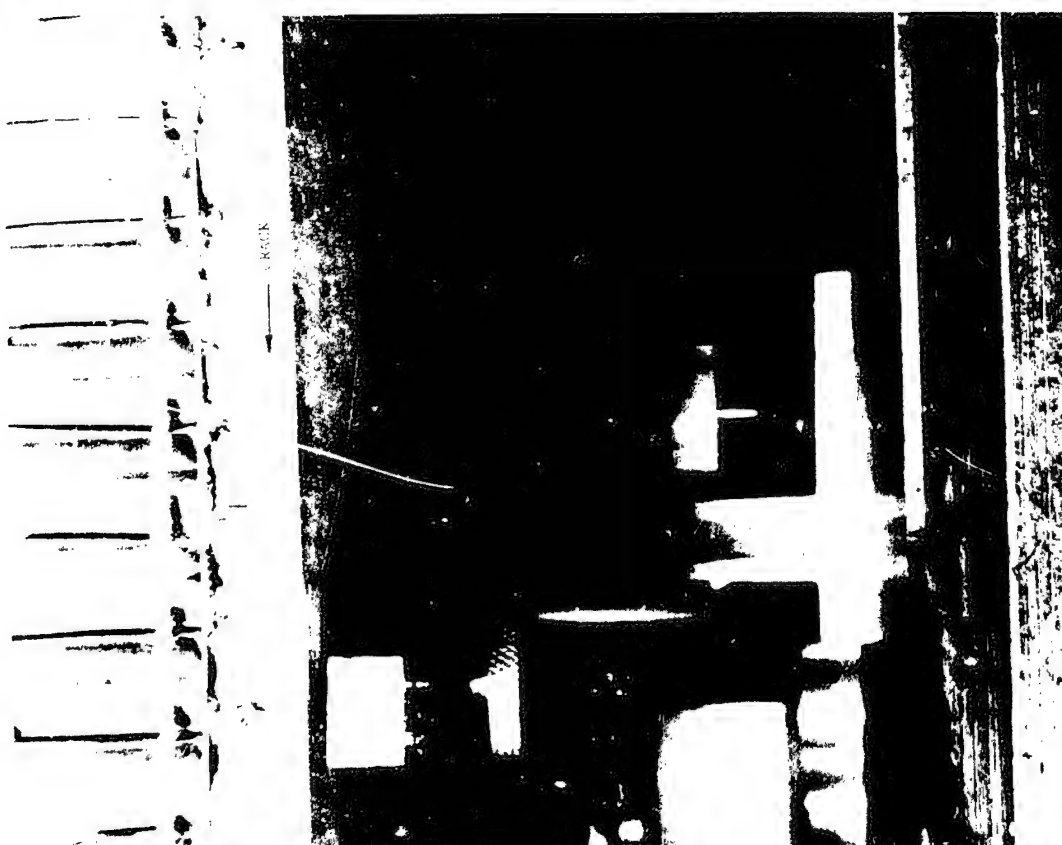
1. Core to facing braze light fillets (LF).
2. Core to facing braze cell wall voids (CWV).
3. Core to facing braze gross voids (GV).
4. Metal to metal or facing surface braze voids (FSV).
5. Core to metal or shear tie braze voids.

Examination of these radiographic inspection reports shows the discrepancies to be principally confined to the metal to metal braze area in the edge members. The core to facing braze imperfections were confined to light fillet areas and small isolated cell wall void areas.

An unacceptable level of braze quality is shown in Figure 37. Note the large area exhibiting cell wall voids and light fillets which also contains a large gross void on both panel faces. These conditions resulted from rework leakage during brazing caused by failure of welded joints in the rework which results in contamination (oxidation) of the protective atmosphere. The net result of oxidized surfaces on the panel components during brazing is inability of the brazing alloy to properly wet the panel surfaces resulting in either very poor fillet formation or none at all.

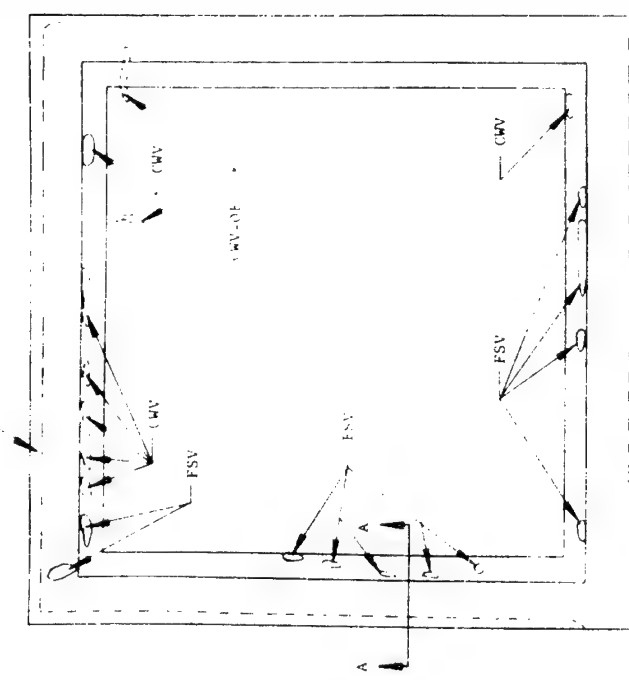
It should be noted that the core to facing braze quality exhibited in Figures 3 through 36 radiographic reports is typical of acceptable braze quality by airframe braze panel standards. The metal to metal and core to metal braze is likewise acceptable.

The following sections contain a detailed analysis of the effect of these five types of braze discrepancies on heat shield panels typical of the 30M12571 design and repair methods where applicable for these conditions.



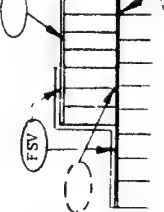
FIGURES 3 THROUGH 35: BRAZE DISCREPANCIES IN HEAT SHIELD PANEL INSULATION AT 30M12571

88



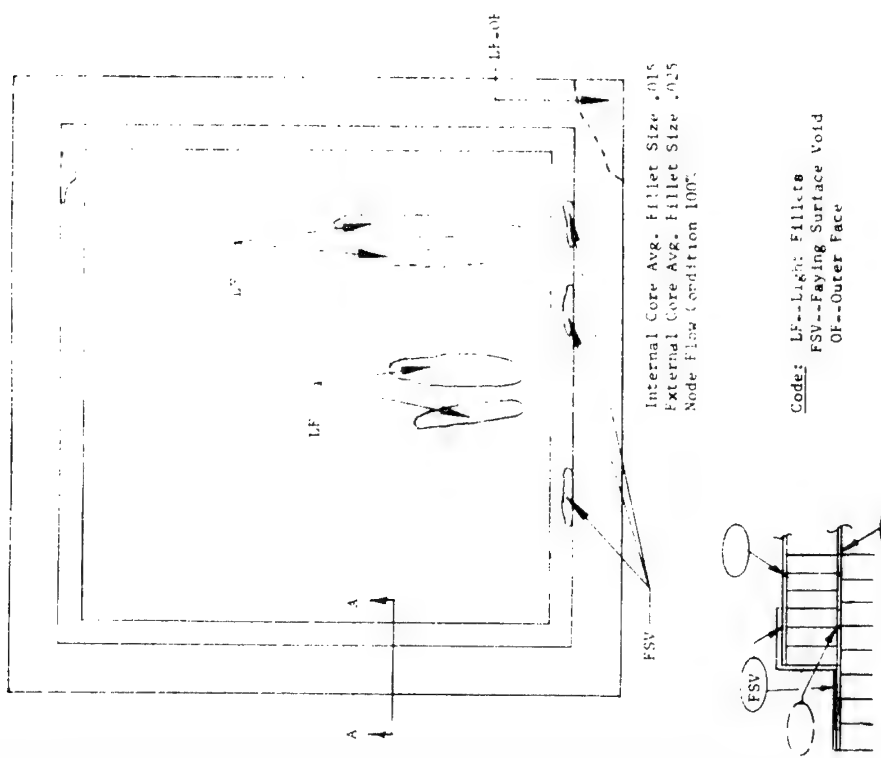
SECTION A-A

Internal Core Avg. Fillet Size .020
External Core Avg. Fillet Size .025
Node Flow Condition 100%



Code: CWV--Cell Wall Void
FSV--Faying Surface Void
OF--Outer Face

Figure 33 Quality Modifying Conditions Revealed by Radiographic Examination



SECTION A-A

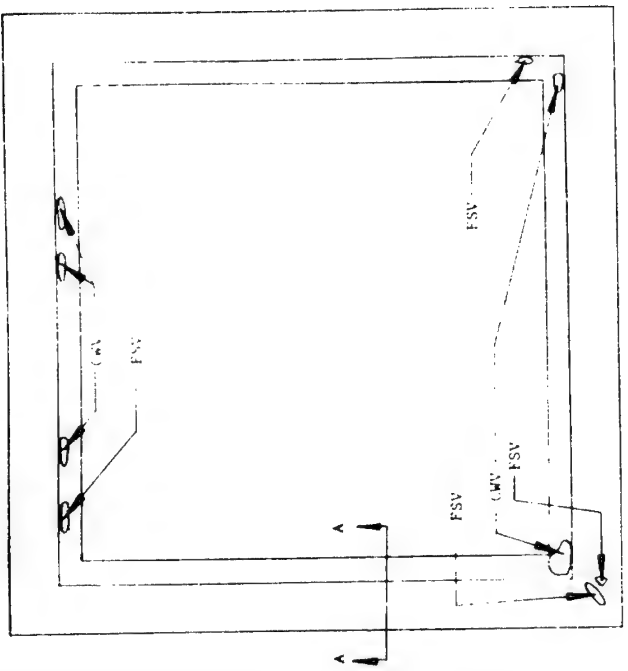
Code: LF--Lip; Fillets
FSV--Faying Surface Void
OF--Outer Face

Figure 34 Quality Modifying Condition Revealed By Radiographic Examination

87

90

89

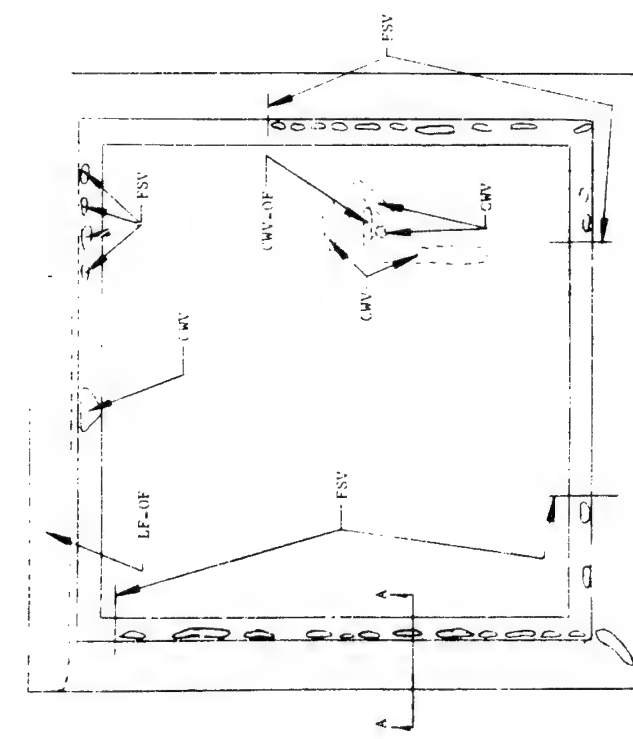


Internal Core Avg. Fillet Size .015
External Core Avg. Fillet Size .030
Node Flow Condition 100%.

Code: CWV--Cell Wall Void
FSV--Faying Surface Void
OF--Outer Face

SECTION A-A

Figure 35 Quality Modifying Conditions Revealed by Radiographic Examination



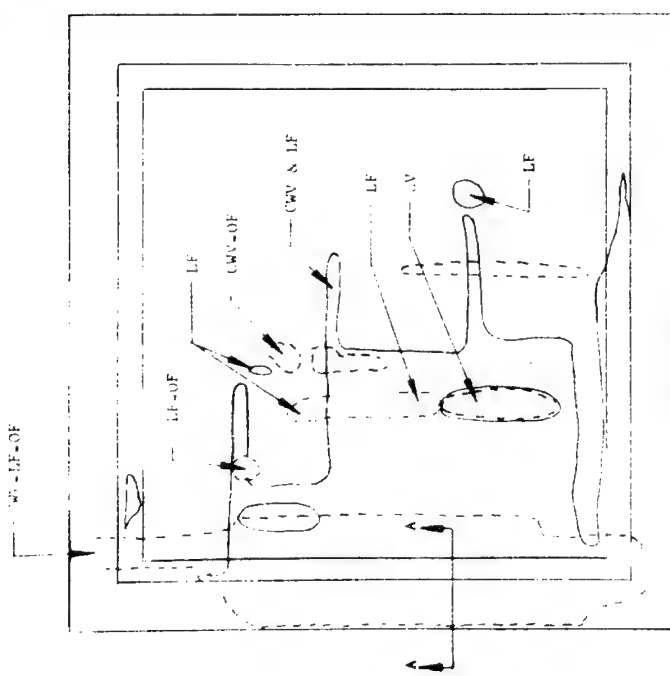
Internal Core Avg. Fillet Size .020
External Core Avg. Fillet Size .025
Node Flow Condition 100%.

Code: LF--Light Fillets
CWV--Cell Wall Void
FSV--Faying Surface Void
OF--Outer Face

SECTION A-A

Figure 36 Quality Modifying Conditions Revealed by Radiographic Examination

91



Internal Core Avg. Fillet Size .015
External Core Avg. Fillet Size .025
Node Flow Condition 100%

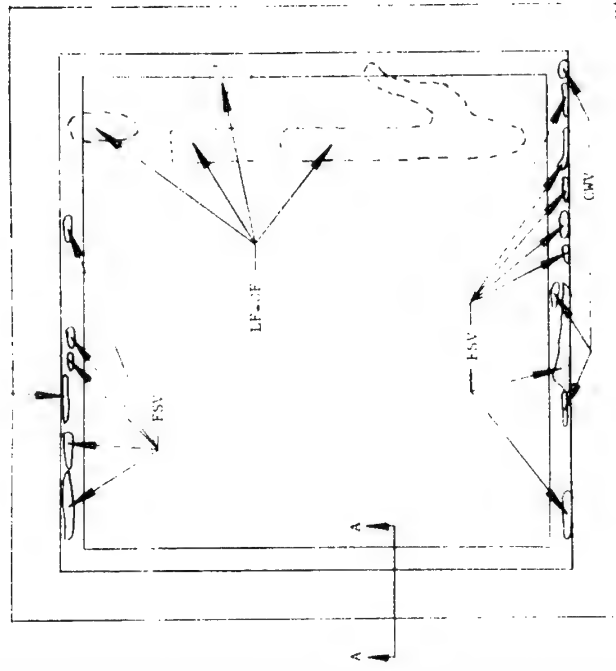
Code: LF--Light Fillets
OF--Outer Face
FSV--Faying Surface Void
GV--Gross Void
CAV--Cell Wall Voids

(Note: Panel Scrapped)

SECTION A-A

Figure 37 Quality Modifying Conditions Revealed by Radiographic Examination

— CMV



Internal Core Avg. Fillet Size .015
External Core Avg. Fillet Size .030
Node Flow Condition 100%

Code: LF--Light Fillets
OF--Outer Face
CMV--Cell Wall Voids
CAV--Cell Wall Voids
FSV--Faying Surface Voids

SECTION A-A

Figure 38 Quality Modifying Conditions Revealed by Radiographic Examination

92

Core to Facing Voids

A core to facing void is an area showing partial or total lack of braze attachment between the honeycomb core and facing sheet. This type of discrepancy is commonly encountered in brazed honeycomb sandwich panels and in numerous variations of size and shape. The effect of such unbraze or unattached areas is a function of size and the type of loading; i.e., tension or compression. Since any sandwich panel subjected to a bending load has one facing in compression while the opposite facing is in tension, the stability of the facing(s) under compression load (in voided or unbraze areas) is of critical importance. Consequently, the analysis of core to facing voids is based on the local buckling strength of the unattached facing sheet under a compression load.

Two types of core to facing voids are commonly encountered. These are:

- Cell Wall Void (CWV)**--The condition where the cell walls are unattached to the face sheet but where attachment is present at the cell nodes. This condition may be continuous or intermittent.
- Gross Void (GV)**--A gross void is a condition where at least one node is unattached to the facing sheet.

Circular Gross Voids

For the condition shown in Figure 39A, the critical unattached area is given by

$$\frac{F_{cr}}{T} \approx 9E \left[\frac{t_f}{d} \right]^{1.5}$$

where γ = plasticity correction factor = $\frac{2E\gamma}{E+E_f}$

E = Modulus of facing material.

E_f = Tangent modulus of facing material from compression stress-strain curve.

Rectangular Gross Voids (Line or Rectangular)

For the condition shown in Figure 39B where dimension b is the loaded edge, the facing behaves as a uniaxially loaded wide plate column. Tests indicate that when the void is surrounded by good braze attachment, the end restraint condition approaches 100% fixity. The local allowable buckling stress for this condition is given by:

$$\frac{F_{cr}}{\eta_1} = \frac{2.62E}{1-b^2} \left[\frac{t_f}{h} \right]^2 \quad (2)$$

η_1 = Poisson's Ratio

where $\eta_1 = \frac{E_f}{E}$ the plasticity correction factor for b the loaded edge.

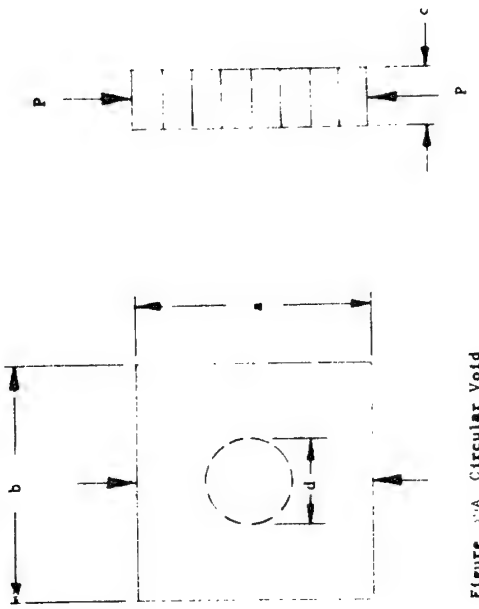


Figure 39A Circular Void

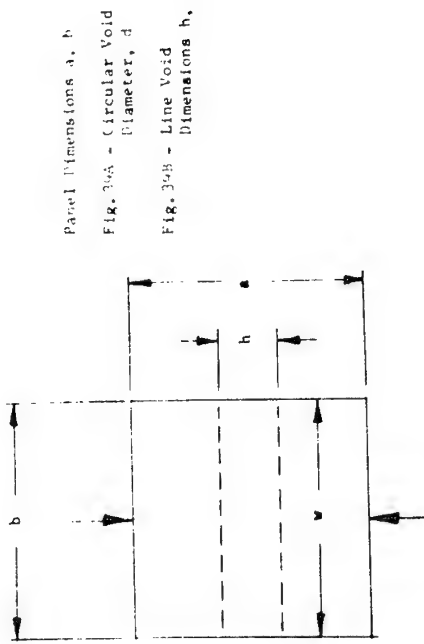
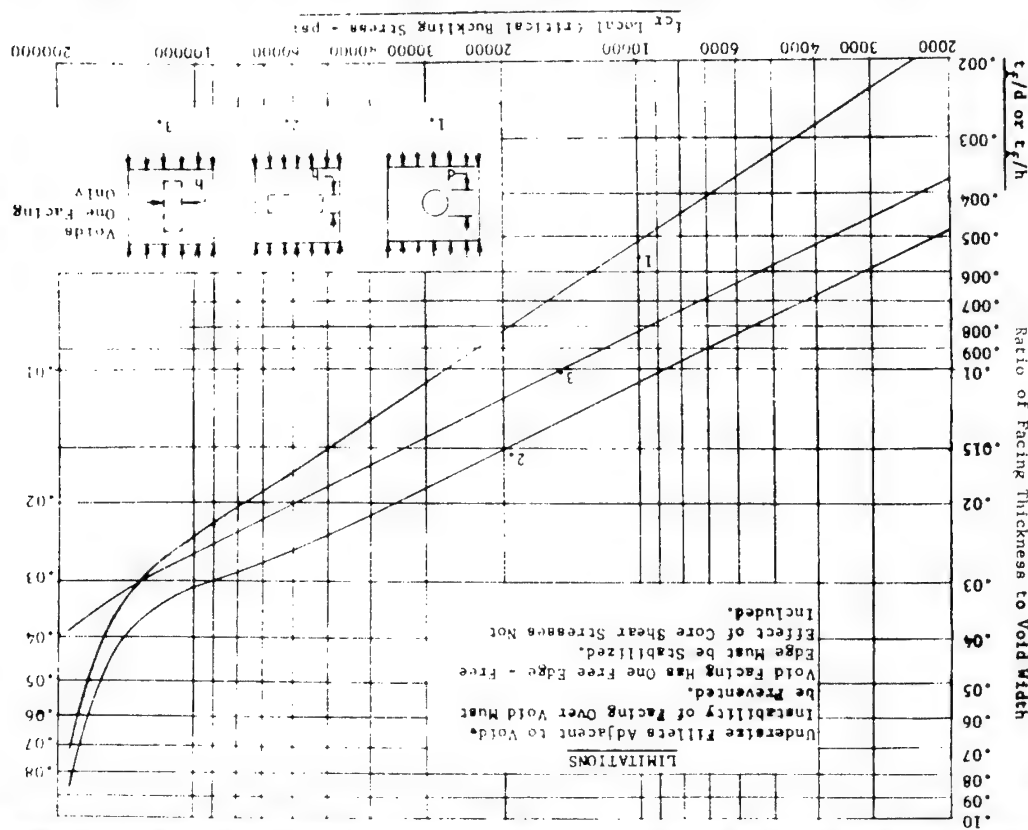


Figure 39B Line Void

Figure 39 Basic Void and Buckling Configurations

פָּלָמָּה ۶۰



Where dimension a is the loaded edge, the rectangular void is considered a long plate elastically restrained on the unloaded edges with intermediate fixity. The buckling stress for this condition is:

$$\frac{f_{cr}}{f_{cr}} = \frac{4.5E}{(1+\eta^2)} \quad (3)$$

$$\eta_{\text{plastic}} = \left[\bar{\varepsilon}_S (0.352 + 0.448 \sqrt{1.25 + \frac{3ET}{4ES}}) \right] \text{ correction factor for the loaded condition}$$

where η_{plastic} is the plasticity

Curves for the preceding equations (1), (2), (3) are shown in Figure 40 and allow ready assessment of the buckling stress for these three one to facing void conditions. Since the maximum stress condition for the 30M125T panel is 35,644 psi, all voids must be stable to this minimum buckling allowable. Voids exhibiting far values below 15,644 psi would be unacceptable "as is" and would require repair. From Figure 40 the maximum circular void size acceptable "as is" without repair would be:

$$\frac{.01}{\beta} = .012$$

line void conditions in Figure 3a; the comparable values for h are (Fig. 4a)

Two conditions of this type of void may be present, a (connected) row of cell walls void or an area with intermittent cell wall voids. The former case may be treated by the use of formulas (2) or (3) for gross line voids. For the latter case (area with intermittent cell wall voids), the following

$$f_{cr} = \frac{2.958 + \log_{10} \left[\frac{r_f}{\delta} \right]}{1 - \frac{3r}{4}} \text{ allowable}$$

fallowable = compression wrinkling stress in facing
(177,000 psi for 4-15 core)

$$\frac{t_f}{t_i} \leq 0.25$$

*Third Monthly Report. Page 37

97

The curve for this equation is shown in Figure 41. For a buckling stress of 35,644 psi, the maximum cell wall void acceptable "is" would be:

$$\frac{35,644}{177,000} = .2 \text{ and } \frac{t_f}{d} = .002$$

for $t = .01"$ $d = 5"$ diameter and $h = 5"$.

(Ref. NAA Structural Repair Manual /buckling equations and curves/).

Fillet Size

For in plane loads a certain minimum fillet size is required to permit development of the face shear allowable in compression loading which in turn subjects the brace fillet to a tensile load. This critical tension stress may be calculated by the following empirical equation:

$$f = \frac{1.75W_f}{S}$$

W = actual brace fillet width at base, inches

S = honeycomb core cell size

f = brace lap shear allowable, p.s.i.

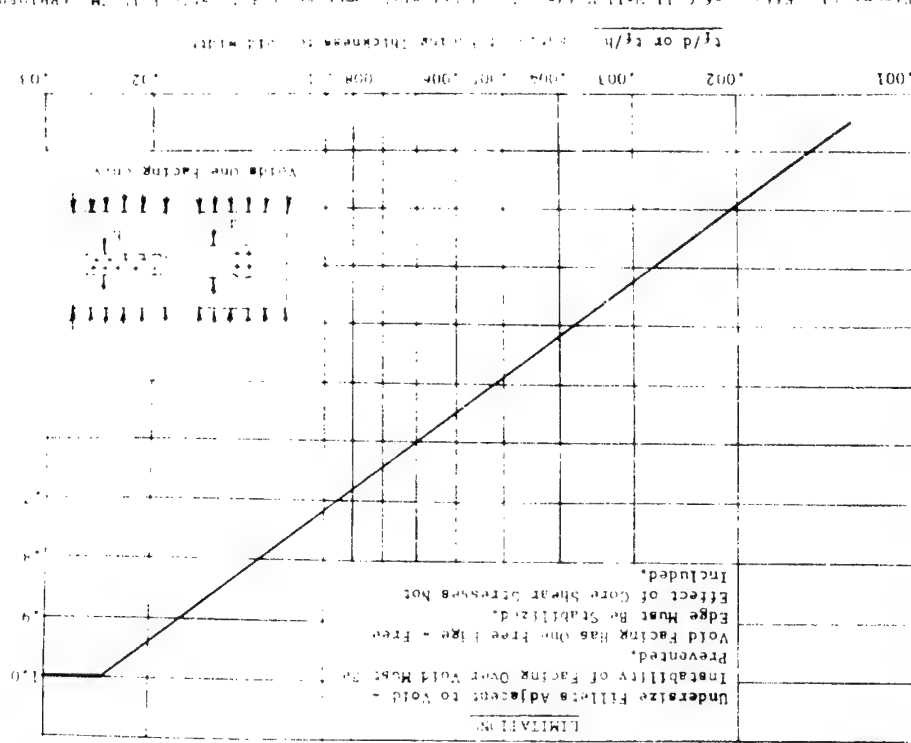
For type 4-15 core and the sterling lithium brace alloy $f_S = 15,000$ psi*, W is 440 psi for the minimum fillet size requirement (0.008") recommended for this application. Typical fillet size for the 30M12574 panels was 0.015". The effect of undersize fillets on face sheet stability is shown in Figure 42.

Node Flow Requirements

For the S-1C heat shield panel applications in question, brazing alloy node flow in the load bearing core is desirable from the standpoint of minimizing the thermal gradient (ΔT), resulting panel deflection and facing stresses rather than providing increased core shear properties.

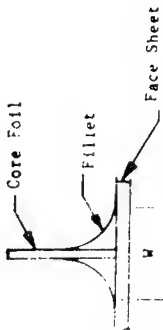
*Ref. Convair Spec. F2S-4-162A

Figure 41. Effect of Cell Wall Void on Allowable Shear Stress



98

However, since the combined facing stresses for a flight condition are quite low (25,238 psi) for the zero net skin loading (AT) condition with a N.S. of 1.0, node flow is not considered a mandatory requirement for heat shield panel acceptance.



Size and Spacing Requirements for Core to Face Voids

The maximum sizes of core to facing voids recommended for acceptance was 1/8" (unprepared) are given in Table 1, which also include the minimum recommended spacing requirements. The spacing requirements, essentially, represent the minimum distance necessary to prevent catastrophic propagation of adjacent voids and are based on empirical standards used for brazed honeycomb sandwich air frame panels. Because of the large N.S. associated with the maximum panel stress (35,644 psi), the maximum permissible acceptable voids void has been defined as 1/8" rather than 0.5 in.

Typical Minimum Voids:

Size Requirement for 1.0" Thick Core

Core Type	W _{req'd}
3-15	.004"
4-15	.008"
6-20	.010"

Repair Procedure:

Repair procedures suitable for core to facing voids in excess of the sizes listed in Tables 1, and 1, consist basically of stabilizing the unbrazed area by means of a doubler which is structurally attached to the facing in the solid panel area surrounding the void as well as the unbrazed facing area. The basic methods of doubler attachment applicable to heat shield panels include:

- Adhesive bonding using a high temperature epoxy type adhesive such as FG-424.
- Spot brazing--A method which employs a lower melting point braze alloy than the sterling lithium braze alloy used for the panel brazing. Localized braze attachment in the form of spots 1/16", 1/4", or 5/16" in diameter is accomplished by electrical resistance heating using a single electrode run applied to one side of the part only. The brazing alloy recommended for this application is the silver-copper eutectic plus 0.2-5% lithium with a melting and flow point of approximately 1400°F.
- Area Brazing--A method using a lower melting point brazing alloy as in item b, with heat applied either locally by means of an indirectly heated copper block or by heating the entire panel using the original brazing tooling. The latter method gives very good results but requires specialized manufacturing facilities and is relatively expensive. The local heating method is highly dependent on operator skill, limited to small size or areas, and frequently results in excessive panel warpage.

*Ref: Monthly Report No. 3, Page 37

99

100

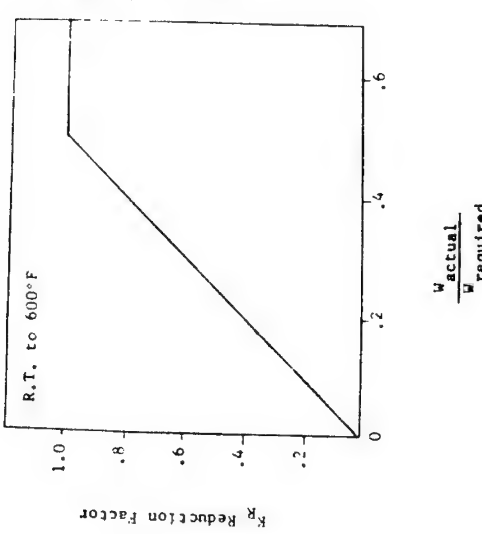


Figure 42 Effect of Undersize Fillet on Face Sheet Stability

Ref: NAA Structural Repair Manual

d. Mechanical Fasteners-Limited use may be made of blind mechanical fasteners such as Influent L-Nickel noisless explosive rivets of the jumbo head type (PN-134A) $0.134 \pm .001$ in. in diameter. The rivet holes must be located in the center of the core cells in the sound braze area to avoid undesirable core to facing braze damage.

Of the foregoing methods, the adhesive bonding, spot brazing and blind panel facing (cold side); the hot side facing bearing the open face honeycomb effectively prevents repairs from being accomplished. Welding as a means of doubler attachment, either directly as along the doubler edge or a fusion spots, burn down welds of pins passing through a doubler and top and bottom facings, is likewise not feasible with conventional TIG welding equipment on panels with 0.010 in. facing essentially because of inadequate control resulting in burn through.

Analysis of Metal to Metal and Core to Metal Voids in 50M12571 Heat Shield Panel

Core to Metal Voids:

The core to metal joint is assumed to carry the entire load. Since the vertical leg of the Zee is $1\frac{1}{4}$ in., the total shear area for the panel is 4 sq. in. ; where a is the length of the core (48.3 in.). The shear load per inch of perimeter then becomes $q = 2/4a$ or $q = 1/4$ psi of wall area. The core to metal attachment area for Type 4.15 core per square inch of surface would be $4 \times 0.005 = 0.020$ in.² of shear area*. The shear stress on the braze attachment is:

$$f_a = \frac{q}{4 \times .02} = \frac{48.3 \times .02}{.08} = 6039 \text{ psi}$$

The shear strength allowable for the silver-copper-lithium braze alloy is $15,000$ psi at R.T. and $12,750$ at 500°F *.

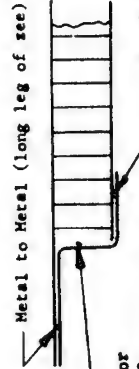
For $q = 2.7$ air load plus 0.72 psi dynamic load (noise and vibration)

$$f_a = 2050 \text{ and } 1025 \text{ psi, respectively.}$$

Thus for the worst condition, the maximum void allowable is

$$1 - \frac{2050}{15000} \times 100 = 85\%$$

Metal to Metal (long leg of zee) Braze



*Ref: Convair Spec. FMS-0036

93

Metal to Metal Voids--Short Leg of Zee Member:

Assume the short leg of the zee must carry the entire panel load as a tensile loading on the facing to short leg zee braze. The width of this braze area is 0.875 in. and the total braze length is 1.125×4.0 in. The panel load is q_a with the tensile stress in the braze given by $q_a = 3.5 \times 12.39$ psi. Applying the worst loading condition, the stress in the braze is 42 psi. The braze tensile allowable is approximately $25,000$ psi, $(15000/42)$ consequently a very large margin is present for this loading condition.

Metal to Metal Voids--Long Leg of Zee Member:

When the composite edge member (long leg of zee) and facing is bent by a shear load at point P the edge P



rotation is given by:

$$\theta = \frac{PL^2}{2EI} - \frac{ML}{EI} = \frac{41.4 \times (.897)^2}{2 \times 29 \times 10^6 \times 1.84 \times 10^{-6}} = .03125 \text{ radians}$$

Where $P = 1 \text{ sq. in.}$ / inch

$$a = 48.3 \text{ in.}$$

$$q = (2.7 + 0.72) = 3.42 \text{ psi}$$

The stress in the braze is:

$$f = \frac{MC}{I} \text{ where } M = \frac{qL}{2}$$

$$f = \frac{2EBC}{L} = \frac{2 \times 10.2 \times 10^6 \times .03125 \times .019}{.897} = 18,500 \text{ psi}$$

Since the braze must withstand the shearing force resulting from bending, the $13,500$ psi value may be compared with the braze shear allowable namely, $15,000$ psi. Actual values, however, for the silver-copper-lithium braze alloy are $19,600$ psi (R.T.)*.

With the panel edge secured by means of bolts to the support beam flanges the principal concern with voids between the facing and see occurs when the facing experiences a compression loading resulting from bending of the .061 in.

103

104

thick composite edge member (flight condition loading). As a result, the facing would tend to buckle in unbrazed areas so that voids might propagate into the core to facing areas, particularly if core to facing voids near the edge members were present. Where no core to facing voids near the panel edge are present, metal to metal void propagation is unlikely since the panel edge rotation is very small. As a consequence, the compressive force required for extensive buckling in metal to metal voided areas will not be produced.

Repair Methods for Metal to Metal Voids

Repair methods applicable to metal to metal braze voids include:

- a. Mechanical Fasteners--Either blind or countersunk rivet fasteners depending on the void location and interference requirements may be used. A recommended fastener is the DuPont Aircraft Blind Expansion Rivet (PN series) of low carbon nickel alloy. This fastener is available with either a modified brazer head or 100% flush head. Expansion of the rivet shank is accomplished by applying a heated tool to the rivet head which activates the sealed internal chemical charge. This type of rivet has been widely used for applicable braze panel repairs with complete success. Certain NASA test panels produced on Contract NAS-6976 were repaired using this type rivet, as shown in Figure 43. Repairs to voids in either the short or long leg of see member can be readily accomplished with this fastening system both in the field as well as by the panel fabricator.
- b. Spot Welds--This joining method has been used for metal to metal repairs where the area to be repaired is accessible; i.e., the long leg of the see and the facing surfaces are sufficiently clean (unoxidized) so a sound nugget can be formed. As a consequence, this method is limited with respect to void location and equipment availability.

- c. Fusion Welding--This is applicable to metal to metal voids between long legs of see and facing that extend the full width (edge to edge). Essentially a burndown weld is performed which joins the facing and edge member. The presence of silver brazing alloy in the fusion zone is not detrimental to the joint however, it does cause some difficulty because of the tendency to "flow out". Consequently, a complete void condition is preferred for this type of repair.

Repair Methods for Core to Metal (Shear Tie) Voids

Repair for core to metal or shear tie voids consists of injection of a foam type adhesive through holes drilled in the vertical leg of the see, curing the adhesive and plugging the drilled holes with a sealer or potting compound.



FIGURE 43. TYPICAL METAL TO METAL Voids AND REPAIR METHODS TO TREAT THEM.

The detail requirements are:

- a. Clean surface (MEN) and lay out bolt pattern using 1.0" hole spacing and drill holes (No. 50 drill).
- b. Inject with a lever type gun (Therm-Foam 67), type I (Hexcel Products). Cover holes with one layer masking tape, reopen holes and add another layer of tape (see separate notes). This provides an expansion area for adhesive overflow during the curing.

c. Attach thermocouple(s) to the area to be repaired and cure in oven at:

180°-190° F for 25-30 min. followed by

225°-240° F for 50-60 min. followed by

325°-350° F for 25-30 min.

d. Reopen holes used for injection to a depth of approximately 0.1" and seal with Silastic RTV.

Braze Quality Standards for Metal to Metal and Cure to Metal Joints

The maximum sizes of metal to metal and core to metal braze voids recommended for acceptance are 1 in. These size and spacing requirements are based on empirical standards modified for the S-1C heat shield panel requirements.

METAL TO METAL AND CORE TO METAL BRAZE REQUIREMENTS

TABLE

Metal to Metal	(Fayling surface void)
Core to Metal	(shear tie void)
Any vertical shear tie 50% or more brazed is	acceptable. The maximum number of unbrazed or
completely void shear ties shall be not more than	3 in any 5 consecutive shear ties.
edge to edge.	
metal to metal void shall not be continuous from	
area for each 1/16" inch of braze joint. A	
the voided area shall not exceed 25% of the joint	
edge to edge.	
metal to metal void shall not be continuous from	
area for each 1/16" inch of braze joint. A	
the voided area shall not exceed 25% of the joint	
edge to edge.	
metal to metal void shall not be continuous from	
area for each 1/16" inch of braze joint. A	
the voided area shall not exceed 25% of the joint	
edge to edge.	

SECTION VI:
ANALYSIS OF HOLES IN PLATE SHELL PANELS

Methods for calculation of stress concentrations factors for round holes in bands which panels are outlined in ANC-23, Part 1, 1951, sections 5.11, 5.12, 5.13, 5.215, 5.2153, 5.2155. Give Figure 4 for notation and tip of hole diameter. The parametric equations describing the boundary of the hole (with no doubler) are:

$$\begin{aligned} x &= A \cos \theta + b \cos 3\theta \\ y &= B \sin \theta + b \sin 3\theta \end{aligned}$$

where $\tan \theta = \frac{y}{x}$

The stress in the facia at the edge of the hole in a tangent direction is given as:

$$\begin{aligned} & \left[(A^2 + b^2) \sin^2 \theta + (B^2 + b^2) \cos^2 \theta - 6b(A + B) \cos^2 \theta + 4b^2 \right] f_t = \\ & = (f_x + f_y) (A^2 \sin^2 \theta + B^2 \cos^2 \theta - 9b^2) - \left\{ f_{xy} (A + B)^2 \left[\frac{A^2 b^2 + b^4}{A + B + 2b} \sin 2\theta \right] + \frac{(A^2 - b^2)(f_x + f_y) - (A + b)^2 (f_x - f_y)}{A + B - 2b} \right. \\ & \quad \left. (A + 3b) \sin^2 \theta - (b - 3b) \cos^2 \theta \right\} \end{aligned}$$

For a round hole where $A = b = 1$ and $b = 0$, the above expression becomes:

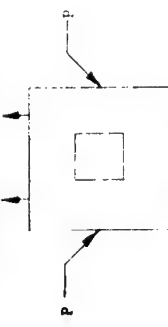
$$\begin{aligned} f_t &= (f_x + f_y) - 4f_{xy} \sin 2\theta - 2(f_x - f_y) \cos 2\theta \\ f_t &= (1 - 2 \cos \theta) f_x + (1 + 2 \cos 2\theta) f_y - 4f_{xy} \sin 2\theta \end{aligned}$$

For an assumed unidirectional condition where $f_y = 0$, we have a maximum value for f_x at $\theta = \pi/2$. Thus $f_t(\pi/2) = 3f_x$.

Thus the maximum stress concentration factor for a round hole in a plate subjected to a uniaxial stress is 3 and is independent of the hole size and the distance of the point of interest from the hole.

The recent analytical work on stress concentration factors in plates by G. H. Savin reported by W. Griffell discloses a factor of 3 for the case of a square but also considers the effect of the distance of the hole from the center of the field of interest with respect to the hole size. Subsequently, it will be seen that the results are considerably to be preferred as will be shown.

For a square hole theory indicates $\sqrt{2}$ as the stress concentration factor at the center (p) of a side parallel to the applied stress.



At the corners the stress concentration factor is a function of the corner radius to side length ratio, $\frac{r}{a}$.

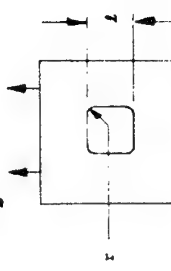


Figure 45 shows a plot of K_c vs $\frac{r}{a}$ for square and diamond holes taken from Savin's data. Table 21 and Figure 44 show the stress concentration factors for different hole shapes and locations.

For the case of a round hole near a boundary edge of the panel for the case where (distance of hole center from edge/hole radius = 2) the stress at the panel edge adjacent to the hole will be zero; at the hole boundary adjacent to the panel edge $K = 3.3$; at the hole boundary opposite to the panel edge $K = 3.1$.

Figure 44 Hole Diagrams, Typical
(See discussion of Stress Concentration Factors, pages 98-104)

113

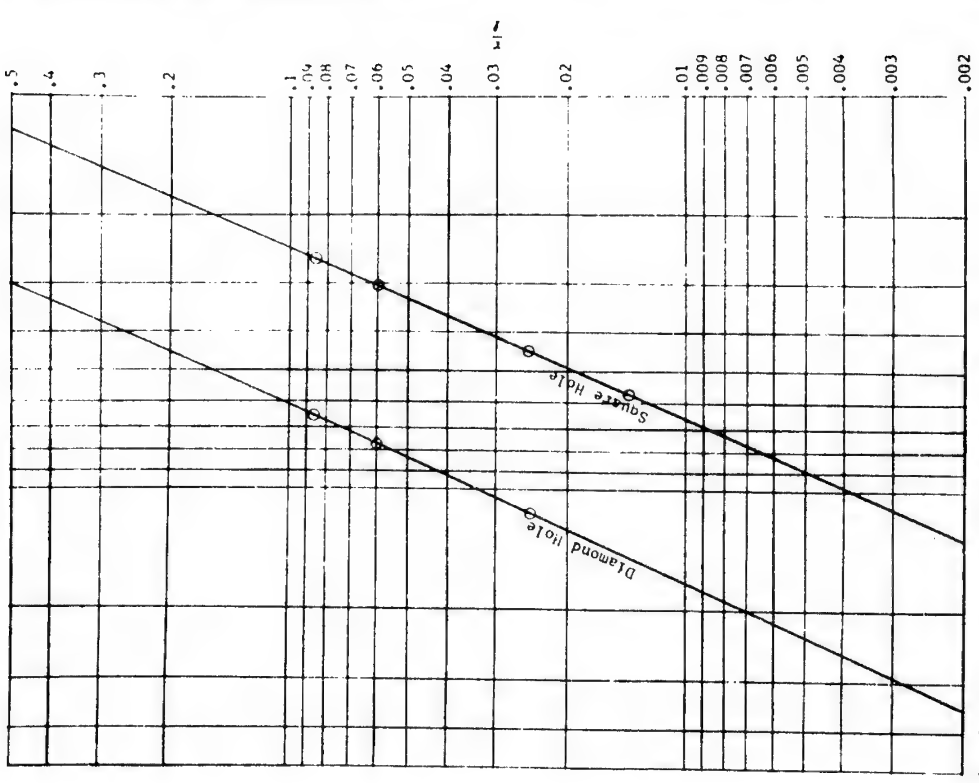


Figure 45 Stress Concentration Factor, K
at $\theta=\pi/4$ for Square and Diamond Holes

114

TABLE 2
VALUES OF K FOR HOLLOW PLATES WITH A UNIDIMENSIONAL HOLE
SHAPED HOLES WHICH ARE EQUILIBRIUM IN A UNIDIMENSIONAL SERIES

	K at $\theta=0$	r at $\theta=\frac{\pi}{2}$	K at $\theta=\pi$	Max. Value
Round Hole (per A.N.C.23)	-1	3	3	
Round Hole (per G. H. Savin)	-1	3	3	
Round Hole ($d=2R$) Near Edge per G. H. Savin	-1	3.3 at A 0 at D 3.1 at B	3.3	
Square Hole $R_c = .086L$ per G. H. Savin	-0.828	1.645	3.3	
Square Hole per $R_c = .086L$ $R_c = .06L$ $R_c = .025L$ $R_c = .014L$				
Diamond Hole per G. H. Savin				
$R_c = .086L$	-.86	1.4	2.8 at 50°*	
$R_c = .06L$	-.8	1.6	3.9 at 50°*	
$R_c = .025L$	-.95	1.8	4.5 at 50°*	
$R_c = .014L$	+1.4	-.9	5.8 at 50°*	
Diamond Hole 1/4 per G. H. Savin				
$R_c = .086L$	+.35	+.35	6.5 at 45°*	
$R_c = .06L$	+.4	+.4	7.8 at 45°*	
$R_c = .025L$	+.5	+.5	11.6 at 45°*	

*These values are 2.6; 3.1; and 4.5, respectively, at
 $\theta = \pi/4$ as shown in Figure 45.

When biaxial stresses are present as will be the case with the heat shield panels and the test samples, the factor for the tangential stress at the boundary of a round hole is a maximum of 4 when $f_x = f_y$, for steady state load conditions.

For dynamic loads (modes and vibration) the stress concentration factor for a round hole is approximately 2.8.

Accordingly, the maximum stress at the boundary of a round hole with no doubler in a heat shield panel is given by:

$$f_t = 4.79 \times (4 \times 2.7 \text{ psi} + 2.8 \times 0.72 \text{ psi}) \times (48.3)^2 = 142,313 \text{ psi}$$

Since this value is well below the yield strength minimum of 170,000 psi and assuming 100% core to facing brace attachment in the panel area surrounding the hole, a positive margin is indicated. If the hole was located in an area of light fillets or voids, the addition of a doubler around the hole would be necessary.

Holes with Doubler Reinforcement

The stress in the facing at the boundary of a round hole with a doubler on one facing where $\frac{R_D}{H} = \frac{3}{2}$ and $\frac{R_1}{R_2} = \frac{1}{2}$ is:

$$f_{t_1} = (f_1 + f_2) C - 4(f_1 - f_2) \left[B + 3P \frac{R_1}{R_2} \right] \cos 2\theta \quad (1)$$

H = extensional stiffness of panel, $2t_F E$

H_D = extensional stiffness of panel in doubler area, $3t_F E$

R_1 = radius of hole, inches

R_2 = outside radius of doubler, inches

f_1, f_2 = thickness of facing and doubler, respectively, inches

The stress in the facing at the junction of the doubler is given by:

$$f_{t_2} = \frac{(f_1 + f_2)}{2} \frac{(1-A)}{2} - \frac{(f_1 - f_2)}{2} (6J-1) \cos 2\theta \quad (2)$$

The values of the parameters A - J for the conditions set forth above are:

*Ref: Dynamical Stress Concentrations in An Elastic Plate, J. of Applied Mechanics, June 1962, Pg. 304.

$$A = \frac{3(1 - \frac{R_1}{R_2}) \frac{H_D}{H} - 5 \frac{R_1^2}{R_2^2} + 3}{5(1 - \frac{R_1}{R_2}) \frac{H_D}{H} + 5 \frac{R_1^2}{R_2^2} - 3}$$

$$C = \frac{8}{5(1 - \frac{R_1}{R_2}) \frac{H_D}{H} + 5 \frac{R_1^2}{R_2^2} - 3} = +0.81$$

$$D = +0.228$$

$$F = -0.537$$

$$J = +0.5272$$

$$H = +0.423$$

$$f_{t_1} = (f_1 + f_2) \cdot 81 - 4(f_1 - f_2) \left[4.23 - 3 \times \frac{+587}{4} \right] \cos 2\theta$$

$$\text{or} \quad f_{t_1} = .88 f_1 \text{ at } \theta = 0; f_{t_1} = +.74 f_1 \text{ at } \theta = \frac{\pi}{2}; \text{ (for } f_2 = 0)$$

$$f_{t_1} = 1.62 f_1 \text{ for all values of } \theta \text{ when } f_1 = f_2$$

For the stress in the facing at the edge of the doubler from Equation (2):

$$f_{t_2} = -1.023 f_1 \text{ at } \theta = 0; f_{t_2} = -1.137 f_1 \text{ at } \theta = \frac{\pi}{2} \text{ (for } f_2 = 0)$$

$$f_{t_2} = 0.114 f_1 \text{ at all } \theta \text{ for } f_1 = f_2; f_{t_2} = 1.08 \text{ at } \theta = \frac{\pi}{2} \text{ (for } f_2 = -f_1)$$

EXPERIMENTAL MEASUREMENT OF
STRESS CONCENTRATIONS AT HOLE BOUNDARIES

Two identical sample panels were fabricated of the same material¹⁶, cire type, facing gage and panel thickness at the heat shield panels. Size of the panels was 20" x 30" x 1.02 thick. A vacuum box (see Fig. 46) to simulate simple support condition was made with the centerline of support 19" x 29". It was believed that the use of corner reaction forces would overcome the slight compressibility of the support ridges around the fixture edge and thus offset the tendency of the panel to curl. Had this been successful, the calculations would have been made much simpler as the face edges would lie in a plane and the formulas and expressions for simple support edge condition would apply. However, no amount of corner reaction force would hold the edges to a straight line. This necessitated considering the deflection of the panel with all four edges elastically supported.

Panel No. 1 was drilled to provide a 2-3/8" hole through the center. Deflection data was recorded and a second 2-3/8" hole placed near a corner with the center distant from the edge, $d/R = 2$. Stresscoat and deflection data were obtained. This test was repeated again with strain gage data also being taken. The center round hole was then cut out to make a square of the same size. A stresscoat pattern was obtained in the vicinity of the square hole, then deflection and strain gage data were recorded. No edge reinforcement doublers around the holes were employed. The test arrangement is shown in Figures 47 and 48. No failures of any nature in the vicinity of the holes occurred during the panel tests.

Table 22 shows the summary of the dial indicator deflection data. Dial indicator locations appear in Figure 49. The deflections tabulated for each test have been adjusted to a common value of 28.5° of mercury. The two corner indicators (No. 1 and No. 7) were used as a reference plane and the mean deflection of the five tests at the other positions on the panel were listed as the observed deflection of the panel. The value of Q_{calc} then computed for each of the indicator positions other than the corners 1 and 7 for a panel aspect ratio of 1.5 with elastically supported edges. These are tabulated. The value of Q_{calc} is 13.768. The tabulated values of W_{calc} are thus 13.768. A comparison of the observed and calculated deflections shows in general good agreement in the central panel area of greatest deflection.

The strain patterns for each condition are clearly shown in Figures 50 through 54 and particularly the areas of stress concentrations around the holes, Figures 51, 52 and 53. Stress concentration factors were determined by the comparative strains at the same points and for the same loading for the panel with holes versus the panel with no holes. Consequently, the simple ratios of hole strain

* See Theory of Plates and Shells,
2nd Ed., page 218, by Timoshenko.

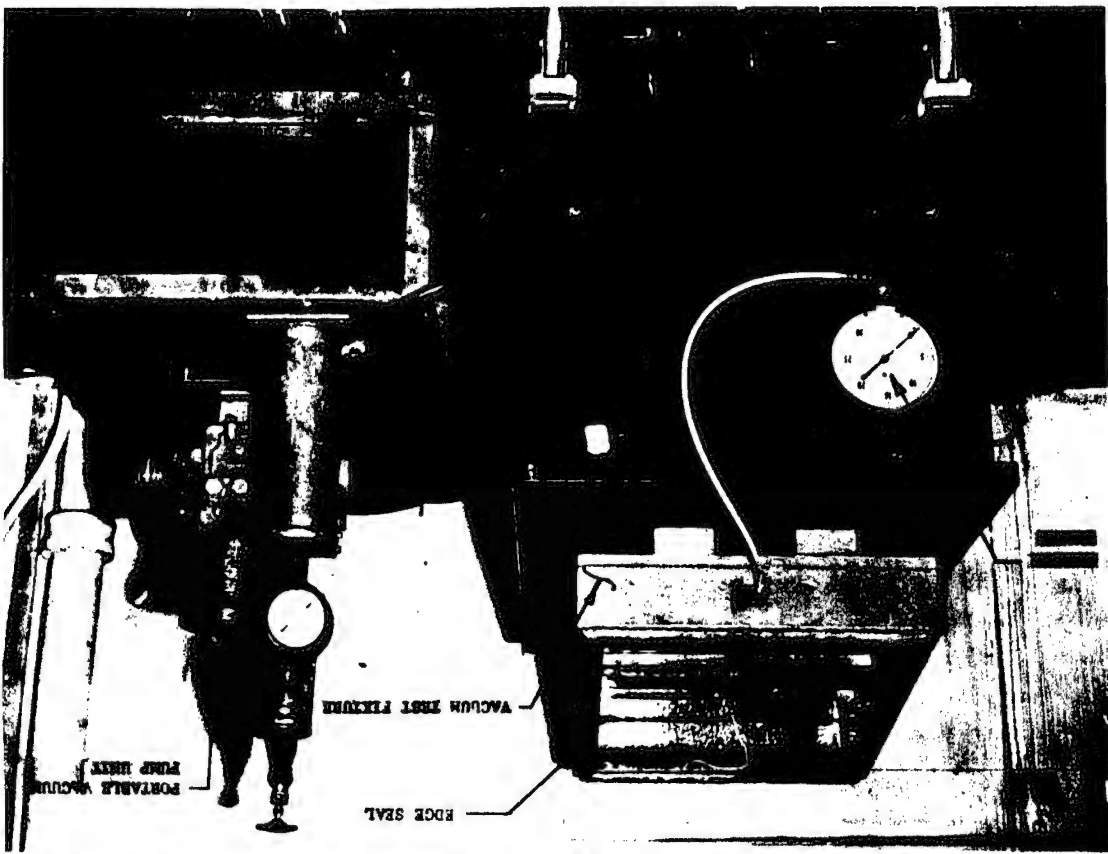


FIGURE 46 Vacuum Box Test Fixture

119

120

122

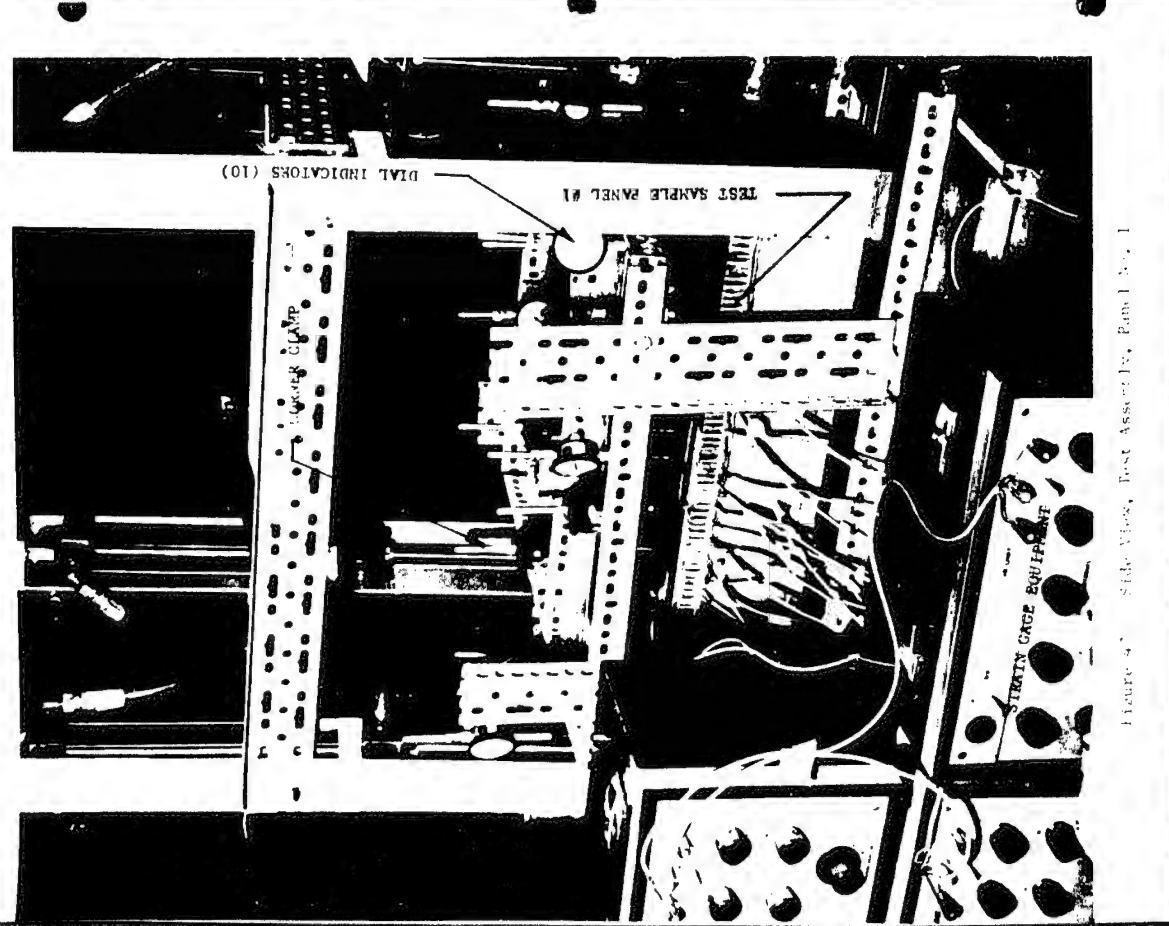
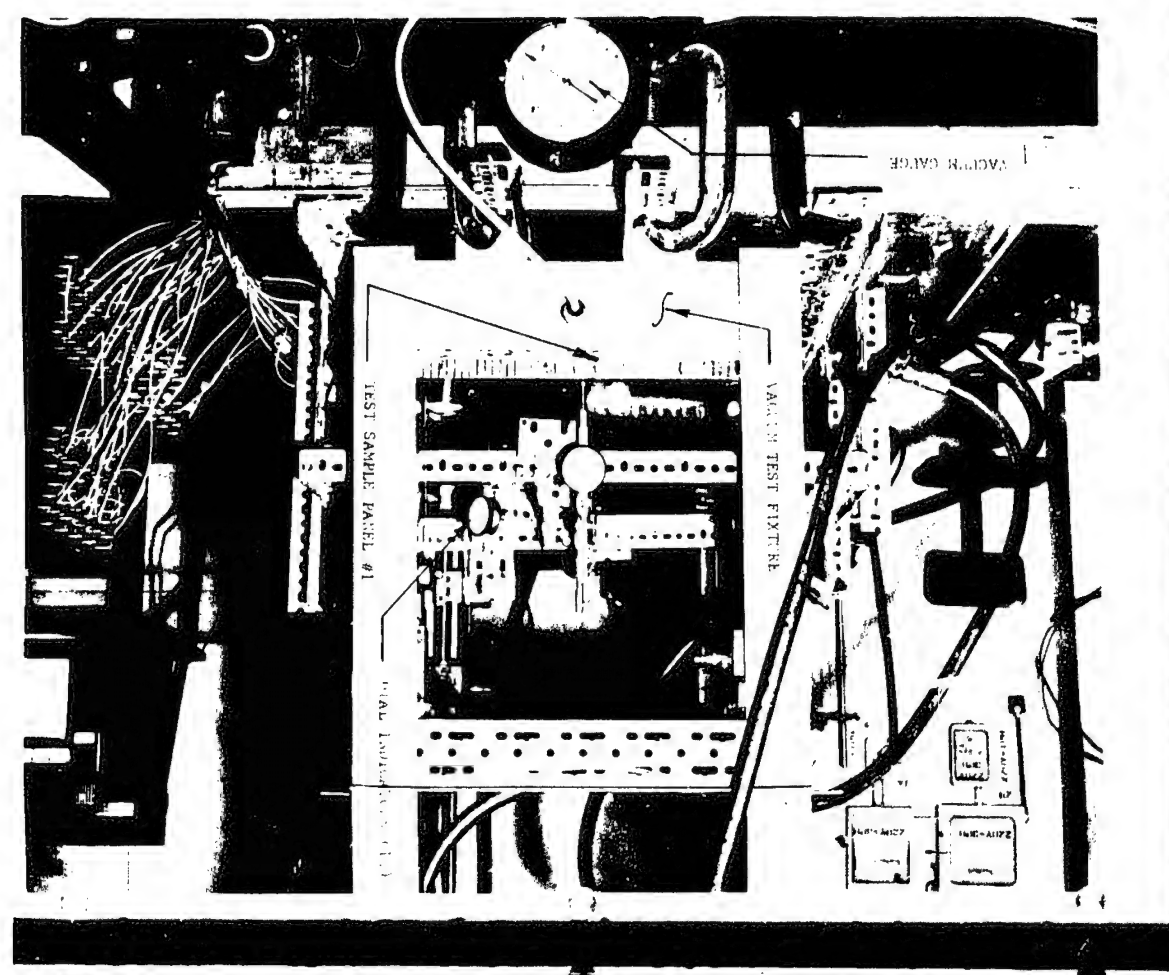
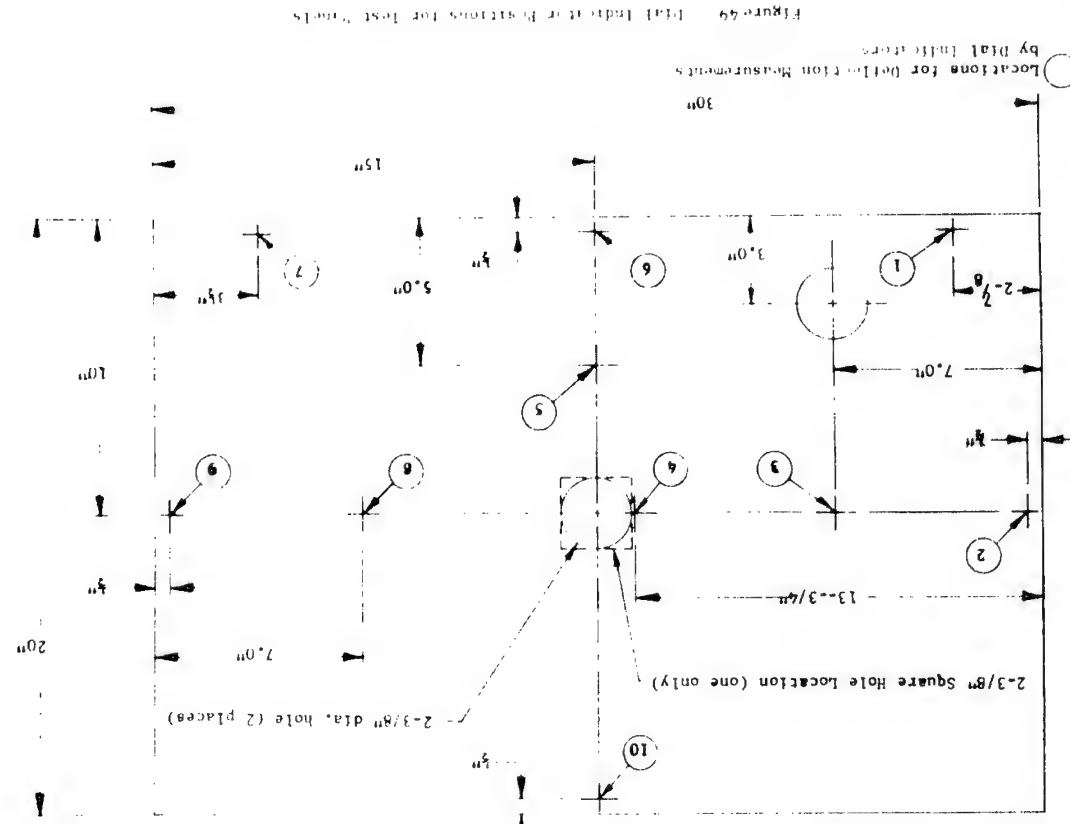


Figure 4. Side view, Test Fixture, Panel No. 1

121

EST PANEL DEFLECTION DATA

TABLE 2



A inches of mercury vacuum on test fixture. Data was reduced to this value for all cases to provide a common reference value. This is an equivalent AP of 13.99 psf.

* It is observed in the deflection below the plane calculated from eq. 4, where $\frac{D}{d} = 13.768$

1	.150	.140	.211	.197	.194	.188	0	---	-
2	.205	.196	.220	.233	.220	.215	.027	.0026	.0
3	.306	.305	.327	.331	.325	.319	.136	.00996	.1
4	.347	.347	.380	.379	.383	.367	.187	.0136	.1
5	.268	.315	.322	.330	.332	.313	.133	.01026	.1
6	.222	.250	.228	.243	.239	.236	.056	.00884	.1
7	.157	.180	.165	.180	.186	.173	0	---	-
8	.306	.296	.324	.317	.328	.314	.141	.00996	.1
9	.220	.190	.211	.194	.201	.203	.030	.0028	.0
10	.396	.267	.316	.301	.303	.309	.120	.00884	.1

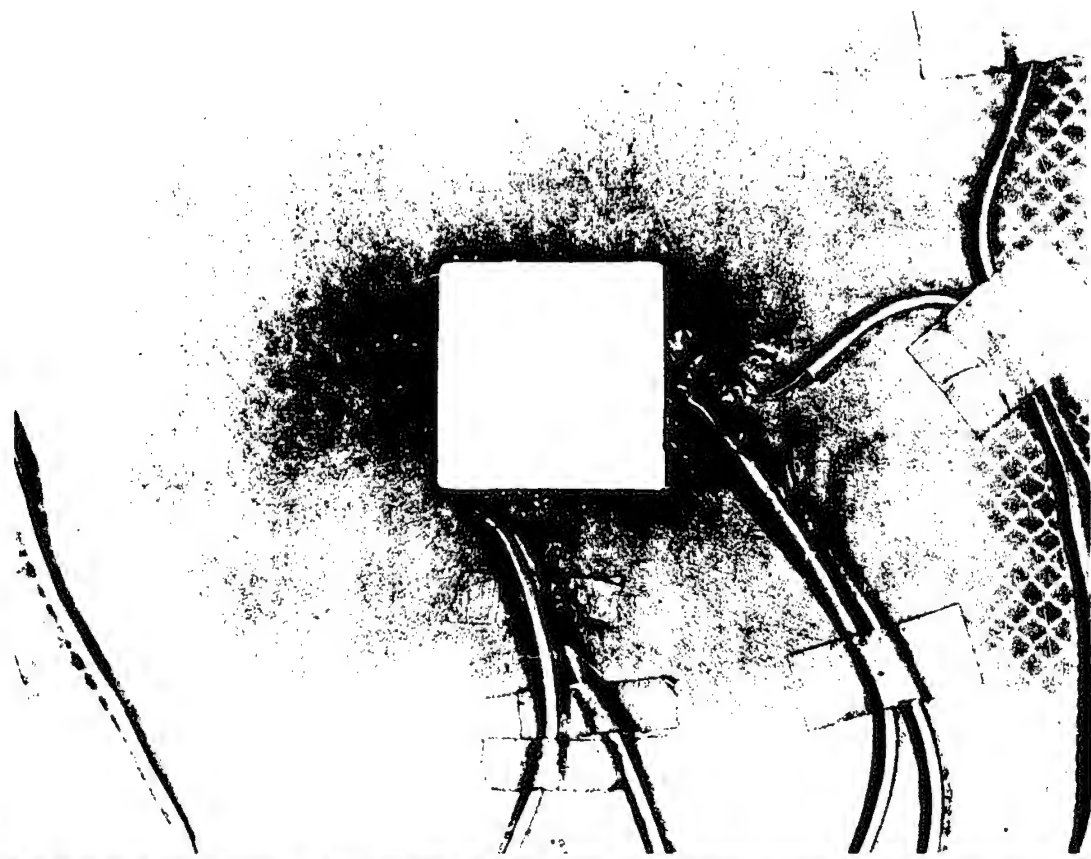
126



125



Figure 53. Connector Hole Stress (Note Loss-of-Preload at Nut Hole) 128



128

127

to no hole strain at the hole boundary gives the critical stress concentration factors for biaxial loading. Theoretical values for the same hole conditions were obtained from published data. The observed and theoretical values are given in Table 2 and the agreement appears satisfactory. The desirability of round holes versus square holes is clearly shown.

Since only steady state loading conditions were evaluated while practical application includes a sizeable thermal and acoustic load, the addition of a smaller equal in thickness to the facings is recommended for all instrumentation holes. Simulated environment testing under combined air, thermal and noise loads of a full size heat shield panel having multiple hole patterns accomplished after panel fabrication is recommended.

129

Figure 54 Panel No. 2, Stresscoat Pattern,

130

TABLE 2:
SUMMARY OF EXPERIMENTAL AND THEORETICAL
VALUES OF STRESS CONCENTRATION FACTOR K FOR BIAXIAL LOADING

Strain Gage Position**	First Test, Panel No. 1 Two Round Holes		Second Test, Panel No. 1 Square Center Hole Round Corner Hole	
	K_{theory} *	$K_{\text{obs.}}$	K_{theory} *	$K_{\text{obs.}}$
A	2.4	2.38C 2.41T	.9	.69C .85T
B	3.9	4.1 T	2.4	2.34T
C			4.5	4.7 T
D			4.5	4.25T
E			6.0	6.20T
F	3.8	3.66T		
G	3.8	3.25T		
H	2.3	1.9T	2.3	2.13T
J	3.4	3.13T	3.4	3.25T

T, Tension Side of Panel
C, Compression Side of Panel

* Theoretical values for biaxial loading from Stresses Around Holes,
W. Griffee, Product Engineering 11/11/63, based on Stress Concentra-
tion Around Holes, G. N. Savit.

** See Figure 55 for locations A through J.

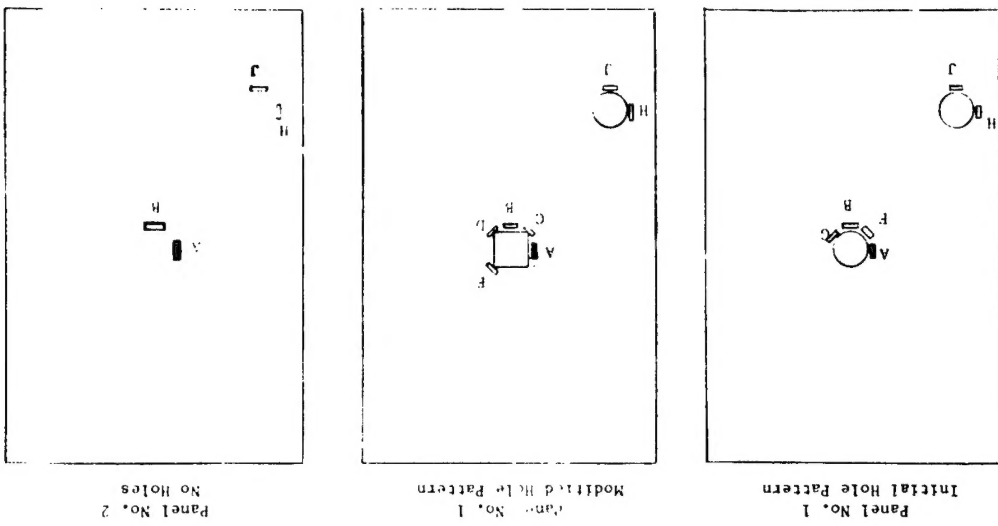


Figure 55: Stress gage locations on test panels used for experimental load tests. The figure shows three panels labeled Panel No. 1, Panel No. 2, and Panel No. 3. Panel No. 1 has a square center hole and round corner holes, with strain gages labeled A through J. Panel No. 2 has two round holes, with strain gages labeled A through F. Panel No. 3 has a square center hole and round corner holes, with strain gages labeled A through H. A legend indicates that 'A' is the tension side and 'C' is the compression side of the panel.

■ Stress Gage Position and Direction of Load
due to Tension and due to Compression (2% error)

Panel No. 1 Initial Hole Pattern
and No. 1
Model 1 Hole Pattern

Panel No. 2 Initial Hole Pattern
and No. 2
Model 2 Hole Pattern

Panel No. 3 Initial Hole Pattern
and No. 3
Model 3 Hole Pattern

SECTION VIII

DESIGN RECOMMENDATIONS FOR 3 1/2" X 4 1/2" SHIELD PANELS

The following recommended design changes for current ~~heat shield panel designs~~ are based on the structural analysis developed on this program and on the heat shield panel fabrication experience on Contract NASA-1276.

1. Honeycomb Reinforcement for M-31 Insulation

Presently specified core configuration for the M-31 insulation reinforcement is Type 8-15 (1/8" cell size - 0.0015" foil core). A slightly heavier core, Type 8-20 (1/8" cell size - 0.001" foil core) is preferred for increased stability in the actual panel brazing as well as the core machining and panel layup operations. The greater stability of the Type 8-20 core during the brazing process will allow the use of a higher vacuum desirable to insure the fit of the panel detail than the presently used 3" mercury or 1.5 psi. Likewise both the core machining and panel layup operations will benefit from the increased stability provided by the Type 8-20 core in:

- a. Improving the resistance to deformation caused by shop handling

- b. Reducing the time required for panel layup.

The difference in weight for the Type 8-20 versus 8-15 core (1/8" in thickness) is very slight, amounting to 0.011 lbs. per square foot or 0.21 lbs. for the 30H12571 panel.

2. Brazing Alloy Thickness for Open Faced Honeycomb Core

The 30H12571 panels produced on Contract NASA-976 utilized 0.002" thick brazing alloy (silver-copper-lithium) for the Type 8-15 open face core to facing attachment because of availability and prior experience on other open face honeycomb brazing applications. A thinner gauge of brazing alloy, namely 0.0015", would be advantageous from a weight viewpoint (0.078 lbs/ft² versus 0.104 lbs/ft² for 0.002" braze alloy) and would provide comparable size braze fillets.

3. Welded Zee Edge Member Frame

The 30H12571 panel utilizes a one piece edge member frame fabricated as a subassembly by fusion welding four (4) zee sections at the corners followed by radiographic inspection of the welds and grinding the weld bead flush with the surface. As a consequence of the welded edge member frame, the completed panel is "sealed" with respect to the structural honeycomb core.

133

134

4. Brazed Zee Edge Member Assembly

The one piece welded edge member frame has many advantages. However, it involves expense and fabrication operations that could be eliminated by using the fully brazed edge member assembly shown in Figure 56. This arrangement, made up of four zee sections brazed together, is also fully sealed by use of a small piece of facing integrally brazed as a doubler at each corner to provide additional strength and close off the corner gap from the core. This is the assembly that is recommended.

5. Core Sealed Edge Member Assembly

For minimum cost the corner joint sealing can be accomplished with a cost savings by using the corner configuration shown in Figure 57 with a high temperature elastomeric sealer such as Coast Pro Seal 700 applied to the corner opening. This type corner joint uses four (4) separate zee sections brazed to the panel facings and eliminates the welding operation, weld fixture, radiographic inspection and weld bead machining--it has likewise been extensively used in brazed panels for airframe application.

6. flare Reduction for Zee Section Edge Member

An 0.030" thick zee section edge member will satisfy the design conditions and afford weight savings of approximately 5 lbs. for the 30MH2571 panel configuration. The analysis for the 0.030" edge member and a comparison with the present 0.050" edge member appears in Section II, Stress Analysis.

7. Treatment of the panel edges for the cup type attachment heat shield panels, particularly for exposed panel edges such as the outboard fairing panels, will be required to protect the structural honeycomb core from thermal and mechanical damage. Presumably, this will be accomplished by completely machining out the honeycomb core approximately 1/8" from the edge of the panel facings and filling the resulting slot with M-31 insulation. It appears unlikely that the unreinforced M-31 edge fill will be retained under the severe noise and vibration environment sustained during ignition and flight. A better edge treatment would be to leave a minimum of 0.25" honeycomb on each panel face in the slot area to provide a more positive attachment for the M-31 insulation. The best edge treatment is a complete insulated metal seal.

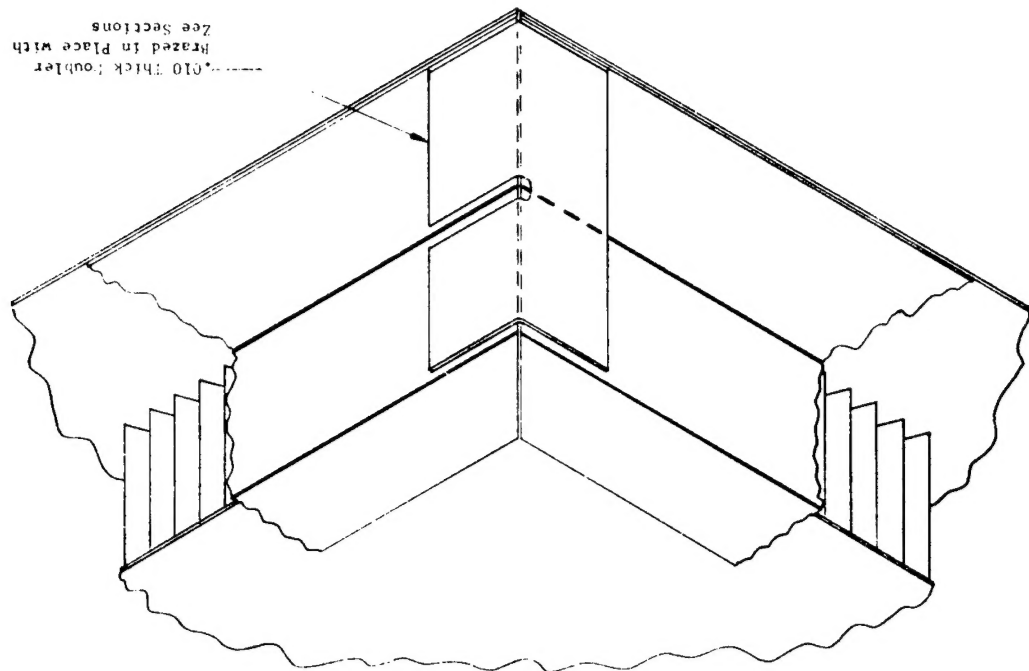
8. The necessity for deformed or crushed open faced honeycomb core to insure the adherence of the M-31 insulation under acoustic and thermal loads was established by the NASA S-IC Heat Shield Panel Test Program. Since the initial core height on both the 30MH2571 and 60B2020 panel designs was 0.125" and then further reduced by deformation or crushing to about 0.075", a thicker open faced core is clearly indicated. A thickness of 0.250" deformed to 0.180" is recommended.

135

136

137

Figure 56 Recommended Zee Section without Joint Assembly



138

Figure 57 Recommended Zee Section with Joint Assembly

